



**HAL**  
open science

## Resveratrol and cyclodextrins, an easy alliance: Applications in nanomedicine, green chemistry and biotechnology

Philippe Jeandet, Eduardo Sobarzo-Sánchez, Md. Sahab Uddin, Roque Bru,  
Christophe Clément, Cédric Jacquard, Seyed Fazel Nabavi, Maryam  
Khayatkashani, Gaber El-Saber Batiha, Haroon Khan, et al.

### ► To cite this version:

Philippe Jeandet, Eduardo Sobarzo-Sánchez, Md. Sahab Uddin, Roque Bru, Christophe Clément, et al.. Resveratrol and cyclodextrins, an easy alliance: Applications in nanomedicine, green chemistry and biotechnology. *Biotechnology Advances*, 2021, 53, pp.107844. 10.1016/j.biotechadv.2021.107844 . hal-03400616

HAL Id: hal-03400616

<https://hal.univ-reims.fr/hal-03400616v1>

Submitted on 16 Oct 2023

**HAL** is a multi-disciplinary open access archive for the deposit and dissemination of scientific research documents, whether they are published or not. The documents may come from teaching and research institutions in France or abroad, or from public or private research centers.

L'archive ouverte pluridisciplinaire **HAL**, est destinée au dépôt et à la diffusion de documents scientifiques de niveau recherche, publiés ou non, émanant des établissements d'enseignement et de recherche français ou étrangers, des laboratoires publics ou privés.



Distributed under a Creative Commons Attribution - NonCommercial 4.0 International License

# 1 Resveratrol and cyclodextrins, an easy alliance: 2 Applications in nanomedicine, green chemistry and 3 biotechnology

4  
5 Philippe Jeandet,<sup>a,b,\*</sup> Eduardo Sobarzo-Sánchez,<sup>c,d</sup> Md. Sahab Uddin,<sup>e,b</sup> Roque Bru,<sup>f</sup> Christophe  
6 Clément,<sup>a</sup> Cédric Jacquard<sup>a</sup>, Seyed Fazel Nabavi<sup>g</sup>, Maryam Khayatkashani<sup>h</sup>, Gaber El-Saber Batiha,<sup>i</sup>  
7 Haroon Khan,<sup>j</sup> Iwona Morkunas,<sup>k</sup> Franscesco Trotta<sup>l</sup>, Adrian Matencio<sup>l</sup> and Seyed Mohammad  
8 Nabavi<sup>g</sup>

9 <sup>a</sup>University of Reims Champagne-Ardenne, RIBP EA 4707 USC INRAE 1488, SFR Condorcet FR CNRS 3417, 51100 Reims Cedex,  
10 France

11 <sup>b</sup>Pharmakon Neuroscience Research Network, Dhaka, Bangladesh

12 <sup>c</sup>Laboratory of Pharmaceutical Chemistry, Faculty of Pharmacy, University of Santiago de Compostela, Campus Vida, 15782  
13 Santiago de Compostela, Spain,

14 <sup>d</sup>Instituto de Investigación e Innovación en Salud, Facultad de Ciencias de la Salud, Universidad Central de Chile, Chile

15 <sup>e</sup>Department of Pharmacy, Southeast University, Dhaka, Bangladesh

16 <sup>f</sup>Plant Proteomics and Functional Genomics Group, Department of Agrochemistry and Biochemistry, Faculty of Science,  
17 University of Alicante, Alicante, Spain

18 <sup>g</sup>Applied Biotechnology Research Center, Baqiyatallah University of Medical Sciences, Tehran 14359-16471, Iran

19 <sup>h</sup>Amol University of Special Modern Technologies, Amol, Iran

20 <sup>i</sup>Department of Pharmacology and Therapeutics, Faculty of Veterinary Medicine, Damanhour University, Damanhour 22511,  
21 AlBeheira, Egypt

22 <sup>j</sup>Department of Pharmacy, Faculty of Chemical and Life Sciences, Abdul Wali Khan University Mardan, 23200, Pakistan.

23 <sup>k</sup>Department of Plant Physiology, Poznań University of Life Sciences, Wołyńska 35, 60-637 Poznań, Poland

24 <sup>l</sup>Department of Chemistry, University of Turin, via P. Giuria 7, 10125, Turin, Italy

25  
26

27 \*Corresponding author: Philippe Jeandet, philippe.jeandet@univ-reims.fr

28  
29

30 **Abstract**

31 Most drugs or the natural substances reputed to display some biological activity are hydrophobic  
32 molecules that demonstrate low bioavailability regardless of their mode of absorption. Resveratrol  
33 and its derivatives belong to the chemical group of stilbenes; while stilbenes are known to possess  
34 very interesting properties, these are limited by their poor aqueous solubility as well as low  
35 bioavailability in animals and humans. Among the substances capable of forming nanomolecular  
36 inclusion complexes which can be used for drug delivery, cyclodextrins show spectacular  
37 physicochemical and biomedical implications in stilbene chemistry for their possible application in  
38 nanomedicine. By virtue of their properties, cyclodextrins have also demonstrated their possible use  
39 in green chemistry for the synthesis of stilbene glucosylated derivatives with potential applications in  
40 dermatology and cosmetics. Compared to chemical synthesis and genetically modified  
41 microorganisms, plant cell or tissue systems provide excellent models for obtaining stilbenes in few  
42 g/L quantities, making feasible the production of these compounds at a large scale. However, the  
43 biosynthesis of stilbenes is only possible in the presence of the so-called elicitor compounds, the  
44 most commonly used of which are cyclodextrins. We also report here on the induction of resveratrol  
45 production by cyclodextrins or combinatory elicitation with methyljasmonate in plant cell systems as  
46 well as the mechanisms by which they are able to trigger a stilbene response. The present article  
47 therefore discusses the role of cyclodextrins in stilbene chemistry both at the physico-chemical level  
48 as well as the biomedical and biotechnological levels, emphasizing the notion of "easy alliance"  
49 between these compounds and stilbenes.

50  
51  
52  
53  
54  
55  
56  
57  
58  
59  
60  
61  
62  
63  
64  
65  
66  
67  
68  
69  
70

71

## 72 1. Introduction

73 Discovered in 1939 by Takaoka in the roots of the white hellebore and subsequently identified as a  
74 phytoalexin, that is, small biocidal molecules produced by plants as a response to stress, in grapevine  
75 (Langcake and Pryce, 1976) and peanut (Ingham, 1976), resveratrol, which belongs to the rather  
76 restricted chemical group of stilbenes, has mainly been the focus of studies undertaken by the  
77 phytopathologists' community until the onset of the 90s (Jeandet et al., 2002; Jeandet et al., 2010;  
78 Jeandet et al., 2021). At the time, works mainly targeted its biosynthetic pathway (Langcake and  
79 Pryce, 1977), antifungal activity (Adrian et al., 1997) and metabolism *in planta* (Jeandet et al., 1997)  
80 as well as by fungi (Breuil et al., 1998). The first reports on the production of resveratrol by grape  
81 berries (Creasy and Coffee, 1988; Jeandet et al., 1991) quickly led to the detection of this compound  
82 in wine by Siemann and Creasy (1992). The originality of the seminal work of these two authors was  
83 to put in relation the already known properties of resveratrol in traditional Chinese and Japanese  
84 medicine (Nonomura et al., 1963) and the cardioprotective effects of a moderate consumption of a  
85 wine rich in polyphenols in a population subjected to a hyperlipidemic diet, the so called famous  
86 "French Paradox" (Renaud and de Lorgeril, 1992). These convergent studies between the  
87 concentration of resveratrol in wine and its possible beneficial effects on human health, has led to a  
88 real explosion of the research on this compound at the end of the 90s, an interest which has not  
89 been denied since. John Pezutto, whose team was the first to demonstrate the cancer  
90 chemoprotective activity of this compound even evoked the "phenomenon resveratrol" (Jang et al.,  
91 1997; Pezzuto, 2011). Resveratrol and its derivatives, the number of which now exceeds a thousand,  
92 have been the subject of relatively recent bibliographic reviews (Jeandet et al., 2021; Keylor et al.,  
93 2015; Rivière et al., 2012; Shen et al., 2009).

94 From a biological point of view, resveratrol exhibits a cytotoxic activity against many  
95 cancer cell lines as well as anti-inflammatory properties (Cai et al., 2015; De Sa Coutinho et al., 2018;  
96 Rauf et al., 2018; Varoni et al., 2016). There is a certain amount of preclinical and clinical evidence of  
97 its efficacy in the treatment of cardiovascular diseases (Zordosky et al., 2015) and of resveratrol  
98 action as a blood pressure lowering agent (Prysyazhna et al., 2019). Resveratrol was also described as  
99 being able to play a protective role in case of neurodegenerative diseases such as Alzheimer,  
100 Huntington and Parkinson, through its antioxidant activity (Bastianetto et al., 2015; Uddin et al.,  
101 2020; Uddin et al., 2021). Resveratrol displays antifungal properties against phytopathogens (Adrian  
102 et al., 1997; Gabaston et al., 2017) or fungi responsible for candidiasis in humans (Houillé et al., 2014).  
103 Finally, resveratrol and its derivatives have excellent cosmetic properties as whitening agents for the  
104 treatment of melanin skin spots (Boo, 2019; Jeandet et al., 2016). One can therefore see without  
105 being exhaustive, that resveratrol and in general stilbenes, possess many biological activities.  
106 However, most of these properties are based on studies conducted *in vitro*. Several obstacles limit  
107 the study of the biological activity of resveratrol and its derivatives *in vivo*. The first one is the weak  
108 water-solubility of most stilbenes as well as their low bioavailability in humans and rats, as observed  
109 after oral administration; these features being quite common with polyphenols (Kapetanovic et al.,  
110 2011; Walle, 2011; Walle et al., 2004). In addition, having these compounds in adequate quantities  
111 for the design of biological tests *in vivo* is hampered by the difficulty of obtaining them by pure

112 chemical synthesis, which is a time-consuming as well as an environmentally unfriendly process  
113 (Keylor et al., 2016; Snyder et al., 2011). Bio-producing stilbenes using biological systems, mainly  
114 plant tissue cultures or cell suspensions in response to molecules capable of eliciting their synthesis,  
115 also provides an interesting alternative in terms of available quantities and green processes (Donnez  
116 et al., 2009; Jeandet et al., 2020; Martinez-Marquez et al., 2016). To address these fundamental  
117 questions, we show in this review how cyclodextrins, which are cyclic molecules built from a few  
118 glucose units, constitute valuable allies in the chemistry of stilbenes. The design of nanomolecular  
119 sponges using cyclodextrins capable of increasing the solubility, inclusion and delivery of stilbenes to  
120 their target cells is a first example. Use of cyclodextrins can also provide interesting applications in  
121 the green synthesis of stilbenes, particularly, for obtaining water-soluble glucosylated derivatives.  
122 Finally, the eliciting properties of cyclodextrins on the biosynthesis of stilbenes, not only of  
123 monomeric stilbenes but also of oligomeric stilbenes, can be applied in plant biotechnology for the  
124 natural sourcing of these compounds.

125

## 126 **2. Stilbene chemistry and biosynthesis: a condensed overview**

127 Phytostilbenes are generally low molecular weight compounds varying from 212 Da for pinosylvin  
128 (3,4-dihydroxystilbene) or 228 Da for resveratrol (3,5,4'-trihydroxystilbene) (Fig. 1) and up to 1587 Da  
129 for pauciflorol D, a resveratrol heptamer identified in *Vatica pauciflora* (Ito et al., 2004). All these  
130 compounds contain a 1,2-diphenylethylene structure based on the C6-C2-C6 backbone. The work of  
131 Stephenson's group has demonstrated very brilliantly that all stilbenes, comprising oligomers varying  
132 in number and structure, are derived from a single block, resveratrol, making this compound the  
133 iconic molecule of this group (Keylor et al., 2015). Resveratrol biosynthesis hails from the  
134 phenylpropanoid pathway, which is common to lignins and flavonoids (Jeandet et al., 2020; Nabavi et  
135 al., 2020) (Fig. 2). This pathway begins with the oxidative deamination of phenylalanine, an amino  
136 acid which drains 30% of all the carbon assimilated during photosynthesis (Qian et al., 2019). This  
137 first reaction, catalyzed by phenylalanine ammonia lyase (PAL), leads to cinnamic acid, the  
138 hydroxylation of which at position 4 yielding *para*-coumaric acid, is ensured by cinnamate-4-  
139 hydroxylase, an enzyme from the cytochrome P450 hydroxylase superfamily. In a secondary way,  
140 *para*-coumaric acid can be obtained directly from tyrosine *via* TAL (tyrosine ammonia lyase) (see  
141 Jeandet et al., 2021 for a review). The final condensation between the *para*-coumaroyl-coenzyme A  
142 formed by ligation of *p*-coumarate with a coenzyme A (CoA) molecule *via* a CoA ligase and three  
143 malonyl-CoA units formed from the glycolysis-derived acetyl-CoA, is catalyzed by stilbene synthase  
144 during an iterative condensation process including the loss of four molecules of CO<sub>2</sub> (Austin and Noel,  
145 2003; Austin et al., 2004).

146 Once the trihydroxystilbene skeleton of resveratrol is built, a high level of chemical  
147 diversification of stilbenes is then obtained thanks to various decorating enzymes like prenylases,  
148 hydroxylases as well as glucosyl and methyltransferases (Jeandet et al., 2021). These enzymes lead to  
149 different monomeric stilbenes, some of which are described in this work: hydroxylated stilbenes,  
150 piceatannol and oxyresveratrol; methylated stilbenes, pterostilbene and glucosylated stilbenes,  
151 polydatin or piceid and 4'-β-O-D-glucosyl resveratrol (Fig. 1). On the other hand, the subsequent  
152 polymerization of resveratrol takes place through the action of plant peroxidases. The condensation

153 of the phenoxy radicals formed from resveratrol upon the action of peroxidases, does not take place  
154 in a randomized manner but in a defined order including various coupling modes (Keylor et al., 2015).  
155 Aside from their glucosylated derivatives, stilbenes, like many polyphenols, are poorly water-soluble  
156 compounds with low bioavailability (Jeandet et al., 2020; Smoliga and Blanchard, 2014).

157

### 158 3. Resveratrol solubility and bioavailability

159 While being less lipophilic than its demethylated derivative pterostilbene (Fig. 1), resveratrol  
160 is a hydrophobic compound as shown by a log P value of 3.0 to compare with that of methylated  
161 stilbenes (log P > 4) (Caruso et al., 2011). Due to its relative lipophilic character, resveratrol can easily  
162 cross membranes and seems to be well transferred in human bioengineered epithelia (Walle et al.,  
163 2006). Although resveratrol displays promising and beneficial properties for human health, most of  
164 the data obtained stemmed from *in vitro* experiments carried out with cell cultures, tissues or  
165 bioengineered tissues (Walle, 2011). The main problem encountered with drugs displaying poor  
166 aqueous solubility is they cannot easily reach the target cells or tissues at sufficient concentrations to  
167 exert their action. *In vivo* studies of resveratrol bioactivity have addressed questions regarding its  
168 absorption and bioavailability. Some key parameters commonly used in pharmacokinetics are the  
169 area under the curve, AUC, the maximal plasmatic concentration,  $C_{max}$  (and the maximal time  $t_{max}$  to  
170 reach  $C_{max}$ ), half-life value,  $t_{1/2}$  and drug bioavailability,  $F$ . Mathematically, the AUC of a given drug  
171 corresponds to the sum of its instantaneous concentrations in the plasma for a given (0 to  $t$ ) time  
172 interval. AUC is described by the following relation in case of a system with one compartment:

173

$$174 \quad AUC_0^t = \int_0^t C_0 e^{-kt}$$

175 Here,  $C_0$  is the initial drug concentration in the plasma and  $k$  is the elimination constant of the drug

176

177 The bioavailability of a drug is the fraction of the drug which reaches the systemic circulation  
178 when it is administered *via* non-intravenous routes as compared to the intravenous one.  $F$  can be  
179 calculated (in %) according to the formula given below with an orally administered drug:

180

$$181 \quad F = \left[ \frac{AUC_{OA} \times \text{dose}_{IVA}}{AUC_{IVA} \times \text{dose}_{OA}} \right] \times 100$$

182

183 Where  $AUC_{OA}$  = AUC oral administration;  $AUC_{IVA}$ , AUC intravenous administration;  $\text{dose}_{IVA}$ , drug dose  
184 *via* the intravenous route and  $\text{dose}_{OA}$ , drug dose *via* oral administration.

185

186 The pioneering studies of Goldberg et al. (2003) and Walle et al. (2004), respectively, have  
187 shown that upon oral administration of 25 mg doses of various wine polyphenols including  
188 resveratrol or the single oral administration of 25 mg radiolabelled resveratrol in humans, this  
189 compound seemed to display an unusual high absorption rate (70%) at the gastro-intestinal tract  
190 level (GIT) when addressing the sum of all its metabolites (both glucuronated and sulfated ones).  
191 However, Walle et al. (2004) concluded that the bioavailability of *non-metabolized* resveratrol

192 remains at a very low level of around 1%. In fact, resveratrol is rapidly transformed in the small  
193 intestine by enterocytes where it undergoes either glucuronidation or sulfation implicating  
194 glucuronidases (Böhmdorfer et al., 2017; Springer and Moco, 2019) and sulfotransferases  
195 (Böhmdorfer et al., 2017; Boocock et al., 2007; Miksits et al., 2005; Springer and Moco, 2019; Wu et  
196 al., 2011), a certain fraction of these sulfo- and glucurono-derivatives entering the portal circulation  
197 (Springer and Moco, 2019). Some studies have reported moderate *F* values for resveratrol following  
198 oral administration as compared to intravenous dosing in rats: 38.8% (Kapetanovic et al., 2011; Lin et  
199 al., 2009) and 29.8% (Kapetanovic et al., 2011). Surprisingly, the more hydrophobic and less polar  
200 pterostilbene (3,5-dimethoxy-resveratrol) was found to reach substantial *F* values, 12.5% (Lin et al.,  
201 2009) and 66.9% (Kapetanovic et al., 2011).

202 Preclinical and clinical experiments conducted in human groups after oral administration of  
203 resveratrol in the form of repeated doses ranging from 30 to 5000 mg per day, revealed varying but  
204 generally low resveratrol peak plasma concentrations ( $C_{max}$ ): 0.56 - 2967.325 ng/mL (Brown et al.,  
205 2010; Draijer et al., 2016; Howells et al., 2011; La Porte et al., 2010; Novotny et al., 2017; Springer  
206 and Moco, 2019; Wightman et al., 2015; Wong et al., 2011), pterostilbene displaying higher total  
207 plasma levels ( $C_{max}$ : 2820-7880 ng/mL) (Kapetanovic et al., 2011). All the afore-mentioned works  
208 underlined poor bioavailability of resveratrol after oral administration *via* single or repeated dosing.  
209 Such limitations have thus opened the way for the search of alternative methods to increase  
210 resveratrol/derivative bioavailability. Some of them such as the use of cyclodextrins as nanocarriers  
211 for the transport of resveratrol as well as utilization of cyclodextrins for the green synthesis of more  
212 polar and soluble resveratrol derivatives, are described in the following sections of this review.

213

#### 214 **4. Cyclodextrins as nanomolecular carriers and their use**

215 Biological membranes represent a barrier for the penetration, delivery and therapeutic  
216 action of many drugs (Bonnet et al, 2015). Targeted drug solubilizers for oral, transdermal,  
217 transmucosal or parenteral formulations are thus needed to overcome these limitations (Stella and  
218 Rajewski, 2020). Drug vectorization has been achieved through use of various nanocarriers including  
219 liposomes, dendrimers and polymeric nanoparticles of range size from 1 to 1000 nm, namely for  
220 cancer treatment (Din et al., 2017). Among these, cyclodextrins have revealed very interesting  
221 properties as nano-vehicles for many drugs (Bonnet et al, 2015; Giwani and Vyas, 2015; Pinho et al,  
222 2014) as well as themselves displaying antiviral properties (Jones et al., 2020) and cytotoxic effects at  
223 high concentrations on diverse cancer cell lines (Argenziano et al., 2020). Cyclodextrins (CDs) have  
224 already been used as nanocarriers for established anticancer drugs like camptothecin (prostate  
225 cancer) (Gigliotti et al., 2016), paclitaxel (ovarian, breast and lung cancers) (Ansari et al., 2011a),  
226 erlotinib (non-small cell lung cancer) (Dora et al., 2016) and tamoxifen (breast cancer) (Torne et al.,  
227 2013). Cyclodextrins were also employed for the release of many other drugs, for example, anti-  
228 inflammatory drugs such as acetyl salicylic acid (Shende et al., 2012), oxaprozin (Mennini et al.,  
229 2016), antivirals such as rilpivirine (Rao et al., 2018), the anti-HIV1 protease inhibitor lopinavir  
230 (Adeoye et al., 2020), antifungals like econazole (Sharma et al., 2011) and antibacterial drugs such as  
231 norfloxacin (Mendes et al., 2018). Cyclodextrin-mediated drug delivery has been experimented in  
232 case of neurodegenerative diseases, as well. Molecularly-imprinted cyclodextrin nanoparticles have

233 indeed been designed for the dihydroxyphenylalanine (DOPA)-prodrug delivery in the treatment of  
234 Parkinson's disease (Trotta et al., 2016a) as well as for facilitating the crossing of the blood-brain  
235 barrier of crocetin, a natural inhibitor of amyloid  $\beta$  plaque formation in the treatment of Alzheimer's  
236 disease (Wong et al., 2020) among other nanovectors used for anti-Alzheimer's drug delivery (Wong  
237 et al., 2019). CDs are safe products approved by the Food and Drug Administration (FDA) (Stella and  
238 Rajewski, 2020). CDs themselves do not display any biological activity unless employed at very high  
239 concentrations (Argenziano et al., 2020).

240 The French Chemist Villiers observed in 1891 that potato starch seeded with *Bacillus*  
241 *amylobacter* (*Clostridium butyricum*) yielded, besides dextrans, two carbohydrates forming "beautiful  
242 crystals" in low amounts, named celluloses and which were attributed a multiple of the following  
243 formula  $[(C_6H_{10}O_5)_2 + 3 H_2O]$  (Crini, 2014). A long time after, the two crystals obtained by Villiers were  
244 identified by Manor and Saenger (1972) as being more likely  $\alpha$ -cyclodextrin with the formula  
245  $[(C_6H_{10}O_5)_6 \cdot 6H_2O]$  and  $\beta$ -cyclodextrin. Cyclodextrins form cyclic oligosaccharidic assemblies  
246 constituted of several  $\alpha$ -1,4-linked glucopyranose units (hereafter named as glucose units). They are  
247 mainly composed of six (CD6) ( $\alpha$ -cyclodextrins), seven (CD7) ( $\beta$ -cyclodextrins) and eight glucose units  
248 (CD8) ( $\gamma$ -cyclodextrins) (Bonnet et al., 2015; Gidwani and Vyas, 2015). This cyclic oligosaccharidic  
249 structure delimits at the supramolecular level a sort of truncated cone as imposed by the peculiar  
250 location of the primary hydroxyl groups of the  $\alpha$ -D-glucopyranose units on one rim of the structure  
251 being the secondary hydroxyl groups on the other (Sandilya et al., 2020) (Fig. 3). CDs thus comprise  
252 an inner hydrophobic cavity with the sugar hydroxyl groups being externally oriented (Bonnet et al.,  
253 2015). Cyclic structures composed of a lower number of glucose units ( $< CD5$ ) were not known and  
254 reputed not to allow stable conformations of glucose units until the recent work of Yamada group  
255 demonstrating the feasibility of the synthesis of smaller cyclodextrins such as CD3 (three glucose  
256 units) and CD4 (four glucose units), which could be utilizable for the inclusion of therapeutic  
257 molecules of very small size (Ikuta et al., 2019).

258 Cyclodextrins not only improve the solubility and above all the bioavailability of hydrophobic  
259 compounds including both synthetic and natural drugs, they provide them with protection against  
260 numerous environmental conditions such as light, pH and temperature variations, oxidation and  
261 enzymatic degradation (Bonnet et al., 2015; Kanaya et al., 2011; Pinho et al., 2014). Internalization of  
262 drugs within cyclodextrins is related to the cyclodextrin cavity size including the inner and outer  
263 diameters which are on average the following: 57/137 nm, 78/153 nm and 95/169 for  $\alpha$ -,  $\beta$ - and  $\gamma$ -  
264 cyclodextrins, respectively (Gidwani and Vyas, 2015; Stella and Rajewski, 2020) (Fig. 3). Torus shape  
265 and opening of  $\alpha$ -cyclodextrins are thought to be too tight to permit the formation of inclusion  
266 complexes with many drugs leading to the preferential use of  $\beta$ -cyclodextrins, even  $\gamma$ -cyclodextrins  
267 for high-molecular weight drugs (Stella and Rajewski, 2020). However, measurement of the binding  
268 affinity energy of various cyclodextrins for resveratrol reported, for example, very close values (-5.4  
269 Kcal/mol and -5.3 Kcal/mol) for  $\beta$ - and  $\gamma$ -CDs, respectively (Haley et al., 2020).

270 As surprising as it may seem,  $\beta$ -cyclodextrins ( $\beta$ -CDs) possess an aqueous solubility eight to  
271 twelve-fold lower than the other two main cyclodextrin groups ( $\alpha$ - and  $\gamma$ -CDs) (Connors, 1997;  
272 Sabadini et al., 2006; Saenger et al., 1998; Sandilya et al., 2020; Szejtli, 1998), though they constitute  
273 the preferred CDs as drug carriers in many experiments for their low cost of production and cavity



274 size best suited for numerous drugs (Stella and Rajewski, 2020). The solubility of  $\beta$ -CDs has thus been  
275 increased through chemical modifications of the glucose secondary hydroxyl groups. These include  
276 methylated  $\beta$ -CDs (mono-, di- and trimethylated CDs as well as randomized methylation of the  
277 cyclodextrin core), hydroxy-alkylated  $\beta$ -CDs (mainly hydroxypropyl- $\beta$ -CDs, HP- $\beta$ -CDs), various  
278 glucosyl- $\beta$ -CDs (glucosyl- $\beta$ -CDs, G1- $\beta$ -CDs and maltosyl- $\beta$ -CDs, G2- $\beta$ -CDs) and sulfonic acid- $\beta$ -CD  
279 derivatives (sulfobutylether- $\beta$ -CDs) (Bonnet et al., 2015; Gidwani and Vyas, 2015; Lucas-Abellan et  
280 al., 2007; Pinho et al., 2014; Stella and Rajewski, 2020; Sandilya et al., 2020) (Fig. 4). Substituting  
281 groups may be chosen with a specific goal. Some studies have selected CD derivatives not subject to  
282 changes of the ionization state of the substituents in relation with pH variations. For instance,  
283 sulfobutylether CDs containing sulfonates or sulfates are stable in the anionic state at physiological  
284 pH (Stella and Rajewski, 2020). CDs such as HP- $\beta$ -CDs, have also been used in combination with  
285 biopolymer-liposomes (Soo et al., 2016; Tan et al., 2021). All these types of CDs have been employed  
286 for the vectorization of resveratrol and its derivatives (see next section).

287 Cyclodextrin chemistry has switched to other ways including the synthesis of hypercross-  
288 linked materials named CD-polymers when consisting of slightly condensed and water soluble  
289 cyclodextrins on one hand, or cyclodextrin-based nanosponges, which are highly polymerized and  
290 insoluble CDs, on the other. CDs of increased site specificity in drug delivery as a response to a given  
291 stimulus are termed stimuli-responsive CD nanosponges and have been developed more recently  
292 (Ciesielska et al., 2020; Dhakar et al., 2019; Palminteri et al., 2021; Yasayan et al., 2020). The three-  
293 dimensional mesh polymer network generated by the cross linking of the CD monomers thus forms  
294 nanocavities for various drug inclusion (Adeoye et al., 2020). Cross linking may occur upon the  
295 condensation of CDs with reagents such as carboxylic acid dianhydrides (pyromellitic dianhydride)  
296 leading to carboxylate CDs (Adeoye et al., 2020; Ciesielska et al., 2020), carbonyldiimidazole yielding  
297 carbonyl-CDs (Ansari et al., 2011b; Dhakar et al., 2019; Yasayan et al., 2020) (Fig. 5) or 1,6-  
298 diisocyanatohexane for the fabrication of polymerized CDs (Haley et al., 2020). For example,  
299 condensation of two  $\beta$ -CDs with pyromellitic dianhydride yielded a CD polymer increasing by 12 to  
300 14- fold the solubility of the anti-HIV1 drug, lopinavir (Adeoye et al., 2020).

301 To deliver drugs in a more specific way, a lot of stimuli-responsive nanosystems-based CDs  
302 were conceived (Palminteri et al., 2021; Tayo, 2017). Inclusion of photochromic moieties into  
303 nanocarriers generates light responsive systems whose light-induced modification can lead to  
304 conformational changes of the carrier and consequently drug release (Babin et al., 2009; Wajs et al.,  
305 2016). Another option for modifying nanocarriers is the addition of ionizable groups such as  
306 carboxylates or amines to build pH-responsive drug transporters (Manchun et al., 2012; Wu et al.,  
307 2016). Differences in pH between tumor and inflammation tissue environments and normal healthy  
308 tissues, with the tumor microenvironment being more acidic than normal tissues (Boedtjker and  
309 Pedersen, 2020), may justify the building of pH-responsive nanosponges for anticancer and anti-  
310 inflammatory drug delivery (Lin et al., 2017; Wu et al., 2016). A similar reasoning applies to the  
311 synthesis of temperature-responsive nanosystems (Cheng et al., 2008; Kim and Matsunaga, 2017)  
312 which is based on the fact that hyperthermia is associated with pathological processes. Redox-  
313 responsive nanocarriers are particularly interesting to exploit the property of certain cancer tissues  
314 to contain significantly higher levels of glutathione (GSH) than normal ones, where these high GSH

315 amounts are linked to tumoral progression and resistance to chemotherapy (Kennedy et al., 2020).  
316 Disulfide bonds present in some redox-responsive nanocarriers are easily reduced by enzymes of the  
317 thioredoxin family localized in the cytoplasm, endoplasmic reticulum or even lysosomes in the  
318 presence of GSH (Arunachalam et al., 2000). Disulfide bond-containing nanovehicles have thus  
319 appeared as particularly useful for site-specific drug delivery and, namely, for resveratrol (Daga et al.,  
320 2016; Trotta et al., 2016b) (Fig. 6).

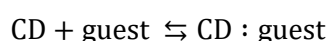
321 Before focusing on resveratrol complexation with CDs, let us remember briefly that CD  
322 encapsulation has already been reported for many polyphenols (Pinho et al., 2014). In order to  
323 improve the water solubility, thermal stability, photostability as well as the bioavailability of these  
324 compounds, numerous works have described the synthesis of inclusion complexes between  
325 flavonoids and CDs, among others:  $\beta$ -CD–rutin complexes for increased antibacterial activity  
326 (Paczkowska et al., 2015),  $\beta$ -CD–quercetin inclusion complexes for establishing potent nose-to-brain  
327 drug carriers (Manta et al., 2020), hydroxypropyl- $\beta$ -CD encapsulation of naringenin for anti-  
328 inflammatory effects (Gratieri et al., 2020), daidzein and genistein inclusion complexes with  
329 hydroxypropyl- and sulfobutylether- $\beta$ -CDs as part of a combined therapy for mucopolysaccharidosis  
330 (Fumic et al., 2018), and curcumin crosslinked CD nanosponges for cancer treatment (Rafati et al.,  
331 2019).

332

### 333 **5. Physico-chemical aspects of resveratrol/stilbene complexation by cyclodextrins:**

334 Formation of inclusion complexes between cyclodextrins and “guest” molecules is defined by two  
335 important physico-chemical parameters, the stoichiometry of the internalization process and the  
336 binding constant  $K$  between cyclodextrins and guest compounds, which are given by the following  
337 equations in case of a 1:1 stoichiometry (Lopez-Nicolas et al., 2009b):

338



340

$$341 K = \frac{[\text{CD} : \text{guest}]}{[\text{CD}] \times [\text{guest}]}$$

342

343 where [CD], [CD-guest] and [guest] are concentrations at the equilibrium.

344

345 A stoichiometry of 1:1 is corresponding to an inclusion formed by one cyclodextrin with one  
346 guest. The stoichiometry becomes 1:2 (or more) in case of a cyclodextrin fixing two (or more) guests  
347 and 2:1 for one guest molecule being complexed with two (or more) molecules of cyclodextrins  
348 (Pinho et al., 2014). A 1:1 stoichiometry in the CD inclusion complexes formed with resveratrol,  
349 pinosylvin, oxyresveratrol, piceatannol (Matencio et al., 2016) or pterostilbene is generally the rule  
350 (see Table 1 and references therein), except pinosylvin where a 1:2 stoichiometry is observed (Silva  
351 et al., 2014). The stability or the complexation constant  $K$  (notated  $K_c$  or  $K_f$ ) measures the strength of  
352 the association between the drug and the ligand. Otherwise speaking,  $K$  characterizes drug affinity  
353 for CDs (Jambhekar and Breen, 2016). The higher this constant, the higher the interaction between  
354 stilbenes and CDs (Bertacche et al., 2006). Values of  $K$  differ according to the structure of the

355 internalized stilbenes and the type of CDs being in the magnitude order of  $10^2$ - $10^4$   $M^{-1}$  (see Table 1  
356 and references therein). The lowest  $K_c$  value recorded was  $606.65 \pm 30.18 M^{-1}$  for oxyresveratrol  
357 complexation on methyl- $\beta$ -CDs (Matencio et al., 2017) and the highest one,  $35864.72 \pm 3415.89 M^{-1}$   
358 for oxyresveratrol inclusion on hydroxypropyl- $\beta$ -CDs (He et al., 2019). According to some authors,  
359 high values of  $K$  may be detrimental to drug release from the inclusion complex (Stella et al., 1999;  
360 Venuti et al., 2014). Increase in the observed anticancer effects of resveratrol-loaded CDs was not  
361 found to be in line with the gain in resveratrol solubility observed upon resveratrol complexation  
362 with various CDs as compared to free resveratrol (Dhakar et al., 2019; Palminteri et al., 2021; Venuti  
363 et al., 2014). For example, around only 65% inhibition of cell viability on MCF-7 human breast cancer  
364 cells were recorded with 150  $\mu$ M resveratrol + sulfobutylether- $\beta$ -CD and 55% inhibition with free  
365 resveratrol despite an increased observed solubility of resveratrol of around 37-fold (0.03 mg/mL  
366 against 1.1 mg/mL). This was attributed to a high complexation constant  $K$  of  $10114 M^{-1}$  maybe  
367 explaining a higher retention of this compound (Venuti et al., 2014). Almost similar results were  
368 obtained regarding inhibition of a DU-145 prostate cell line: 75% inhibition with a carbonyl- $\beta$ -CD and  
369 65% with resveratrol at 100  $\mu$ M for a 3-fold enhanced solubility of resveratrol (0.04 mg/mL against  
370 0.12 mg/mL) (Dhakar et al., 2019).

371 Among the various CDs available, the common ones,  $\alpha$ -CDs,  $\beta$ -CDs and  $\gamma$ -CDs have been used  
372 for the complexation of resveratrol and its derivatives (Fig. 7) (Bertacche et al., 2006; He et al., 2019;  
373 Kumpugdee-Vollrath et al., 2012; Li et al., 2018; Lopez-Nicolas et al., 2009a and 2009b; Lu et al.,  
374 2009; Lucas-Abellan et al., 2007; Soussi et al., 2019). There are many studies reporting on the  
375 application of derivatized CDs to form inclusion complexes with resveratrol: hydroxypropyl- $\beta$ -CDs  
376 (HP- $\beta$ -CDs) (Berta et al., 2010; Bertacche et al., 2006; He et al., 2019; Kong et al., 2020; Kumpugdee-  
377 Vollrath et al., 2012 ; Li et al., 2018; Lim et al., 2020; Lopez-Nicolas et al., 2009a and 2009b; Lu et al.,  
378 2009; Matencio et al., 2017; Sapino et al., 2009.; Silva et al., 2021), glucosylated- $\beta$ -CDs like the  
379 maltosyl- $\beta$ -CD (G2- $\beta$ -CD) (Lucas-Abellan et al., 2008), methylated or ethylated- $\beta$ -CDs such as  
380 monomethylated/ethylated- $\beta$ -CDs (Li et al., 2018; Lopez-Nicolas et al., 2009a and 2009b; Matencio et  
381 al., 2017; Trollope et al., 2014), dimethylated- $\beta$ -CDs (DIMEB) (Bertacche et al., 2006; Kumpugdee-  
382 Vollrath et al., 2012) and randomly-methylated- $\beta$ -CDs (RAMEB) (Duarte et al., 2015) (Table 1). As  
383 aforementioned, sulfobutylether  $\beta$ -CDs are well suited for both neutral and cationic substrates due  
384 to their stability in the anionic state at various pH values (Stella and Rajewski, 2020; Venuti et al.,  
385 2014).

386 Finally, hypercross-linked CD nanosponges where the 3D mesh between CD units is  
387 established through carbonyl, carboxylate and disulfide bonds (Ansari et al., 2011b; Dhakar et al.,  
388 2019; Matencio et al., 2020; Palminteri et al., 2021; Pushpalatha et al., 2018) or constituted of  
389 polymerized  $\alpha$ -,  $\beta$ - and  $\gamma$ -CDs with 1,6-diisocyanotohexane (Haley et al., 2020), have been employed  
390 for resveratrol vectorization. In these intricaded systems, resveratrol is internalized both in the inner  
391 cavities of CDs and the interstitial spaces managed between the cross-linked CDs thus increasing  
392 resveratrol loading efficiency (Dhakar et al., 2019). The most promising vectors for resveratrol are  
393 represented by the so-called bio-responsive nanosponges which constitute site-specific delivery  
394 systems for this compound (Ciesielska et al., 2020; Dhakar et al., 2019; Palminteri et al., 2021, Trotta  
395 et al., 2016b; Yasayan et al., 2020).

396 Generally, resveratrol solubility increases in parallel with the resveratrol-CD molar ratio,  
397 solubility being optimal for a resveratrol-CD ratio of 1:4 (Pushpalatha et al., 2018; Sapino et al., 2009)  
398 (see Table 1). A solubility diagram of resveratrol recorded at pH 6 revealed an increasing solubility of  
399 this stilbene with increased CD concentrations approaching a plateau at the 1:4 resveratrol-CD ratio  
400 (Sapino et al. 2009). Resveratrol solubility may also depend on chemical modifications of CDs taking  
401 place on hydroxyl groups upon its complexation with CDs. Phase solubility diagrams showed an 8.5-  
402 fold increase in resveratrol solubility with  $\beta$ -CD and a 24-fold increased solubility with a HP- $\beta$ -CD,  
403 these values almost doubling when the respective CD concentrations underwent a two-fold increase  
404 (Lu et al., 2012). Stilbene or resveratrol complexation with CDs always leads to an increase in their  
405 water-solubility ranging from 2-fold (Dhakar et al., 2019) to the unbelievably high value of 700,000-  
406 fold recorded by Silva et al. (2014) (Table 1). Resveratrol Inclusion complexes formed with  $\gamma$ -CDs  
407 were also reported as enhancing its solubility in lemon juices from 4.8% to 43.1%, *i.e.*, a 9-fold  
408 increase (Silva et al., 2021). In some studies, a higher solubility of resveratrol (Lu et al., 2009) or  
409 polydatin (Li et al., 2018) was observed with HP- $\beta$ -CDs than with non-derived  $\beta$ -CDs (Table 1).

410 Two parameters are particularly useful in drug nanoformulation: drug loading on- and drug  
411 release from the nanoparticles. These factors are essential for determining the efficiency of the drug  
412 delivery process. Resveratrol loading on nanoparticles which can be expressed as %, is the ratio  
413 between entrapped resveratrol and CD weight (Palminteri et al., 2021). Its values vary from 4 to 7%  
414 in polymerized  $\alpha$ ,  $\beta$  and  $\gamma$ -CDs depending on the CD type (Haley et al., 2020), from 9.95 to 16.12% in  
415 GSH-responsive nanosponges as a function of the resveratrol/CD weight ratio (Palminteri et al., 2021)  
416 and from 30-40% in carbonyl nanosponges (Ansari et al., 2011b; Matencio et al., 2020) to more than  
417 90% in both carboxylate and carbonyl nanosponges (Pushpalatha et al., 2018) (Table 1). The notion  
418 of drug loading can also be extended to the determination of the drug encapsulation efficiency (%),  
419 which is defined as the ratio between entrapped resveratrol in CDs and total resveratrol  
420 concentration in the mobile phase (Palminteri et al., 2021). The values of around 80% obtained for  
421 resveratrol and oxyresveratrol confirm a high encapsulation rate of stilbene compounds in  
422 nanosponges (Dhakar et al, 2019; Palminteri et al., 2021) though it can be lower (29%) (Wang et al.,  
423 2020). Resveratrol loading efficiency is enhanced in conjunction with the stilbene-CD weight ratio of  
424 the inclusion complex (Ansari et al., 2011b; Palminteri et al., 2021). Resveratrol loading passed from  
425 9.95% to 16.12% on glutathione-responsive nanosponges for weight ratios of respectively 1:2 and 1:4  
426 (Palminteri et al., 2021) and 11.93% (1:2 weight ratio) to 16.78% (1:6 weight ratio) for oxyresveratrol  
427 (Dhakar et al., 2019).

428 Release of resveratrol (or derivatives) from CDs or CD-nanosponges was expressed as the  
429 drug dissolution rate with time using the membrane diffusion method (Dhakar et al, 2019; Palminteri  
430 et al., 2021) or determined by measuring resveratrol release from resveratrol-loaded polymerized  
431 CDs in a liquid medium (Haley et al., 2020). Release of resveratrol or oxyresveratrol from various CDs  
432 and CD-nanosponges increased by 2 to 8 fold at different timing (1, 3 or 24 h) compared to their  
433 dissolution rate in the free forms (Bertacche et al., 2006; Dhakar et al., 2019; Palminteri et al., 2021;  
434 Pushpalatha et al., 2018). Resveratrol complexation with HP- $\beta$ -CDs and its further inclusion into  
435 biopolymer-liposomes led to a 100% loading, a value superior to its incorporation to both the CD and

436 the double layer of liposomes (94.4%), though the former complex allowed a two-fold increase in  
437 resveratrol delivery (Table 1) (Soo et al., 2016).

438

#### 439 **6. Pharmacokinetic profile of resveratrol formulated with cyclodextrins**

440 There are numerous *in vitro* studies describing the characteristics of stilbene-CD inclusion complexes  
441 (Table 1), however, works on the pharmacokinetic parameters of resveratrol complexed with CDs  
442 stemming from *in vivo* studies and following different modes of administration are less numerous  
443 (Das et al., 2008; Kong et al., 2020; Pushpalatha et al., 2018) compared to flavonoids (Dos Santos  
444 Lima et al., 2019). The seminal work of Das et al. (2008) provided the first pharmacokinetic profiles  
445 regarding resveratrol-CD formulations. In this study, intravenous administration of resveratrol was  
446 carried out in rats with HP- $\beta$ -CD while oral absorption of resveratrol was performed using RAMEB- $\beta$ -  
447 CD (randomly methylated- $\beta$ -CD) and compared to a suspension of this compound in  
448 carboxymethylcellulose (CMC). Although resveratrol internalization with CDs increased its solubility  
449 by 59,500 fold, the  $AUC_{0\rightarrow 5h}$  (505.9 ng x h/mL) following resveratrol-HP- $\beta$ -CD intravenous  
450 administration at a dosing of 10 mg/kg did not significantly differ from intravenous injection of the  
451 plain compound (10 mg/kg resveratrol in a sodium salt suspension) with an  $AUC_{0\rightarrow 5h}$  of 532.9 ng x  
452 h/mL. Oral formulation of resveratrol with RAMEB- $\beta$ -CD at the dose of 50 mg/kg both increased  $C_{max}$   
453 and  $t_{max}$  without significantly modifying  $AUC_{0\rightarrow 8h}$  (1009 ng x h/mL) nor resveratrol bioavailability  
454 ( $F=39.9\%$ ) as compared to the CMC resveratrol suspension ( $AUC_{0\rightarrow 8h}= 981$  ng x h/ mL;  $F = 38.8\%$ ) (Das  
455 et al., 2008) (Table 2). However, using two sorts of resveratrol-CD nanosponges, one carbonyl  
456 nanosponge formed by crosslinking  $\beta$ -CD with diphenylcarbonate (R-NS I) and a carboxylate one  
457 fabricated from  $\beta$ -CD and pyromellitic dianhydride (R-NS II), a significant resveratrol loading  
458 efficiency of around 91% (Tables 1 and 2) was recorded in rats following a 20 mg/kg oral absorption  
459 of R-NS I and R-NS II compared to resveratrol alone as well as a two-fold increase in  $C_{max}$  and  
460 AUC values ( $AUC_{0\rightarrow 24h}$  : 4145 and 3917 ng x h/ mL vs 2080 ng x h/ mL) (Pushpalatha et al., 2018)  
461 (Table 2).

462 In a comparative study performed in rats, pulmonary administration (oro-tracheal intubation)  
463 of resveratrol-HP- $\beta$ -CD inclusion complexes in various dosages were evaluated against intravenous,  
464 intra-gastric and nasal inhalation administration (Kong et al., 2020). Reported data showed better  
465 pharmacokinetic profiles ( $C_{max}$ ,  $AUC_{0\rightarrow 10h}$ ,  $AUC_{0\rightarrow \infty}$ ) according to the trans-pulmonary route vs all  
466 other routes with decreasing  $F$  values, 92.95% (pulmonary administration), 76.31% (nasal inhalation)  
467 and only 16.68% (intra-gastric route) (Table 2). A 5-fold increase in resveratrol bioavailability was thus  
468 recorded between pulmonary administration and the intra-gastric route.

469 These studies therefore indicate that resveratrol bioavailability upon inclusion with  
470 cyclodextrins can be increased by a factor 2 when using CD-nanosponges compared to oral  
471 administration of the unloaded compound (Das et al., 2008; Pushpalatha et al., 2018). It also depends  
472 on its mode of administration (Kong et al., 2020).

473

#### 474 **7. Stilbene/cyclodextrin inclusions increase stilbene photostability**

475 Generally, the complexation of stilbenes with CDs or nanosponges has a positive effect on their  
476 photostability (Allan et al., 2009; Bertacche et al., 2006; Cheng et al., 2018; Dhakar et al., 2019; He et

477 al., 2019; Li et al., 2018; Pushpalatha et al., 2018; Sapino et al., 2009; Silva et al., 2014) and  
478 thermostability (He et al., 2019). Light exposure can indeed be very detrimental to highly  
479 photosensitive compounds or drugs. Complexation with CDs has namely been described to delay  
480 photodegradation of the light versatile vasodilator nifedipine (Bayomi et al., 2002). It is well  
481 established that the natural isomer of resveratrol (and its derivatives) is the *trans* form which easily  
482 yields the *cis* isomer within a few minutes of UV or sunlight exposure (Jeandet et al., 1997; Trela and  
483 Waterhouse, 1994). Bertacche et al. (2006) reported that only  $\alpha$ -CD was efficient in protecting  
484 resveratrol from sunlight as compared to the larger  $\beta$ - and  $\gamma$ -CDs, though all CDs were found to  
485 confer resveratrol stability against UV radiations of 254 and 365 nm. It was suggested that the three-  
486 dimensional network constituted by CDs (Sapino et al., 2009) or nanosponges (Dhakar et al., 2019;  
487 Pushpalatha et al., 2018) negatively affects light scattering due to a screening effect.

488

## 489 **8. Reported benefits of stilbene/cyclodextrin inclusion complexes**

490 All data tend to demonstrate that inclusion of resveratrol and its derivatives in CDs improves their  
491 solubility as well as loading on-and release from CDs (Table 1 and references therein). Most of the  
492 experiments conducted *in vitro* or *in vivo* which have been put in place to validate the benefits of  
493 stilbene internalization in CDs on their biological activity, may principally resume in the study of the  
494 antioxidant capabilities and cytotoxic actions of the complexes obtained. Besides, other works have  
495 reported the usefulness of stilbene inclusion with CDs for biomedical applications *in vivo* (Haley et al.,  
496 2020; Lacerda et al., 2017; Lacerda et al., 2018; Soussi et al., 2019).

497

### 498 **8.1. Antioxidant activity of stilbene-cyclodextrin inclusion complexes**

499 The antioxidant activity of stilbene-CD inclusion complexes was mainly evaluated by their capacity to  
500 enhance scavenging of stable radicals such as DPPH $\cdot$  (Dhakar et al., 2019; Duarte et al., 2015; Haley  
501 et al., 2020; Li et al., 2018; Lu et al., 2009; Sapino et al., 2009), ABTS $^{+}$  and SO $^{+}$  (Silva et al., 2021) or  
502 the lipid peroxidation state (Lu et al., 2012). There is converging evidence in some studies that  
503 internalization of stilbenes in CDs or nanosponges increases their antioxidant properties compared to  
504 the free compounds. For example, the reducing power of polydatin as determined with the  
505 Fe $^{3+}$ /ferricyanide complex as well as its DPPH $\cdot$  radical scavenging activity were respectively enhanced  
506 by 2 and 1.5-fold upon inclusion with CDs, the best performances being observed with HP- $\beta$ -CD (Li et  
507 al., 2018) (Table 3). Dhakar et al. (2019) recorded a 75% DPPH $\cdot$  radical inhibition activity with  
508 resveratrol-carbonyl- $\beta$ -CD nanosponges vs 45% (1.7 fold-increase) with the plain compound at a 100  
509  $\mu$ M concentration. The same trend was also reported with oxyresveratrol-carbonyl- $\beta$ -CD  
510 nanosponges at the 50  $\mu$ M level. Supplementation of lemon juice with resveratrol- $\gamma$ -CD complexes  
511 allowed to maintain juices' antioxidant capacity over 28 days compared to free resveratrol  
512 supplementation possibly leading to pertinent application in functional food (Silva et al., 2021). In the  
513 same way, a strong inhibition of lipid peroxidation was described with resveratrol-CD complexes (Lu  
514 et al., 2012). Haley et al. (2020) showed in a pilot study, that localized resveratrol delivery performed  
515 with polymerized  $\alpha$ -,  $\beta$ - and  $\gamma$ -CDs maintained a significant DPPH $\cdot$  radical scavenging activity in the  
516 oxidative stress microenvironment generated by implanted intracortical microelectrodes, which are

517 used in the treatment of several neurological disorders increasing their operating time. This work  
518 thus adds value to the utilization of resveratrol inclusion CD complexes for potential applications in  
519 neurology (Table 3).

520 At the opposite, no beneficial role of resveratrol encapsulation with CDs was demonstrated  
521 in other studies, its antioxidant capabilities being unchanged from resveratrol to resveratrol-CD  
522 complexes (Duarte et al., 2015; Lu et al. 2009; Sapino et al., 2009). A strong interaction between CDs  
523 and stilbenes and possibly low drug release was reported as a plausible cause for the observed non-  
524 significant differences in the scavenging radical capacities of free resveratrol and its inclusion  
525 complex with methyl- $\beta$ -CD despite an increase in resveratrol solubility and loading (Duarte et al.,  
526 2015) (Tables 1 and 3). Here, a low enhancement (1.5-fold) in resveratrol release may account for  
527 this discrepancy (Duarte et al., 2015).

528

## 529 *8.2. Anticancer activity of stilbene-cyclodextrin inclusion complexes*

530 All experimental studies conducted *in vitro* have shown a reduction of the cell viability of various  
531 malignant cell lines upon inclusion of resveratrol with CDs or nanosponge complexes *vs* free  
532 resveratrol (Table 3). For example, Pushpalatha et al. (2018) noted IC<sub>50</sub> values for the *in vitro*  
533 cytotoxicity of resveratrol carbonyl- $\beta$ -CD or resveratrol carboxylate- $\beta$ -CD nanosponges, 65% lower  
534 (IC<sub>50</sub>= 110.70  $\mu$ M and 117.34  $\mu$ M) than those of the unloaded compound (IC<sub>50</sub>=169.98  $\mu$ M) on MCF-7  
535 human breast cancer cells. A reduced IC<sub>50</sub> value of 20  $\mu$ M was observed upon resveratrol inclusion  
536 with HP- $\beta$ -CD for inhibiting the proliferation of 7,12-dimethylbenz[a]anthracene-induced oral cancer  
537 cells (HCPC-1 oral squamous cell carcinoma) compared to resveratrol alone (45  $\mu$ M) (Berta et al.,  
538 2010). Moreover, a spectacular regression of exophytic lesions displaying oral squamous cell  
539 carcinoma characters was recorded in hamster cheek pouches following topical applications of  
540 resveratrol-CD complexes *vs* free resveratrol (Berta et al., 2010). A significantly higher inhibition of  
541 cell viability was also reported for oxyresveratrol (-75%) and resveratrol (-70%) loaded on carbonyl  
542 nanosponges at the 100  $\mu$ M concentration on DU-145 prostate cancer cells compared to the free  
543 compounds (-60 and -50%, respectively) (Dhakar et al., 2019) (Table 3). At the same 100  $\mu$ M  
544 concentration, a 1.5 fold-increase (40 to 60%), a 4 fold-increase (20 to 80%) and a 6 fold-increase (10  
545 to 60%) were observed in the inhibition of cell viability (from unloaded resveratrol to resveratrol  
546 nanosponges) for one prostate cancer line (PC-3) and two colon cancer lines (HT-29 and HCT-116),  
547 respectively (Matencio et al., 2020). Reduction in the viability of HT-29 colon cancer cells also shifted  
548 from 15% with plain resveratrol to 40% with dual liposome-CD-resveratrol encapsulation complexes  
549 at a dose of 100  $\mu$ M (Soo et al., 2016).

550 Very marked effects of resveratrol-HP- $\beta$ -CD or resveratrol- $\beta$ -CD complexes have been  
551 reported regarding the cell viability decrease of HeLa cervical carcinoma cells (-40%) and Hep3B  
552 hepatocellular liver cancer cells (-43 to -46%) compared to the only 5% recorded with unloaded  
553 resveratrol (Lu et al., 2012). Extensive alterations of the cellular morphology including membrane  
554 collapse were also observed with CDs loaded with resveratrol though no such alterations were seen  
555 with free resveratrol (Lu et al., 2012). Similar reduction of cell viability (> 90%) was reported upon  
556 resveratrol inclusion with other types of CDs such as RAMEB- $\beta$ -CD *vs* resveratrol (70%) in Caco-2  
557 human epithelial colorectal adenocarcinoma cells (Duarte et al., 2015) or sulfobutylether- $\beta$ -CDs

558 (65%) in the MCF-7 breast cancer line than with resveratrol alone (55%) (Venuti et al., 2014). In this  
559 latter case, the slight difference observed in the reduction of the cell viability of those cancer cells  
560 was attributed to a high binding constant between resveratrol and CDs thus limiting resveratrol  
561 release efficiency. Resveratrol-sulfobutylether- $\beta$ -CDs encapsulated in poly (lactic-co-glycolic acid)  
562 nanoparticles, which have been proposed as an inhalable system for resveratrol delivery, displayed a  
563 remarkable inhibition of the cell viability of non-small cell lung cancer cells, reducing by respectively  
564 15.39 and 50-fold the  $IC_{50}$  against the A549 and H358 cell lines compared to plain resveratrol (Wang  
565 et al., 2020).

566 Glutathione (GSH)-responsive nanosponges were used to selectively target cancer cells with  
567 elevated contents of GSH such as some ovarian and breast tumorigenic cell lines (Palminteri et al.,  
568 2021). The 3-D mesh of these nanosponges is constituted by the CD cavities and the interstitial  
569 spaces managed by the cross linkage of the CDs with pyromellitic dianhydride and disulfure bridges  
570 (Fig. 6). The latter are lysed by endocellular enzymes of the thioredoxin family in the presence of high  
571 amounts of GSH thus facilitating release of resveratrol in the cell. Nanosponges are internalized in  
572 the cells through different endocytosis pathways (Palminteri et al., 2021). At resveratrol  
573 concentrations from 100 to 200  $\mu$ M, a 50-80% inhibition of the cell viability of the OVCAR-3 ovarian  
574 cancer cell line and the MDA-MB-231 breast cancer cell line was reported with the resveratrol  
575 nanosponges, while a lower reduction in cell viability (-15%) was noted with the resveratrol  
576 nanosponges on normal human fibroblasts, the human mammary epithelial cell line MCF-10A or the  
577 SK-OV-3 human ovarian malignant cells, demonstrating the selective toxicity of these nanosponges  
578 (Palminteri et al., 2021).

579

### 580 *8.3. Applications of stilbene-cyclodextrin inclusion complexes in vivo*

581 Stilbene inclusion in CDs and its recognized benefits to increasing the solubility, release and  
582 bioavailability of these compounds has received some interesting applications in nanomedicine. For  
583 example, Vectisol<sup>®</sup> formulation of resveratrol, *i.e.* its encapsulation in a monopropene diamino- $\beta$ -CD,  
584 turned out to allow the early recovery of proximal tubular function and glomerular filtration as well  
585 as a slowdown of loss of the renal functions in a kidney transplantation preclinical study in pigs  
586 thanks to the resveratrol antioxidant properties (Soussi et al., 2019). By reducing oxidative stress in  
587 the right ventricle of rats displaying monocrotaline-induced pulmonary hypertension in a *cor*  
588 *pulmonale* model, inclusion of pterostilbene with HP- $\beta$ -CDs ameliorates the systolic function of the  
589 ventricle as well as prevents it from structural alterations such as hypertrophy through an increase of  
590 pterostilbene bioavailability (Lacerda et al., 2017). Likewise, pterostilbene encapsulation with HP- $\beta$ -  
591 CDs was shown to preserve *via* a decrease of lipid peroxidation and the regulation of some  
592 antioxidant mechanisms, the function of the left ventricle following induced myocardial infarction in  
593 rats (Lacerda et al., 2018). Additionally, inclusion of stilbenes in CDs may also have a positive effect  
594 by increasing their antimicrobial capabilities. These compounds are indeed known for possessing  
595 various antifungal and antimicrobial activities (Vestergaard and Ingmer, 2019). Complexation of  
596 pterostilbene with HP- $\beta$ -CDs, which is reputed to display higher fungitoxicity than its non-methylated  
597 counterpart resveratrol, was reported to diminish by 7.5-fold the minimum inhibiting concentration  
598 and by 4-fold the minimum bactericidal concentration on growth of *Fusobacterium nucleatum*, a



599 bacterial pathogen associated with periodontitis, compared to unloaded pterostilbene dissolved in  
600 DMSO (Lim et al., 2020).

601 Numerous works have provided a large piece of evidence that stilbene compounds, mainly  
602 resveratrol (Aziz et al., 2005; Boo, 2019; Costa et al., 2016, Lin et al. 2021; Osmond et al., 2012) or  
603 pterostilbene (Sirerol et al., 2015) are efficient in preventing ultraviolet-B induced damages of skin,  
604 treating cutaneous herpes (Docherty et al., 2004), psoriasis (Kjaer et al., 2015), modulating skin  
605 cancer mechanisms or improving melanoma treatment with potential applications in onco-  
606 dermatology. CDs have been shown to constitute interesting agents as good vehicles for stilbene  
607 delivery and for ensuring high levels of compound penetration as well as safety of the tissues for the  
608 treatment of skin or mucosal cancers (Ansari et al., 2011b; Berta et al., 2010; Sapino et al., 2009).  
609 Experiments with various matrices including rabbit mucosa (Ansari et al., 2011b), porcine skin  
610 (Sapino et al., 2009) and porcine ear skin (Pushpalatha et al., 2019), revealed an increased *ex vivo*  
611 skin penetration of resveratrol with resveratrol CD or nanosponge formulations. Resveratrol-  
612 nanosponges accumulated at a two-fold higher rate (600  $\mu\text{g}/\text{cm}^2$ ) than the plain compound (300  
613  $\mu\text{g}/\text{cm}^2$ ) in porcine ear skin (Pushpalatha et al., 2019). A similar trend was reported with resveratrol-  
614 HP- $\beta$ -CDs in porcine skin (Sapino et al., 2009) and resveratrol-carbonyl nanosponges in rabbit mucosa  
615 (Ansari et al., 2011b).

616

### 617 **9. Implication of cyclodextrins for the green synthesis of stilbene glucosides**

618 Glucosylation of stilbene compounds not only increases their aqueous solubility for potential uses in  
619 cosmetic and onco-dermatology but substitution by a glucosyl group at the 4'-position of stilbenes  
620 also protects them from oxidation by polyphenol-oxidases such as tyrosinases (Regev-Shoshani et al.,  
621 2003). A lot of stilbene  $\beta$ -D-glucosides have been identified so far in plants, namely the 3-O- $\beta$ -D-  
622 glucosyl-resveratrol (piceid or polydatin), the 4'-O- $\beta$ -D-glucosyl-resveratrol (resveratrolside) and the  
623 4'-O- $\beta$ -D-glucosyl-piceatannol (Fig. 1) (Jeandet et al., 2020). Research has moved over the past few  
624 years toward the synthesis of their  $\alpha$ -anomeric counterparts whose aqueous solubility and surfactant  
625 properties are superior (Gonzalez-Alfonso et al., 2018; Marié et al., 2018; Ioannou et al., 2021;  
626 Shimoda et al., 2015).

627 The major drawback in the green synthesis of stilbene glucosides is the compatibility of the  
628 solvent employed for both the glucose acceptor (here the starting stilbenes) and the enzyme used for  
629 glucosylation. For this reason, oftentimes, a compromise between enzyme stability and stilbene  
630 solubility is necessary (Jeandet et al., 2020). Making use of green solvents could be the right answer  
631 to this paradox. The green synthesis of 3-O- $\alpha$ -D-glucosyl resveratrol with sucrose and not CDs as a  
632 glucose donor, has already been performed under the catalytic action of a phosphorylase from  
633 *Bifidobacterium adolescentis* using a combination of an ionic liquid and a buffer, which considerably  
634 increases resveratrol solubility (De Winter et al., 2013). Several works have reported achievement of  
635 stilbene O-glucosylation with cyclodextrin glucosyl-(glucano)-transferases (CGTases) from various  
636 sources as biocatalysts utilizing starch or CDs as glucose donors (Gonzalez-Alfonso et al., 2018;  
637 Ioannou et al., 2021; Marié et al., 2018; Mathew et al., 2012; Shimoda et al., 2015; Torres et al.,  
638 2011) (Table 4). CGTases have indeed often been employed for the biosynthesis of various  
639 polyphenolic glucoside derivatives: epicatechin glucosides (Aramsangtienchai et al., 2011),

640 kaempferol glucoside (Choung et al., 2017), genistein diglucoside (Han et al., 2017), flavonol and  
641 flavanone glucosides (Lee et al., 2017), pinosresinol glucoside (Khummanee et al., 2019) or  $\alpha$ -arbutin  
642 (Mathew et al., 2013). Torres et al. (2011) have described the use of a monophasic solvent system  
643 constituted of a mixture of one organic solvent (DMSO) and acetate buffer for the synthesis of a  
644 series of glucoside derivatives of resveratrol. In this synthesis, starch was employed as the primary  
645 glucose donor, glucosylation being ensured by the CGTases of *Thermoanaerobacter* or *Bacillus*  
646 *macerens*. Under these conditions, various glucosides of resveratrol were obtained with quite good  
647 50% glucosylation yield, suggesting that CDs arising from the partially hydrolyzed starch were directly  
648 implicated in the transfer of the glucosyl moiety to stilbene acceptors. In a similar manner, the  
649 enzymatic production of a 4'-O- $\alpha$ -glucoside of pterostilbene whose solubility is lower than that of  
650 hydroxystilbenes, was described in a monophasic solvent system constituted by DMSO and buffer  
651 with the CGTase of *Thermoanaerobacter* and starch as the primary source for glucosyl groups  
652 (Gonzalez-Alfonso et al., 2018). However, the high proportion of DMSO in the solvent mixture  
653 renders this synthetic route unsuitable for the green production of stilbene glucosides.

654 As aforementioned, CDs allow the increasing of the internalization rate of compounds poorly  
655 soluble in water such as stilbene aglycones. Their use is thus particularly conducive to the green  
656 synthesis of stilbene glucoside derivatives (Ioannou et al., 2021; Jeandet et al., 2020; Marié et al.,  
657 2018). The transfer of an  $\alpha$ -glucoside group or more groups from the donor (the cyclodextrin) to the  
658 acceptor (the stilbene) may proceed through coupling of the cyclodextrin and the stilbene, which  
659 randomly attach to the active site of the CGTase (Lim et al., 2021; Mathew et al., 2012). A plausible  
660 mechanism for the formation of a series of piceid (referred as picG<sub>1</sub>) derivatives considerably varying  
661 in the number of the glucosyl groups, has been deciphered under the action of the CGTase of *B.*  
662 *macerans* (Mathew et al., 2012) (Fig. 8). A primary nucleophilic attack of the 4'-hydroxyphenyl group  
663 of piceid (picG<sub>1</sub>) on the Carbon 1 at the reducing end of an opened  $\alpha$ -CD,  $\alpha$ -maltohexaose, results in  
664 an  $\alpha$ -(1,4) linkage between piceid and the maltohexaose leading to the release of an initial coupling  
665 product called picG<sub>7</sub>. Following successive disproportionation reactions of picG<sub>7</sub>, various glucoside  
666 derivatives of picG<sub>1</sub> like picG<sub>2</sub>, picG<sub>3</sub>, etc...are then obtained (Mathew et al., 2012). This mechanism  
667 may explain not only the recovery of monoglucosides but also of di and tri-glucosides during  
668 resveratrol glucosylation in the presence of CGTases (see below) (Ioannou et al., 2021; Marié et al.,  
669 2018, Torres et al., 2011). Polyglucosylated derivatives of 4'-O- $\beta$ -resveratrol-glucoside like 4'-O- $\beta$ -  
670 maltoside, 4'-O- $\beta$ -maltotrioside, 4'-O- $\beta$ -maltotetraoside and 4'-O- $\beta$ -maltopentaoside acting as  
671 potent inhibitors of phosphodiesterase activity and displaying possible neuroprotective properties,  
672 were obtained through a synthetic route including  $\alpha$ -CD and a plant CGTase in a medium totally free  
673 from organic solvent (Shimoda et al., 2015). One may pay attention to the fact that in this case, only  
674 the  $\beta$ -anomeric forms were obtained instead of the commonly recovered  $\alpha$ -glucosides (Table 4).

675 The CGTase-catalyzed synthesis of hundred milligrams of  $\alpha$ -O-D- mono and diglucosides of  
676 resveratrol (3 and 4'- $\alpha$ -O-D-glucosyl resveratrol as well as 3 and 4'- $\alpha$ -O-D-maltosyl resveratrol) was  
677 performed more recently at the 2-L bioreactor scale in water (MES buffer) with the CGTase from  
678 *Thermoanaerobacter* sp. (*Toruzyme*) and  $\beta$ -CD as a glucose donor (Marié et al., 2018) (Fig. 9).  
679 Maximization of the glucosylation transfer was achieved *via* the optimization of multiple factors such  
680 as pH, temperature, enzyme and donor amount as well as the resveratrol:CD ratio, performing a 35%

681 yield based on molar concentrations. This yield increases up to 50% when a 1 kDa cut-off membrane  
682 is coupled to the enzymatic reactor thus allowing retention of the resveratrol  $\beta$ -CD inclusion complex  
683 in the medium and increasing the transfer rate of the glucoside derivatives formed in the permeate  
684 such that they are protected from further hydrolysis (Ioannou et al., 2021). The production rates of  
685 the 3 and the 4'-O- $\alpha$ -glucosides of resveratrol were almost similar indicating the absence of any  
686 regioselectivity in the glucosylation process on the stilbene moiety (Marié et al., 2018) (Table 4).

687 Glucosylation of stilbenes increases their water-solubility making them utilizable for topical  
688 applications in case of cutaneous disorders for cosmetics and onco-dermatology (Intagliata et al.,  
689 2019). Torres et al. (2011) indeed noted a 67-fold increase in the solubility of resveratrol- $\alpha$ -  
690 glucosides compared to resveratrol. Likewise, pterostilbene, which is an almost insoluble compound  
691 in water, has its solubility reaching 0.1 g per liter upon glucosylation (Gonzalez-Alfonso et al., 2018).  
692 Except the study of Shimoda et al. (2015) reporting an increase in the inhibition of  
693 phosphodiesterase activity with resveratrol glucosides that suggests their potential for the treatment  
694 of neurodegenerative diseases, other works conducted on the biological activity of stilbene  
695 glucosides tend to show paradoxically a decrease in their antioxidant and cytotoxic effects with  
696 regards to the aglycones (Table 4). By taking resveratrol as the reference compound with an  
697 antioxidant activity of 100%, the relative activities of the 3 and the 4'-O- $\alpha$ -glucosides of resveratrol  
698 were respectively of only 40 and 70% (Marié et al., 2018; Torres et al., 2011) as confirmation that  
699 glucosylation on the 4'-position of stilbenes is less detrimental to their biological activity (Regev-  
700 Shoshani et al., 2003). Similarly, Gonzalez-Alfonso et al. (2018) reported a near 40% decrease in the  
701 antioxidant activity of 4'-O- $\alpha$ -glucoside of pterostilbene as well as a significantly lower toxicity on HT-  
702 29 colon cancer cells compared to the aglycone.

703 Apart from the synthesis of stilbene glucosides, use of RAMEB- $\beta$ -CDs was also found to  
704 facilitate hydroxylation of the stilbene core with engineered cytochrome P450 leading to various di-  
705 and trihydroxystilbenes and limiting the use of organic solvents to a few percents (Ruhlmann et al.,  
706 2017).

707

## 708 **10. Cyclodextrins for the induction of stilbene production in plant cell systems**

709 As aforementioned, one major feature of CDs is their ability to form inclusion complexes with poor  
710 water-soluble organic molecules due to the hydrophobic character of their central cavity, which thus  
711 serve as nano-sized carriers for these molecules in aqueous solutions. In addition to such a  
712 remarkable property, CDs are able to interact with plant cells in which they can trigger a defense  
713 response. This makes them useful tools to study plant biochemistry and physiology as well as  
714 biotechnology aspects. The first evidence for a CD-plant cell interaction arose from experiments run  
715 with grapevine cell cultures treated with the phytoalexin resveratrol, either unloaded or complexed  
716 with the dimethyl- $\beta$ -CD (DM- $\beta$ -CD) in order to evaluate its efficacy as a protecting agent against the  
717 phytopathogen *Xylophylus ampelinus*. Although unloaded resveratrol completely disappeared within  
718 48 h, resveratrol loaded on DM- $\beta$ -CD remained stable in the medium. Unexpectedly, controls treated  
719 only with DM- $\beta$ -CD exhibited an accumulation of resveratrol evidencing for the first time that CDs  
720 may act as inducers of *de novo* resveratrol synthesis in grapevine cells (Morales et al., 1998).

721 As seen before, CDs display a high chemical diversity, including CDs of natural origin with free  
722 hydroxyl groups, and the ones of synthetic origin with chemical groups attached to the glucosidic OH  
723 groups (Bonnet et al., 2015). The capability of a limited number of  $\beta$ -CDs to induce resveratrol  
724 bioproduction was first evaluated in grapevine cell cultures (Bru et al., 2003; Bru et al., 2006). Only  
725 chemically modified CDs, *e.g.* methyl- or hydroxypropyl-CDs, induced a strong resveratrol production  
726 unlike the natural CDs, which yielded a very weak response. However, sulfated  $\beta$ -CDs, which are  
727 frequently used as carriers in pharmaceutical formulations (Stella and Rajewski, 2020), brought about  
728 a hypersensitive response in grapevine cells. Bru group's study thus highlighted the importance of  
729 the chemical nature of CD-linked groups to raise a cellular response and suggested that one plausible  
730 reason for the reported elicitor activity of CDs is their structural similarity to the oligosaccharidic  
731 elicitors released from plant cell walls upon plant-fungal interactions. Dimethylated- $\beta$ -CDs also well-  
732 known as DIMEB thus became the gold standard in subsequent research works. Another piece of  
733 evidence that CDs differentially interact with plant cells is the species- and genotype-dependent cell  
734 resveratrol production observed as a response to a particular cyclodextrin type (Zamboni et al.,  
735 2006).

736 CDs are almost non-toxic for cell cultures and display a superior eliciting activity than other  
737 oligosaccharides like chitosan, a major component of fungal cell walls (Ferri et al., 2009). Among the  
738 elicitors used to induce stilbene biosynthesis by plant cell or tissue systems, CDs lead to the highest  
739 production yields (in the g/L range) (Bru et al., 2003; Bru et al., 2006; Nivelle et al., 2017) compared  
740 to other common eliciting molecules derived from jasmonate, like methyljasmonate (MeJA) with  
741 reported production levels of only milligrams per liter (Krisa et al., 1999; Tassoni et al., 2005;  
742 Santamaria et al. 2010). Further works have shown empirically that combinatory elicitation with CDs  
743 and MeJA and, to a lesser extent, CDs plus coronatine, the jasmonate-Ile analog, synergize the effects  
744 of each elicitor increasing the production of resveratrol by 5 to 8-fold in grapevine cell suspensions  
745 (Almagro et al., 2015; Belchí-Navarro et al., 2012; Lijavetzky et al., 2008; Oilva et al., 2018).  
746 Spectroscopic approaches for understanding the synergistic mechanisms existing between CDs and  
747 MeJA have reported that resveratrol, CDs and MeJA together in solution formed binary complexes,  
748 respectively CD-resveratrol and CD-MeJA but no ternary inclusion complexes (Oliva et al., 2018). CDs  
749 were demonstrated to improve the aqueous solubility of the reputed hydrophobic molecule, MeJA,  
750 resulting in an increase of resveratrol production by grapevine cells.

751 Cost is a key issue in biotechnology and the utilization of elicitors like DIMEB and coronatine  
752 could turn out to be quite expensive for large scale applications in bioreactors. Attempts to reduce  
753 the production costs incurred by CDs have led to a new strategy, such as the use of CD polymers  
754 coated with magnetic nanoparticles for the easy recover and reutilization of the elicitor in plant cell  
755 cultures for optimizing resveratrol production (Almagro et al., 2020). The obtained results are  
756 promising as HP- $\beta$ -CD coated polymers can be reused up to three times yielding resveratrol levels  
757 ranging from 0.3 and 0.5 g/L.

758 Stilbene production based on the use of CDs has also been accomplished in plant tissue  
759 systems like the hairy roots of *Arachis hypogaea*, *Vitis rotundifolia* and *V. vinifera* leading to the  
760 accumulation of tens of mg/g dry weight (DW) of resveratrol, piceid and resveratrol dimers in the  
761 elicited tissues of grapevine or peanut (Medina-Bolivar et al., 2007; Nopo-Olazabal et al., 2013;

762 Tisserant et al., 2016). Elicitation resulted in a successful strategy to both enhance the production  
763 level of those stilbenes and promote their extracellular accumulation, which is particularly useful for  
764 facilitating their extraction from the culture medium. Use of DIMEB was also reported to induce the  
765 production as well as modifying the profiles of some isoprenylated stilbenes belonging to the  
766 arachidin family (Fig. 1) in the hairy roots of *A. Hypogaea* (Yang et al., 2015; Fang et al., 2020).

767 Once the feasibility of producing a natural compound or drug by tissue or cell cultures has  
768 been demonstrated, the problem arises of transferring the results obtained from the laboratory scale  
769 to the industrial production in bioreactors (Donnez et al., 2009; Jeandet et al., 2014; Jeandet et al.,  
770 2016). The high stilbene levels recovered in plant cell systems as a response to elicitation with CDs,  
771 particularly in grapevine cell cultures, have led to scale up the cultures from shaken flasks to  
772 bioreactors. Most grapevine cell cultures well tolerate the typical shear stress of the bioreactor  
773 environment, even with a stirred tank (Aumont et al., 2004; Lambert et al., 2019; Nivelle et al., 2017;  
774 Vera-Urbina et al., 2013), although some genotypes seem to be more sensitive (Donnez et al., 2011;  
775 Ferri et al., 2011). Both bubble column (Vera-Urbina et al., 2013) and disposable bag wave  
776 bioreactors (Eibl and Eibl, 2008) are suitable for this purpose. Elicitation of stilbene production with  
777 DM- $\beta$ -CD was successfully performed in bioreactors using the *V. vinifera* and *V. labrusca* cell lines.  
778 Recovered stilbene amounts well correlated with the respective achievements in shaken flasks  
779 though being slightly higher in bioreactors, most likely due to a better mass transfer. When using  
780 DM- $\beta$ -CD alone, accomplished resveratrol yields were 2.2 and 3 mg/g fresh weight (FW) for *V.*  
781 *vinifera* cv Gamay cultures in V-shaped bubble columns and in stirred tank bioreactors, respectively.  
782 Resveratrol amounts rose to 13.5 mg/g FW in each bioreactor (Vera-Urbina et al., 2013) and even  
783 reached 14.3 mg/g FW in a 20-litre stirred tank bioreactor upon combinatory elicitation with DM- $\beta$ -  
784 CD and MeJA (Lambert et al., 2019), which further confirms the synergistic effect already mentioned  
785 in shaken flasks (Lijavetzky et al., 2008).

786 Elicitation with cyclodextrins combined with plant metabolic engineering has been disclosed  
787 as a successful strategy to diversify the profile of stilbenes and other specialized metabolites  
788 produced by cell suspension cultures. For instance, grapevine cells transformed with the *human*  
789 *hydroxylase CYP1B1* (Martinez-Marquez et al., 2016) or the *Rosa hybrida orcinol-O-methyltransferase*  
790 (Martinez-Marquez et al., 2018) produced significant levels of resveratrol derivatives like piceatannol  
791 and pterostilbene, respectively, in addition to resveratrol upon elicitation. Likewise, the  
792 transformation of *Sylibum marianum* cultures with the *grapevine stilbene synthase 3* yielded 12 mg/L  
793 resveratrol upon elicitation with DM- $\beta$ -CD, in addition to the accumulation of silymarin and coniferyl  
794 alcohol as in the wild lines (Hidalgo et al., 2017).

795

## 796 **11. Mechanisms of induction of stilbene production by cyclodextrins**

797 Although CDs, and particularly DM- $\beta$ -CDs, are known to induce a phytoalexin response in grapevine  
798 cells ending up in both the production and the extracellular accumulation of various stilbenes, the  
799 understanding of the cellular and molecular mechanisms involved in this response is far from being  
800 elucidated. Such events obviously include perception of CDs or their hydrolyzing products at the  
801 membrane level and induction of the related signaling pathways, followed by regulation of the key  
802 enzymes of stilbene biosynthesis, gene transcription changes as well as modifications of some

803 membrane transporters. The mechanisms by which CDs are able to trigger the production of  
804 resveratrol and related stilbenes in the cell, remain unexplained. A good comparison can be drawn  
805 with the induction of a phytoalexin response in soybean cotyledons by middle-chain  
806 oligogalacturonides released from the plant cell wall by fungal endo-polygalacturonases (Cervone et  
807 al., 1989). It is likely that opening of the CD ring and subsequent hydrolysis of the glucosidic chain  
808 may also generate oligosaccharides such as maltoheptaose and maltohexaose with potent eliciting  
809 activities on resveratrol biosynthesis.

810 To decipher the early signaling events taking place during resveratrol biosynthesis induction  
811 in the presence of DM- $\beta$ -CD or DM- $\beta$ -CD + MeJA, the effect of blockers of extracellular Ca<sup>2+</sup> fluxes,  
812 inhibitors of MAP kinases, NADPH oxidases and Tyr phosphatases as well as NO scavengers was  
813 studied in grapevine cell suspensions (Belchi-Navarro et al., 2013). DM- $\beta$ -CD / MeJA combination  
814 turned out to relieve the action of blockers of extracellular Ca<sup>2+</sup> fluxes, MAPKs inhibitors and NO/H<sub>2</sub>O<sub>2</sub>  
815 scavengers indicating that Ca<sup>2+</sup> mobilization, NO and H<sub>2</sub>O<sub>2</sub> production, MAP kinases and  
816 phosphatases are involved in the early signalization to reach resveratrol production (Fig. 10) (Belchi-  
817 Navarro et al., 2013). Remarkably, these effects on signaling pathways resemble those reported for  
818 grapevine cell cultures treated with the microbial protein elicitor PG1 (Poinssot et al., 2003, Vandelle  
819 et al., 2006).

820 Transcription factors are major components in the regulation of cellular metabolic events  
821 fine-tuning the control of numerous biosynthetic routes including the resveratrol one comprising for  
822 example, the *Vitis vinifera* transcription factors VvWRKY24 and VvMyB14 being able to up-regulate  
823 *STS* gene expression on one hand, and the negative regulator VvWRKY8 of *STS* gene expression on  
824 the other (Fig. 10) (Duan et al., 2016; Jeandet et al., 2019; Jiang et al., 2019; Vanzozi et al., 2018;  
825 Wong and Matus, 2017). Transcription factors like MYB15 which activates the transcription of  
826 stilbene synthase (*STS*) (Höll et al., 2013) and the NAC-type which promotes the biosynthesis of  
827 phenylpropanoids and monolignols (Mitsuda et al., 2007), are up-regulated by DM- $\beta$ -CD and further  
828 enhanced by DM- $\beta$ -CD + MeJA (Fig. 10) (Almagro et al., 2014). Numerous biosynthetic enzymes from  
829 the connected pathways of shikimate, phenylalanine, phenylpropanoid (PAL, C4H, 4CL), malonyl CoA  
830 and stilbene (*STS*) biosynthesis are up-regulated by DM- $\beta$ -CD, and DM- $\beta$ -CD + MeJA to allow a  
831 marked carbon flow toward resveratrol biosynthesis (Almagro et al., 2014). Omics analyses  
832 conducted on grapevine cell cultures offered an overall picture of the major metabolic events  
833 following combined DM- $\beta$ -CD and MeJA elicitation (Almagro et al., 2014; Martinez-Esteso et al.,  
834 2011; Martinez-Marquez et al., 2017). Proteomic changes strongly correlate with transcriptional  
835 events, particularly during changes in the activity of the enzymes catalyzing the late resveratrol  
836 biosynthetic steps (PAL, *STS*) (Martinez-Esteso et al., 2011). Taken altogether, it would seem that CDs  
837 and combinatory elicitation with CDs and MeJA orchestrate resveratrol accumulation by two  
838 strategic actions: (i) activation of *STS* genes transcription; (ii) increase of the precursor supply taking  
839 into account that all the precursors of resveratrol biosynthesis are also shared by major competing  
840 pathways; *i.e.* monolignol and flavonoid routes. These omic studies also revealed the co-expression  
841 of certain glutathione-S-transferase isoforms at both the transcript and protein levels. Interestingly,  
842 overexpression of a tau class glutathione-S-transferase (VvGST U10a) possibly implicated in the  
843 transport of resveratrol was observed in grapevine cells upon elicitation with DM- $\beta$ -CD or DM- $\beta$ -CD +

844 MeJA (Martinez-Marquez et al., 2017). Otherwise, combinatory elicitation with DIMEB and MeJA in  
845 peanut hairy roots, led to the up-regulation of stilbene dimethylallyltransferases, which are  
846 implicated in the transfer of a dimethylallyl pyrophosphate group to various stilbenic compounds, in  
847 addition to STS (Yang et al. 2018). This confirms the accumulation of prenylated stilbenes at levels  
848 similar with those of resveratrol (Fig. 10) (Yang et al. 2015). Combinatory elicitation is thus also able  
849 to activate metabolic steps downstream resveratrol biosynthesis to diversify stilbene profiles.

850

## 851 **12. Conclusions and future prospects**

852 The involvement of CDs in the chemistry of resveratrol at both the physico-chemical level  
853 as well as the biomedical and biotechnological levels, was underlined in this work. Cyclodextrins can  
854 serve as nanomolecular-scale transporters for stilbenes to improve their solubility and bioavailability,  
855 thereby ensuring their delivery at the cellular level. Inclusion of resveratrol and stilbenes in  
856 cyclodextrins increases their water solubility by a factor of 10 up to 10,000 depending on the studies,  
857 allowing them to be used in green chemistry particularly for the synthesis of glucosylated derivatives  
858 without the need for organic solvents. Finally, the reported eliciting properties of CDs on the  
859 production of stilbenes by tissue or cell cultures in quantities of the order of a few grams, constitutes  
860 a third aspect of what we have defined as the easy alliance between stilbenes and cyclodextrins.

861 As regard the nano-transport of resveratrol and its derivatives, it has generally been shown  
862 that CDs improve both their solubility in water and their bioavailability in animal models and,  
863 consequently, their anticancer and antioxidant activity as well as their biological properties during  
864 experiments carried out *in vivo*, compared to unloaded resveratrol. However, even if the percentage  
865 of resveratrol loaded on CDs is elevated, its release from CDs may be hampered in case of high  
866 resveratrol-CD association constants. Some authors have indeed suggested that the lack of  
867 differences recorded in the biological activity between free and CD-encapsulated resveratrol could  
868 be linked to high values of this constant. Regarding bioavailability, it seems that resveratrol inclusion  
869 with CDs modifies this parameter increasing it by a factor two when using CD-nanosponges; a  
870 significant improvement in bioavailability (more than 5-fold) was also recorded depending on its  
871 mode of administration (pulmonary, nasal or intra-gastric) (Das et al., 2008; Kong et al., 2020;  
872 Pushpalaha et al., 2018). Further studies are thus needed to study the pharmacokinetic profiles of  
873 stilbenes *in vivo* upon nano-encapsulation with CDs.

874 Stilbene vectorization using CDs is now moving towards the production of more specific  
875 systems such as bioresponsive-cyclodextrin nanosponges targeting particular cell types or  
876 microenvironments. Trotta's group recently described the inexpensive synthesis of a GSH-responsive  
877 CD nanosponge capable of selectively targeting certain types of cancer cells. The crosslinking in this  
878 nanosystem contains disulfide bridges whose lysis in the presence of endogenous GSH and  
879 endocellular enzymes facilitates drug release. These nanosponges have successfully been studied  
880 using the anticancer drug, doxorubicin during *in vitro* experiments (Trotta et al., 2016b). The method  
881 was transposed very recently to the design of GSH-bioresponsive nanosponges dedicated to the  
882 transport of resveratrol (Palminteri et al., 2021). This type of resveratrol-nanosponges preferentially  
883 targets certain models of cancer cells *in vitro* (ovarian, breast and lung cancer cells), which contain  
884 higher levels of GSH than other cancer cell types and normal cells. GSH-responsive nanoparticles

885 transporting resveratrol would therefore have to be further tested *in vivo* for the treatment of  
886 specific tumors and the modulation of tumor extracellular matrices in relation to the high GSH levels  
887 released by tumor-associated fibroblasts (Palminteri et al., 2021).

888 Use of CDs for the green synthesis of glucosides of resveratrol and its derivatives has a  
889 double benefit, CDs both serve as donors of glucosyl moieties during the complex reactions of  
890 transglucosylation in the presence of CGTases and allow the solubilization of these compounds in  
891 water and buffer solutions (Ioannou et al., 2021; Marié et al., 2018; Shimoda et al., 2015) or limit to  
892 small amounts the incorporation of organic solvents (Gonzalez-Alfonso et al., 2018; Mathew et al.,  
893 2012). Quantities of the order of a few hundred milligrams of resveratrol  $\alpha$ -glucosides have already  
894 been obtained from only 2 g of resveratrol in presence of a  $\beta$ -CD in 2 L-reactors, thus paving the way  
895 toward the application to syntheses on a larger scale (Marié et al., 2018). Coupling the enzymatic  
896 reactors with membranes with a cut-off threshold of 1 kDa already makes it possible to optimize the  
897 accomplished yields (Ioannou et al., 2021).

898 Unexpectedly, CDs were reported the ability of inducing the production of resveratrol at the  
899 gram scale as well as yielding various profiles of stilbenes including hydroxylated, isoprenylated,  
900 glucosylated, methylated and oligomeric forms in plant cell or tissue systems. Research in this area  
901 will face two challenges: up-scaling the bioproduction of stilbenes at the industrial level and  
902 deciphering the mechanisms at the basis of their biosynthesis by plant cells and tissues. There are  
903 indeed still many gaps to bridge in the knowledge of the mechanisms by which CDs elicit resveratrol  
904 production in grapevine and other plant culture systems. All this requires further efforts, such as the  
905 discovery of receptor- and signaling cascade-specific proteins, additional transcriptional regulation  
906 players as well as membrane transporters enabling the extracellular accumulation of stilbenes. It  
907 would be interesting to carry out a targeted gene expression analysis to explore whether MYB and  
908 WRKY transcription factors do respond or not to CD elicitation or combinatory elicitation with MeJA,  
909 and which *STS* paralogs are activated to obtain a more complete picture of the regulatory stilbene  
910 biosynthesis network in grapevine.

911  
912 **Acknowledgements:** Part of this work is the result of an aid to the postdoctoral training and  
913 improvement abroad for Dr Adrián Matencio (number 21229/PD/19) and financed by the Fundación  
914 Séneca (Región de Murcia, Spain).

915

916



917 **Legends of the figures:**

918 **Figure 1: Biosynthesis of stilbenes starting from phenylalanine and the alternative route from**  
919 **tyrosine.** Abbreviations used: PAL, phenylalanine ammonia lyase; TAL, tyrosine ammonia lyase; C4H,  
920 cinnamate-4-hydroxylase; 4CL, 4-cinnamoyl-CoA ligase; STS, stilbene synthase; CHS, chalcone  
921 synthase; ROMT, resveratrol-*O*-methyltransferase; GT, glucosyltransferases; UDPG, UDP-Glucose;  
922 PER, peroxidases

923  
924 **Figure 2: Chemical structures of some stilbene monomers described in this review.**  
925 Hydroxystilbenes, resveratrol, piceatannol, oxyresveratrol and pinosylvin; stilbene glucosides, piceid,  
926 4'-*O*- $\beta$ -glucosyl-resveratrol (resveratrolside); methylated stilbenes, pterostilbene; isoprenylated  
927 stilbenes; arachidin-1, arachidin-2 and arachidin-3

928  
929 **Figure 3: Schematic representation of the truncated cones formed by the cyclic oligosaccharides of**  
930  **$\alpha$ -(CD6),  $\beta$ -(CD7) and  $\gamma$ -cyclodextrins (CD8).** The cyclic oligosaccharidic assembly delimits at the  
931 supramolecular level a sort of truncated cone whose inner diameters are increasing according to the  
932 CD type.

933  
934 **Figure 4: Simplified structures of some modified  $\beta$ -cyclodextrins (CD7).** **1;** R = H,  $\beta$ -cyclodextrin, R = -  
935 CH<sub>2</sub>-CH(OH)-CH<sub>3</sub>, 2-hydroxypropyl- $\beta$ -cyclodextrin; **2,** R = -CH<sub>3</sub>, methyl- $\beta$ -cyclodextrin; **3, 3a,** R = -SO<sub>3</sub>Na,  
936  $\beta$ -cyclodextrin sulfate, **3b,** R = -[CH<sub>2</sub>]<sub>4</sub>-SO<sub>3</sub>Na, sulfobutylether- $\beta$ -cyclodextrin.

937  
938 **Figure 5: 3D representation of a carbonyl CD nanosponge.** This type of nanosponge is obtained by  
939 reaction of a  $\beta$ -CD with carbonyldiimidazole yielding the carbonyl CD nanosponge and imidazole.  
940 Linking carbonyl groups are colored in red and blue

941  
942 **Figure 6: 3D representation of a GSH-responsive  $\beta$ -CD nanosponge.**  $\beta$ -cyclodextrin cycles made of  
943 seven  $\alpha$ -D-glucose units are linked with the crosslinker pyromellitic dianhydride and ethyldisulfide  
944 bridges. Diethylsulfide bridges are colored in yellow, oxygen atoms in red and oxygen-hydrogen  
945 bonds in white

946  
947 **Figure 7: Inclusion of resveratrol within the cavity of a  $\beta$ -cyclodextrin (realized by molecular**  
948 **docking)**

949  
950 **Figure 8: Hypothetical mechanism of the formation of stilbene glucosides from cyclodextrins.**  
951 Cleavage of the cycle of the  $\alpha$ -cyclodextrin yields an opened  $\alpha$ -cyclodextrin named  $\alpha$ -maltohexaose.  
952 A primary nucleophilic attack of the hydroxyl situated at the 4'-position of piceid on the C1 at the  
953 reducing end of maltohexaose leads to an intermediate compound whose disproportionation leads  
954 to various piceid glucoside derivatives

955  
956 **Figure 9: Green synthesis of various *O*- $\alpha$ -glucosylated derivatives starting from  $\beta$ -cyclodextrin as a**  
957 **glucose donor with a cyclodextrin glucosyl transferase.** **A,** General scheme of the synthesis; **B,**  
958 schematic representation of resveratrol inclusion inside the  $\beta$ -cyclodextrin cavity. **1** and **2,** 3 and 4'-  
959  $\alpha$ -*O*-D-glucosyl resveratrol; **3** and **4,** 3 and 4'- $\alpha$ -*O*-D-maltosyl resveratrol. Abbreviations: R,  
960 resveratrol;  $\beta$ -CD,  $\beta$ -cyclodextrin; CGTase, cyclodextrin glucanotransferase (according to Ioannou et  
961 al., 2021)

962

963 **Figure 10: Regulation of stilbene biosynthesis through combinatory elicitation with dimethyl- $\beta$ -CD**  
964 **(DIMEB) and MeJA elicitors in grapevine cells.** Stilbene biosynthesis involves the production of the  
965 early precursors erythrose 4-P (E4P) and phosphoenolpyruvate (PEP) from a carbon source through  
966 central carbohydrate pathways. The two direct precursors of resveratrol are produced through two  
967 different pathways: *p-coumaroyl CoA* is a final product of the two early precursors processed *via* the  
968 shikimate/aromatic aminoacid biosynthesis/phenylpropanoid serial pathways, and *Malonyl CoA*  
969 comes from a parallel processing of PEP through three enzymatic steps. The first stilbene,  
970 resveratrol, may undergo derivatization reactions out of which only two have been well  
971 characterized to date: methylation by resveratrol-*O*-methyltransferases in grapevine (VvROMT), and  
972 prenylation by resveratrol dimethylallyl transferases in peanut (AhR4/3'DT). Resveratrol and  
973 prenylated derivatives are found in the extracellular medium, as well. In grapevine cell cultures upon  
974 elicitation with DIMEB and DIMEB + MeJA, a tau class glutathione *S*-transferase (VvGSTU2) is  
975 putatively involved in the extracellular accumulation of resveratrol as free form or complexed with  
976 CDs. Elicitors such as DIMEB and MeJA trigger early signaling events starting from  $Ca^{2+}$  income from  
977 the apoplasmic space that ends up in transcriptional regulation through a only partly established  
978 pathway where production of NO,  $H_2O_2$  and participation of protein tyrosine phosphatases (TyrPase)  
979 and MAPK is involved. In *Vitis quinquangularis*, a MAPKKK38 transcription factor has been described  
980 to enhance the transcription of *STS* genes likely *via* the transcriptional activation of MYB14. In *V.*  
981 *amurensis*, Ca-dependent protein kinases activate the transcription of specific *STS* paralogs. In *V.*  
982 *vinifera*, the best characterized transcriptional activators of *STS* genes are MYB14/15 TFs, that are  
983 also able to activate the transcription of shikimate pathway key genes as well as those of *PAL* and  
984 *ROMT*. MYB14, WRKY8 and resveratrol are components of a regulatory loop in which MYB14  
985 promotes the production of resveratrol; resveratrol activates the transcription of WRKY8, likely  
986 through undisclosed effector proteins, and WRKY8 interacts with MYB14 to block it, thus down-  
987 regulating resveratrol levels. Such a negative loop was discovered upon UV light irradiation which  
988 activates the transcription of MYB14. Other steps of the phenylpropanoid pathway have also specific  
989 transcriptional activators such as WRKY2 and MYB5a, and NAC TFs which are active up-regulators of  
990 some key steps of the shikimate pathway. Regulatory entities described in relation with combinatory  
991 elicitation with DIMEB and MeJA are shown in orange colour. Blue arrows indicate possible hierarchy  
992 between early signaling events. Green and red arrows stand for transcriptional up- and down-  
993 regulation respectively; solid lines indicate that the evidence has been validated in targeted  
994 experiments while slashed lines means the evidence only comes from omics analysis. Genes  
995 encoding for TFs have been labelled in their promoter regions according to the stimulus they  
996 respond: elicitor responding (ERE), hormone responding (HRE), UV light responding (UVRE) and  
997 resveratrol responding (RRE). DIMEB are symbolized by small truncated structures

998

999

1000 **References**

1001

- Adeoye, O.; Bartolo, I.; Conceição, J.; Da Silva, A.B.; Duarte, N.; Francisco, A.P.; Taveira, N.; Cabral-Marques, H. 2020. Pyromellitic dianhydride crosslinked soluble cyclodextrin polymers: Synthesis, lopinavir release from sub-micron sized particles and anti-HIV-1 activity. *Int. J. Pharm.* 583, 119356.
- Adrian, M.; Jeandet, P.; Veneau, J.; Weston, L.A.; Bessis, R. 1997. Biological activity of resveratrol, a stilbenic compound from grapevine against *Botrytis cinerea*, the causal agent for gray mold. *J. Chem. Ecol.* 23 1689-1702.
- Allan, K.E.; Lenehan, C.E.; Ellis, A.V. 2009. UV light stability of  $\alpha$ -cyclodextrin/resveratrol host-guest complexes and isomer stability at varying pH. *Aust. J. Chem.* 62, 921-926.
- Almagro, L.; Belchí-Navarro, S.; Martínez-Marquez, A.; Bru-Martinez, R.; Pedreño, M.A. 2015. Enhanced extracellular production of trans-resveratrol in *Vitis vinifera* suspension cultured cells by using cyclodextrins and coronatine. *Plant Physiol. Biochem.* 97, 361-367.
- Almagro, L.; Carbonell-Bejerano, P.; Belchí-Navarro, S.; Bru-Martinez, R.; Martínez-Zapater, J.M.; Lijavetzky, D.; Pedreño, M.A. 2014. Dissecting the transcriptional response to elicitors in *Vitis vinifera* cells. *PLoS ONE* 9, e109777.
- Almagro, L.; De Gea-Abellán, A.; Rodríguez-López, M.I.; Núñez-Delicado, E.; Gabaldón, J.A.; Pedreño, M.A. 2020. A smart strategy to improve t-resveratrol production in grapevine cells treated with cyclodextrin polymers coated with magnetic nanoparticles. *Polymers* 12, e991.
- Ansari, K.A.; Torne, J.; Vavia, S.; Trotta, F.; Cavalli, R. 2011a. Paclitaxel loaded nanosponges: *in vitro* characterization and cytotoxicity study on MCF-7 cell line culture. *Curr. Drug Deliv.* 8, 194-202.
- Ansari, K.A.; Vavia, P.R.; Trotta, F.; Cavalli, R. 2011b. Cyclodextrin-based nanosponges for delivery of resveratrol: *In vitro* characterization, stability, cytotoxicity and permeation study. *AAPS PharmSciTech* 12, 279-286.
- Aramsangtienchai, P.; Chavasiri, W.; Ito, K.; Pongsawasdi, P. 2011. Synthesis of epicatechin glucosides by a  $\beta$ -cyclodextrin glycosyltransferase. *J. Mol. Catal. B Enzym.* 73, 27-34.
- Argenziano, M.; Foglietta, F.; Canaparo, R.; Spagnolo, R.; Della Pepa, C.; Caldera, F.; Trotta, F.; Serpe, L.; Cavalli, R. 2020. Biological effect evaluation of glutathione-responsive cyclodextrin-based nanosponges: 2D and 3D studies. *Molecules* 25, 2775.
- Arunachalam, B.; Phan, U.T.; Geuze, H.J.; Cresswell, P. 1990. Enzymatic reduction of disulfide bonds in lysosomes: Characterization of a gamma-interferon-inducible lysosomal thiol reductase (GILT). *Proc. Natl Acad. Sci. USA* 97, 745-750.
- Aumont, V.; Larronde, F.; Richard, T.; Budzinski, H.; Decendit, A.; Deffieux, G.; Krisa, S.; Mérillon, J.M. 2004. Production of highly  $^{13}\text{C}$ -labeled polyphenols in *Vitis vinifera* cell bioreactor cultures. *J. Biotechnol.* 109, 287-294.
- Austin, M.B.; Bowman, M.E.; Ferrer, J.L.; Schröder, J.; Noel, J.P. 2004. An aldol switch discovered in stilbene synthases mediates cyclisation specificity of type III polyketide synthases. *Chem. Biol.* 11, 1179-1194.
- Austin, M.B.; Noel, J.P. 2003. The chalcone synthase of type III polyketide synthases. *Nat. Prod. Rep.* 20, 79-110.

- Aziz, M.H.; Afaq, F.; Ahmad, N. 2005. Prevention of ultraviolet-B radiation damage by resveratrol in mouse skin is mediated via modulation in survivin. *Photochem. Photobiol.* 81, 25-31.
- Babin, J.; Pelletier, M.; Lepage, M.; Allard, J.F.; Morris, D.; Zhao, Y. 2009. A new two-photon sensitive block copolymer nanocarrier. *Angew. Chem. Int Ed.* 48, 3329-3332.
- Bastianetto, S.; Ménard, C.; Quirion, R. 2015. Neuroprotective action of resveratrol. *Biochim. Biophys. Acta Mol. Basis Dis.* 1852, 1195-1201.
- Bayomi, M.A.; Abanumay, K.A.; Al-Angary, A.A. 2002. Effect of inclusion complexation with cyclodextrins on photostability of nifedipine in solid state. *Int. J. Pharm.* 243, 107-117.
- Belchí-Navarro, S.; Almagro, L.; Lijavetzky, D.; Bru, R.; Pedreño, M.A. 2012. Enhanced extracellular production of trans-resveratrol in *Vitis vinifera* suspension cultured cells by using cyclodextrins and methyljasmonate. *Plant Cell Rep.* 31, 81-89.
- Belchí-Navarro, S.; Almagro, L.; Sabater-Jara, A.B.; Fernández-Pérez, F.; Bru-Martinez, R.; Pedreño, M.A. 2013. Early signaling events in grapevine cells elicited with cyclodextrins and methyl jasmonate. *Plant Physiol. Biochem.* 62, 107-110.
- Berta, G.N.; Salamone, P.; Sprio, A.E.; Di Scipio, F.; Marinos, L.M.; Sapino, S.; Carlotti, M.E.; Cavalli, R.; Di Carlo, F. 2010. Chemoprevention of 7,12-dimethylbenz[a]anthracene (DMBA)-induced oral carcinogenesis in hamster cheek pouch by topical application of resveratrol complexed with 2-hydroxypropyl- $\beta$ -cyclodextrin. *Oral Oncol.* 46, 42-48.
- Bertacche, V.; Lorenzi, N.; Nava, D.; Pini, E.; Sinico, C. 2006. Host-guest interaction study of resveratrol with natural and modified cyclodextrins. *J. Incl. Phenom. Macrocycl. Chem.* 55, 279-287.
- Boedtkjer, E.; Pedersen, S.F. 2020. The acidic tumor microenvironment as a driver of cancer. *Annu. Rev. Physiology* 83, 103-126.
- Böhmdorfer, M.; Szakmary, A.; Schiestl, R.; Vaquero, J.; Riha, J.; Brenner, S.; Thalhammer, T.; Szekeres, T.; Jäger, W. 2017. Involvement of UDP-glucuronosyltransferases and sulfotransferases in the excretion and tissue distribution of resveratrol in mice. *Nutrients* 9, 1347.
- Bonnet, V.; Gervaise, C.; Djedaïni-Pilard, F.; Furlan, A.; Sarazin, C. 2015. Cyclodextrin nanoassemblies: a promising tool for drug delivery. *Drug Discov. Today* 20, 1120-1126.
- Boo, Y. C. 2019. Human skin lightening efficacy of resveratrol and its analogs: From *in vitro* studies to cosmetic applications. *Antioxidants* 8, 322.
- Boocock, D.J.; Faust, G.E.; Patel, K.R.; Schinas, A.M.; Brown, V.A.; Ducharme, M.P.; Booth, T.D.; Crowell, J.A.; Perloff, M.; Gescher, J.A.; Steward, W.P.; Brenner, D.E. 2007. Phase I dose escalation pharmacokinetic study in healthy volunteers of resveratrol, a potential cancer chemopreventive agent. *Cancer Epidemiol. Biomark. Prev.* 16, 1246-1252.
- Breuil, A.C.; Adrian, M.; Pirio, N.; Meunier, P.; Bessis, R.; Jeandet, P. 1998. Metabolism of stilbene phytoalexins by *Botrytis cinerea*: Characterization of a resveratrol dehydrodimer. *Tetrahedron Lett.* 39, 537-540.
- Brown, V.A.; Patel, K.R.; Viskaduraki, M.; Crowell, J.A.; Perloff, M.; Booth, T.D.; Vasilinin, G.; Sen, A.; Schinas, A.M.; Piccirilli, G.; Brown, K.; Steward, W.P.; Gescher, A.J.; Brenner, D.E. 2010. Repeat dose study of the cancer chemopreventive agent resveratrol in healthy volunteers: Safety, pharmacokinetics, and effect on the insulin-like growth factor axis. *Cancer Res.* 70, 9003-9011.

- Bru, M.R.; Pedreno, M.A. 2003. Method for the production of resveratrol in cell cultures. US patent WO/2003/062406.
- Bru, R.; Selles, S.; Casado-Vela, J.; Belchi-Navarro, S.; Pedreño, M.A. 2006. Modified cyclodextrins are chemically defined glucan inducers of defence responses in grapevine cell cultures. *J. Agric. Food Chem.* 54, 65-71.
- Cai, H.; Scott, E.; Kholghi, A.; Andreadi, C.; Rufini, A.; Karmokar, A.; Britton, R.G.; Horner-glistler, E.; Greaves, P.; Jawad, D.; James, M.; Howells, L.; Ognibene, T.; Malfatti, M.; Goldring, C.; Kitteringham, N.; Walsh, J.; Viskaduraki, M.; West, K.; Miller, A.; Hemingway, D.; Steward, W.P.; Gescher, A.J.; Brown, K. 2015. Cancer chemoprevention: Evidence of a nonlinear dose response for the protective effects of resveratrol in humans and mice. *Sci. Transl. Med.* 7, 298ra117.
- Caruso, F.; Mendoza, L.; Castro, P.; Cotoras, M.; Aguirre, M.; Matsuhira, B.; Isaacs, M.; Rossi, M.; Viglianti, A.; Antonioletti, R. 2011. Antifungal activity of resveratrol against *Botrytis cinerea* is improved using 2-furyl derivatives. *PLoS One* 6, e25421.
- Cervone, F.; Hahn, M.G.; De Lorenzo, G.; Darvill, A.; Albersheim, P. 1989. Host-pathogen interactions XXXIII. A plant protein converts a fungal pathogenesis factor into an elicitor of plant defense responses. *Plant Physiol.* 90, 542-548.
- Cheng, J.G.; Tian, B.R.; Huang, Q.; Ge, H.R.; Wang, Z.Z. 2018. Resveratrol functionalized carboxymethyl- $\beta$ -cyclodextrin: Synthesis, characterization and photostability. *J. Chem.* 2018, 6789076.
- Cheng, C.; Wei, H.; Shi, B.X.; Cheng, H.; Li, C.; Gu, Z.W.; Cheng, S.X.; Zhang, X.Z.; Zhuo, R.X. 2008. Biotinylated thermoresponsive micelle self-assembled from double-hydrophilic block copolymer for drug delivery and tumor target. *Biomaterials* 29, 497-505.
- Choung, W.J.; Hwang, S.H.; Ko, D.S.; Kim, S.B.; Kim, S.H.; Jeon, S.H.; Choi, H.D.; Lim, S.S.; Shim, J.H. 2017. Enzymatic synthesis of a novel kaempferol-3-O- $\beta$ -D-glucopyranosyl-(1 $\rightarrow$ 4)-O- $\alpha$ -D-glucopyranoside using cyclodextrin glucanotransferase and its inhibitory effects on aldose reductase, inflammation, and oxidative stress. *J. Agric. Food Chem.* 65, 2760-2767.
- Ciesielska, A.; Ciesielski, W.; Girek, B.; Girek, T.; Koziel, K.; Kulawik, D.; Lagiewka, J. 2020. Biomedical application of cyclodextrin polymers cross-linked via dianhydrides of carboxylic acids. *Appl. Sci.* 10, 8463.
- Connors, K.A. 1997. The stability of cyclodextrin complexes in solution. *Chem. Rev.* 97, 1325-1358.
- Costa, A.; Bonner, M.Y.; Arbiser, J.L. 2016. Use of polyphenolic compounds in dermatologic oncology. *Am. J. Clin. Dermatol.* 17, 369-385.
- Creasy, L.L.; Coffee, M. 1988. Phytoalexin production potential of grape berries. *J. Am. Soc. Hortic. Sci.* 113, 230-234.
- Crini, G. 2014. Review: A history of cyclodextrins. *Chem. Rev.* 114, 10940-10975.
- Daga, M.; Ullio, C.; Argenziano, M.; Dianzani, C.; Cavalli, R.; Trotta, F.; Ferretti, C.; Zara, G.P.; Gigliotti, C.L.; Ciamporcerro, E.S.; Pettazzoni, P.; Corti, D.; Pizzimenti, S.; Barrera, G. 2016. GSH-targeted nanospheres increase doxorubicin-induced toxicity "in vitro" and "in vivo" in cancer cells with high antioxidant defenses. *Free Radic. Biol. Med.* 97, 24-37.
- Das, S.; Lin, H.S.; Ho, P.C.; Ng, K.Y. 2008. The impact of aqueous solubility and dose on the pharmacokinetic profiles of resveratrol. *Pharm. Res.* 25, 2593-2600.

- De Sa Coutinho, D.; Pacheco, M.T.; Frozza, R.L.; Bernardi, A. 2018. Anti-inflammatory effects of resveratrol: mechanistic insights. *Int. J. Mol. Sci.* 19, 1812.
- De Winter, K.; Verlinden, K.; Kren, V.; Weignerova, L.; Soetaert, W.; Desmet, T. 2013. Ionic liquids as cosolvents for glycosylation by sucrose phosphorylase: balancing acceptor solubility and enzyme stability. *Green Chem.* 15, 1949-1955.
- Dhakar, N.K.; Matencio, A.; Caldera, F.; Argenziano, M.; Cavalli, R.; Dianzani, C.; Zanetti, M.; Lopez-Nicolas, J.M.; Trotta, F. 2019. Comparative evaluation of solubility, cytotoxicity and photostability studies of resveratrol and oxyresveratrol loaded nanosponges. *Pharmaceutics* 11, 545.
- Din, F.U.; Aman, W.; Ullah, I.; Qureshi, O.S.; Mustapha, O.; Shafique, S.; Zeb, A. 2017. Effective use of nanocarriers as drug delivery systems for the treatment of selected tumors. *Int. J. Nanomed.* 12, 7291-7309.
- Docherty, J.J.; Smith, J.S.; Fu, M.M.; Stoner, T.; Booth, T. 2004. Effect of topically applied resveratrol on cutaneous herpes simplex virus infections in hairless mice. *Antivir. Res.* 61, 19-26.
- Donnez, D.; Jeandet, P.; Clément, C.; Courot, E. 2009. Bioproduction of resveratrol and stilbene derivatives by plant cells and microorganisms. *Trends Biotechnol.* 27, 706-713.
- Donnez, D.; Kim, K.H.; Antoine, S.; Conreux, A.; De Luca, V.; Jeandet, P.; Clément, C.; Courot, E. 2011. Bioproduction of resveratrol and viniferins by an elicited grapevine cell culture in a 2L stirred bioreactor. *Process Biochem.* 46, 1056-1062.
- Dora, C.P.; Trotta, F.; Kushwah, V.; Devasari, N.; Singh, C.; Suresh, S.; Jain, S. 2016. Potential of erlotinib cyclodextrin nanosponge complex to enhance solubility, dissolution rate, *in vitro* cytotoxicity and oral bioavailability. *Carbohydr. Polym.* 137, 339-349.
- Dos Santos Lima, B.; Shanmugam, S.; de Souza Siqueira Quintans, J.; Quintans Jr, L.J.; De Souza Araujo, A.A. 2019. Inclusion complexes with cyclodextrins enhances the bioavailability of flavonoid compounds: A systematic review. *Phytochem. Rev.* 18, 1337-1359.
- Draijer, R.; Van Dorsten, F.A.; Zebregs, Y.E.; Hollebrands, B.; Peters, S.; Duchateau, G.S.; Grün, C.H. 2016. Impact of proteins on the uptake, distribution, and excretion of phenolics in the human body. *Nutrients* 8, 814.
- Duan, D.; Fischer, S.; Merz, P.; Bogs, J.; Riemann, M.; Nick, P. 2016. An ancestral allele of grapevine transcription factor MYB14 promotes plant defence. *J. Exp. Bot.* 67, 1795-1804.
- Duarte, A.; Martinho, A.; Luis, A.; Figueiras, A.; Oleastro, M.; Domingues, F.C.; Silva, F. 2015. Resveratrol encapsulation with methyl- $\beta$ -cyclodextrin for antibacterial and antioxidant delivery applications. *LWT-Food Sci. Technol.* 63, 1254-1260.
- Eibl, R.; Eibl, D. 2008. Design of bioreactors suitable for plant cell and tissue cultures. *Phytochem. Rev.* 7, 593-598.
- Fang, L.; Yang, T.; Medina-Bolivar, F. 2020. Production of prenylated stilbenoids in hairy root cultures of peanut (*Arachis hypogaea*) and its wild relatives *A. ipaensis* and *A. duranensis* via an optimized elicitation procedure. *Molecules* 25, 509.
- Ferri, M.; Dipalo, S.C.; Bagni, N.; Tassoni, A. 2011. Chitosan elicits mono-glucosylated stilbene production and release in fed-batch bioreactor cultures of grape cells. *Food Chem.* 124, 1473-1479.

- Fumic, B.; Jablan, J.; Cincic, D.; Zovko Koncic, M.; Jug, M. 2018. Cyclodextrin encapsulation of daidzein and genistein by grinding: implication on the glycosaminoglycan accumulation in mucopolysaccharidosis type II and III fibroblasts. *J. Microencapsul.* 35, 1-12.
- Gabaston, J.; Cantos-Villar, E.; Biais, B.; Waffo-Teguo, P.; Renouf, E.; Corio-Costet, M.F.; Richard, T.; Mérillon, J.M. 2017. Stilbenes from *Vitis vinifera* L. wastes: A sustainable tool for controlling *Plasmopara viticola*. *J. Agric. Food Chem.* 65, 2711-2718.
- Gidwani, B.; Vyas, A. A 2015. comprehensive review on cyclodextrin-based carriers for delivery of chemotherapeutic cytotoxic anticancer drugs. *BioMed Res. Int.* 2015, 198268.
- Gigliotti, C.L.; Minelli, R.; Cavalli, R.; Occhipinti, S.; Barrera G.; Pizzimenti, S.; Cappellano, G.; Boggio, E.; Conti, L.; Fantozzi, R.; Giovanelli, M.; Trotta, F.; Dianzani, U.; Dianzoni, C. 2016. *In vitro* and *in vivo* therapeutic evaluation of camptothecin-encapsulated  $\beta$ -cyclodextrin nanosponges in prostate cancer. *J. Biomed. Nanotechnol.* 12, 114-127.
- Goldberg, D.M.; Yann, J.; Soleas, G.J. 2003. Absorption of three-wine-related polyphenols in three different matrices by healthy subjects. *Clin Biochem.* 36, 79-87.
- Gonzalez-Alfonso, J.L.; Rodrigo-Frutos, D.; Belmonte-Reche, E.; Penalver, P.; Poveda, A.; Jimenez-Barbero, J.; Ballesteros, A.O.; Hirose, Y.; Polaina, J.; Morales J.C.; Fernandez-Lobato, M.; Plou, F.J. 2018. Enzymatic synthesis of a novel pterostilbene  $\alpha$ -glucoside by the combination of cyclodextrin glucanotransferase and amyloglucosidase. *Molecules* 23, 1271.
- Gratieri, T.; Pinho, L.A.G.; Almeida Oliveira, M.; Sa-Barreto, L.L.; Marreto, R.M., Silva, I.C.; Gelfuso, G.M.; de Souza Siqueira Quintans, J.; Quintans Jr, L.J.; Cunha-Filho, M. 2020. Hydroxypropyl- $\beta$ -CD-complexed naringenin by solvent change precipitation for improving anti-inflammatory effect *in vivo*. *Carbohydr. Polym.* 231, 115769.
- Haley, R.M.; Zuckerman, S.T.; Dakhllallah, H.; Capadona, J.R.; von Recum, H.A.; Ereifej, E.S. 2020. Resveratrol delivery from implanted cyclodextrin polymers sustained antioxidant effect on implanted neural probes. *Int. J. Mol. Sci.* 21, 3579.
- Han, R.; Ge, B.; Jiang, M.; Xu, G.; Dong, J.; Ni, Y. 2017. High production of genistein diglucoside derivative using cyclodextrin glycosyltransferase from *Paenibacillus macerans*. *J. Ind. Microbiol. Biotechnol.* 44, 1343-1354.
- He, J.; Guo, F.; Lin, L.; Chen, H.; Chen, J.; Cheng, Y.; Zheng, Z.P. 2019. Investigating the oxyresveratrol  $\beta$ -cyclodextrin and 2-hydroxypropyl- $\beta$ -cyclodextrin complexes: The effects on oxyresveratrol solution, stability, and antibrowning activity on fresh grape juice. *LWT-Food Sci. Technol.* 100, 263-270.
- Hidalgo, D.; Martínez-Márquez, A.; Cusidó, R.; Bru-Martínez, R.; Palazón, J.; Corchete, P. 2017. *Silybum marianum* cell cultures stably transformed with *Vitis vinifera* stilbene synthase accumulate t-resveratrol in the extracellular medium after elicitation with methyl jasmonate or methylated  $\beta$ -cyclodextrins. *Eng. Life Sci.* 17, 686-694.
- Höll, J.; Vannozzi, A.; Czemplin, S.; D'Onofrio, C.; Walker, A.R.; Rausch, T.; Lucchin, M.; Boss, P.K.; Dry, I.B.; Bogs, J. 2013. The R2R3-MYB transcription factors MYB14 and MYB15 regulate stilbene biosynthesis in *Vitis vinifera*. *Plant Cell* 25, 4135-4149.
- Houillé, B.; Papon, N.; Boudesocque, L.; Bourdeaud, E.; Besseau, S.; Courdavault, V.; Enguehard-Gueiffier, C.; Delanoue, G.; Guérin, L.; Bouchara, J.P.; Clastre, M.; Giglioli-Guivarc'h, N.; Guillard, J.; Lanoue, A.

2014. Antifungal activity of resveratrol derivatives against *Candida* species. *J. Nat. Prod.* 77, 1658-1662.
- Howells, L.M.; Berry, D.P.; Elliott, P.J.; Jacobson, E.W.; Hoffmann, E.; Hegarty, B.; Brown, K.; Steward, W.P.; Gescher, A.J. 2011. Phase I randomized, double-blind pilot study of micronized resveratrol (SRT501) in patients with hepatic metastases—safety, pharmacokinetics, and pharmacodynamics. *Cancer Prev. Res.* 4, 1419-1425.
- Ikuta, D.; Hirata, Y.; Wakamori, S.; Shimada, H.; Tomabechi, Y.; Kawasaki, Y.; Ikeuchi, K.; Hagimori, T.; Matsumoto, S.; Yamada, H. 2019. Conformationally supplemented glucose monomers enable synthesis of the smallest cyclodextrins. *Science* 364, 674-677.
- Ingham, J. L. 1976. 3,5,4'-trihydroxystilbene as a phytoalexin from groundnuts (*Arachis hypogaea*). *Phytochemistry* 15, 1791-1793.
- Intagliata, S.; Modica, M.N.; Santagati, L.; Montenegro, L. 2019. Strategies to improve resveratrol systemic and topical bioavailability: An update. *Antioxidants* 8, 244.
- Ioannou, I.; Barboza, E.; Willig, G.; Marié, T.; Teixeira, A.; Darne, P.; Renault, J.H.; Allais, F. 2021. Implementation of an enzyme membrane reactor to intensify the  $\alpha$ -O-glycosylation of resveratrol using cyclodextrins. *Pharmaceuticals* 14, 319.
- Ito, T.; Tanaka, T.; Inuma, M.; Nakaya, K.; Takahashi, Y.; Sawa, R.; Murata, J.; Darnaedi, D. 2004. Three new stilbene oligomers from the stem bark of *Vatica pauciflora*. *J. Nat. Prod.* 67, 932-937.
- Jambhekar, S.S.; Breen, P. 2016. Cyclodextrins in pharmaceutical formulations II: solubilization, binding constant, and complexation efficiency. *Drug Discov. Today* 21, 363-368.
- Jang, M.; Cai, L.; Udeani, G.O.; Slowing, K.V.; Thomas, C.F.; Beecher, C.W.W.; Fong, H.H.S.; Farnsworth, N.R.; Kinghorn, A.D.; Metha, R.G.; Moon, R.C.; Pezzuto, J.M. 1997. Cancer chemopreventive activity of resveratrol, a natural product derived from grapes. *Science* 275, 218-220.
- Jeandet, P.; Bessis, R.; Gautheron, B. 1991. The Production of resveratrol (3,5,4'-trihydroxystilbene) by grape berries in different developmental stages. *Am. J. Enol. Vitic.* 42, 41-46.
- Jeandet, P.; Breuil, A.C.; Adrian, M.; Weston, L.A.; Debord, S.; Meunier, P.; Maume, G.; Bessis, R. 1997. HPLC analysis of grapevine phytoalexins coupling photodiode array detection and fluorometry. *Anal. Chem.* 69, 5172-5177.
- Jeandet, P.; Clément, C.; Cordelier, S. 2019. Regulation of resveratrol biosynthesis in grapevine: new approaches for disease resistance? *J. Exp. Bot.* 70, 375-378.
- Jeandet, P.; Clément, C.; Courot, E. 2014. Use of plant cell suspensions as a basis for large-scale production of resveratrol in bioreactors. *Eng. Life Sci.* 14, 622-632.
- Jeandet, P.; Clément, C.; Tisserant, L.P.; Crouzet, J.; Courot, E. 2016. Use of grapevine cell cultures for the production of phytoalexins of cosmetic interest. *C.R. Chimie* 19, 1062-1070.
- Jeandet, P.; Delaunois, B.; Conreux, A.; Donnez, D.; Nuzzo, V.; Cordelier, S.; Clément, C.; Courot, E. 2010. Biosynthesis, metabolism, molecular engineering and biological functions of stilbene phytoalexins in plants. *BioFactors* 36, 331-341. 933.
- Jeandet, P.; Douillet, A.C.; Weston, L.A.; Debord, S.; Sbaghi, M.; Bessis, R.; Adrian, M. 2002. Phytoalexins from the Vitaceae: biosynthesis, phytoalexin gene expression in transgenic plants, antifungal activity, and metabolism. *J. Agric. Food Chem.* 50, 2731-2741.



- Jeandet, P.; Sobarzo-Sánchez, E.; Sanches Silva, A.; Clément, C.; Nabavi, S.F.; Battino, M.; Rasekhian, M.; Belwal, T.; Habtemariam, S.; Koffas, M.; Nabavi, S.M. 2020. Whole-cell biocatalytic, enzymatic and green chemistry methods for the production of resveratrol and its derivatives. *Biotechnol. Adv.* 38, 107461.
- Jeandet, P.; Vannozzi, A.; Sobarzo-Sanchez, E.; Uddin, M.S.; Bru, R.; Martinez-Marquez, A.; Clément, C.; Cordelier, S.; Manayi, A.; Nabavi, S.F.; Rasekhian, M.; Batiha, G.E.S.; Khan, H.; Morkunas, I.; Belwal, T.; Jiang, J.; Koffas, M.; Nabavi, S.M. 2021. Phytostilbenes as agrochemicals: biosynthesis, bioactivity, metabolic engineering and biotechnology. *Nat. Prod. Rep.*, 28, 1282-1329.
- Jiang, J.; Xi, H.; Dai, Z.; Lecourieux, F.; Yuan, L.; Liu, X.; Patra, B.; Wei, Y.; Li, S.; Wang, L. 2019. VvWRKY8 negatively regulates VvSTS through direct interaction with VvMYB14 to balance resveratrol biosynthesis in grapevine. *J. Exp. Bot.* 70, 715-729.
- Jones, T.J.; Cagno, V.; Janecek, M.; Ortiz, D.; Gasilova, N.; Piret, J.; Gasbarri, M.; Constant, D.A.; Han, Y.; Vukovic, L.; Kral, P.; Kaiser, L.; Huang, S.; Constant, S.; Kirkegaard, K.; Boivin, G.; Stellacci, F.; Tapparell, C. 2020. Modified cyclodextrins as broad-spectrum antivirals. *Sci. Adv.* 6, eaax9318.
- Kanaya, A.; Takashima, Y.; Harada, A. 2011. Double-threathed dimer and supramolecular oligomer formed by stilbene modified cyclodextrin: Effect of acyl migration and photostimuli. *J. Org. Chem.* 76, 492-499.
- Kapetanovic, I.M.; Muzzio, M.; Huang, Z.H.; Thompson, T.N.; McCormick, D.L. 2011. Pharmacokinetics, oral bioavailability, and metabolic profile of resveratrol and its dimethylether analog, pterostilbene, in rats. *Cancer Chemother Pharm.* 68, 593-601.
- Kennedy, L.; Sandhu, J.K.; Harper, M.E.; Cuperlovic-Culf, M. 2020. Role of glutathione in cancer: from mechanisms to therapies. *Biomolecules* 10, 1429.
- Keylor, M.H.; Matsuura, B.S.; Griesser, M.; Chauvin, J.P.; Harding, R.A.; Kirillova, M.S.; Zhu, X.; Fischer, O.J.; Pratt, D.K.; Stephenson, C.R.J. 2016. Synthesis of resveratrol tetramers via a stereoconvergent radical equilibrium. *Science* 354, 1260-1265.
- Keylor, M.H.; Matsuura, B.S.; Stephenson, C.R.J. 2015. Chemistry and biology of resveratrol-derived natural products. *Chem. Rev.* 115, 8976-9027.
- Khummanee, N.; Rudeekulthamrong, P.; Kaulpiboon, J. 2019. Cyclodextrin glycosyltransferase-catalyzed synthesis of pinoresinol- $\alpha$ -D-glucoside having antioxidant and anti-inflammatory activities. *Appl. Biochem. Microbiol.* 55, 360-370.
- Kim, Y.J.; Matsunaga, Y.T. 2017. Thermo-responsive polymers and their application as smart biomaterials. *J. Mater. Chem. B* 5, 4307-4321.
- Kjaer, T.N.; Thorsen, K.; Jessen, N.; Stenderup, K.; Pedersen, S.B. 2015. Resveratrol ameliorates imiquimod-induced psoriasis-like skin inflammation in mice. *PLoS One* 10, e0126599.
- Kong, D.; Ren, C.; Ning, C.; Cheng, Y.; Cai, H.; Xing, H.; Zhang, Y.; Li, N.; Lu, Y.; Chen, X.; Zhao, D. 2020. Pulmonary administration of resveratrol/hydroxypropyl- $\beta$ -cyclodextrin inclusion complex: *in vivo* disposition and *in vitro* metabolic study. *J. Drug Deliv. Sci. Technol.* 60, 101995.
- Krisa, S.; Larronde, F.; Budzinski, H.; Decendit, A.; Deffieux, G.; Mérillon, J.M. 1999. Stilbene production by *Vitis vinifera* cell suspension cultures: methyl jasmonate induction and  $^{13}\text{C}$  biolabeling. *J. Nat. Prod.* 62, 1688-1690.

- Kumpugdee-Vollrath, M.; Ibold, Y.; Sriamornsak, P. 2012. Solid state characterization of trans resveratrol complexes with different cyclodextrins. *JAASP* 1, 125-136.
- Lacerda, D.; Ortiz, V.; Türck, P.; Campos-Carraro, C.; Zimmer, A.; Teixeira, R.; Bianchi, S.; Luz de Castro, A.L.; Schenkel, P.C.; Bello-Klein, A.; Bassani, V.L.; da Rosa Araujo, A.S. 2018. Stilbenoid pterostilbene complexed with cyclodextrin preserves left ventricular function after myocardial infarction in rats: possible involvement of thiol proteins and modulation of phosphorylated GSK-3 $\beta$ . *Free Rad. Res.* 52, 988-999.
- Lacerda, D.; Türck, P.; de Lima-Seolin, B.G.; Colombo, R.; Duarte Ortiz, V.; Poletto Bonetto, J.H.; Campos-Carraro, C.; Bianchi, S.E.; Bello-Klein, A.; Bassani, V.L.; da Rosa Araujo, A.S. 2017. Pterostilbene reduces oxidative stress, prevents hypertrophy and preserves systolic function of right ventricle in *cor pulmonale* model. *Br. J. Pharmacol.* 174, 3302-3314.
- Lambert, C.; Lemaire, J.; Auger, H.; Guilleret, A.; Reynaud, R.; Clément, C.; Courot, E.; Taidi, B. 2019. Optimize, modulate, and scale-up resveratrol and resveratrol dimers bioproduction in *Vitis labrusca* L. cell suspension from flasks to 20 l bioreactor. *Plants* 8, e567.
- Langcake, P.; Pryce, R.J. 1976. The production of resveratrol by *Vitis vinifera* and other members of the Vitaceae as a response to infection or injury. *Physiol. Plant Pathol.* 9, 77-86.
- Langcake, P.; Pryce, R.J. 1977. The production of resveratrol and the viniferins by grapevines in response to ultraviolet irradiation. *Phytochemistry* 16, 1193-1196.
- La Porte, C.; Voduc, N.; Zhang, G.; Seguin, I.; Tardiff, D.; Singhal, N.; Cameron, D.W. 2010. Steady-state pharmacokinetics and tolerability of trans-resveratrol 2000mg twice daily with food, quercetin and alcohol (ethanol) in healthy human subjects. *Clin. Pharmacokinet.* 49, 449-454.
- Lee, Y.S.; Woo, J.B.; Ryu, S.I.; Moon, S.R.; Han, N.S.; Lee, S.B. 2017. Glucosylation of flavonol and flavanones by *Bacillus* cyclodextrin glucosyltransferase to enhance their solubility and stability. *Food Chem.* 229, 75-83.
- Li, S.; Yuan, L.; Zhang, B.; Zhou, W.; Wang, X.; Bai, D. 2018. Photostability and antioxidant activity studies on the inclusion complexes of *trans*-polydatin with  $\beta$ -cyclodextrin and derivatives. *RSC Adv.* 8, 25941.
- Lijavetzky, D.; Almagro, L.; Belchí-Navarro, S.; Martínez-Zapater, J.M.; Bru, R.; Pedreño, M.A. 2008. Synergistic effect of methyljasmonate and cyclodextrin on stilbene biosynthesis pathway gene expression and resveratrol production in Monastrell grapevine cell cultures. *BMC Res. Notes* 1, e132.
- Lim, H.C.; Rasti, B.; Sulistyono, J.; Hamid, M. A. 2021. Comprehensive study on transglucosylation of CGTase from various sources. *Helyon* 7, e06305.
- Lim, Y.R.I.; Preshaw, P.M.; Lim, L.P.; Ong, M.M.A.; Lin, H.S.; Tan, K.S. 2020. Pterostilbene complexed with cyclodextrin exerts antimicrobial and anti-inflammatory effects. *Sci. Rep.* 10, 9072.
- Lin, J.T.; Du, J.K.; Yang, Y.Q.; Li, L.; Zhang, D.W.; Liang, C.L.; Wang, J.; Mei, J.; Wang, G.H. 2017. pH and redox dual stimulate-responsive nanocarriers based on hyaluronic acid coated mesoporous silica for targeted drug delivery. *Mater. Sci. Eng. C Mater. Biol. Appl.* 81, 478-484.
- Lin, M.H.; Hung, C.F.; Sung, H.C.; Yang, S.C.; Yu, H.P.; Fang, J.Y. 2011. The bioactivities of resveratrol and its naturally occurring derivatives on skin. *J. Food Drug Anal.* 29, 15-38.
- Lin, H.S.; Yue, B.D.; Ho, P.C. 2009. Determination of pterostilbene in rat plasma by a simple HPLC-UV method and its application in pre-clinical pharmacokinetic study. *Biomed. Chromatogr.* 23, 1308-1315.

- Lopez-Nicolas, J.M.; Rodriguez-Bonilla, P.; Garcia-Carmona, F. 2009a. Complexation of pinosylvin, an analogue of resveratrol with high antifungal and antimicrobial activity, by different types of cyclodextrins. *J. Agric. Food Chem.* 57, 10175-10180.
- Lopez-Nicolas, J.M.; Rodriguez-Bonilla, P.; Mendez-Carzola, L.; Garcia-Carmona, F. 2009b. Physicochemical study of the complexation of pterostilbene by natural and modified cyclodextrins. *J. Agric. Food Chem.* 57, 5294-5300.
- Lu, Z.; Chen, R.; Fu, R.; Xiong, J.; Hu, Y. 2012. Cytotoxicity and inhibition of lipid peroxidation activity of resveratrol/cyclodextrin inclusion complexes. *J. Incl. Phenom. Macrocycl. Chem.* 73, 313-320.
- Lu, Z.; Cheng, B.; Hu, Y.; Zhang, Y.; Zou, G. 2009. Complexation of resveratrol with cyclodextrins: Solubility and antioxidant activity. *Food Chem.* 113, 17-20.
- Lucas-Abellan, C.; Fortea, M.I.; Gabaldon, J.A.; Nunez-Delicado, E. 2008. Complexation of resveratrol by native and modified cyclodextrins: Determination of complexation constant by enzymatic, solubility and fluorimetric assays. *Food Chem.* 111, 262-267.
- Lucas-Abellan, C.; Fortea, M.I.; Lopez-Nicolas, J.M.; Nunez-Delicado, E. 2007. Cyclodextrins as resveratrol carrier system. *Food Chem.* 104, 39-44 (2007).
- Manchun, S.; Dass, C.R.; Sriamornsak, P. 2012. Targeted therapy for cancer using pH-responsive nanocarrier systems. *Life Sci.* 90, 381-387.
- Manor, P.; Saenger, W. 1972. Water molecule in hydrophobic surroundings: structure of  $\alpha$ -cyclodextrin-hexahydrate ( $C_6H_{10}O_5$ )<sub>6</sub>·6H<sub>2</sub>O. *Nature* 237, 392-393.
- Manta, K.; Papakyriakopoulou, P.; Chountoules, M.; Diamantis, D.A.; Spaneas, D.; Valaki, V.; Naziris, N.; Chatziathanasiadou, M.V.; Andreadelis, I.; Moschovou, K.; Athanasiadou, I.; Dallas, P.; Rekkas, D.M.; Demetzos, C.; Colombo, G.; Banella, S.; Javornik, U.; Plavec, J.; Mavromoustakos, T.; Tzakos, A.G.; Valsami, G. 2020. Preparation and biophysical characterization of quercetin inclusion complexes with  $\beta$ -cyclodextrin derivatives to be formulated as possible nose-to-brain quercetin delivery systems. *Mol. Pharmaceutics* 17, 4241-4255.
- Marié, T.; Willig, G.; Teixeira, A.R.S.; Barboza, E.G.; Kotland, A.; Gratia, A.; Courot, E.; Hubert, J.; Renault, J.H.; Allais, F. 2018. Enzymatic synthesis of resveratrol  $\alpha$ -glycosides from  $\beta$ -cyclodextrin-resveratrol complex in water. *ACS Sustainable Chem. Eng.* 6, 5370-5380.
- Martínez-Esteso, M.J.; Sellés-Marchart, S.; Vera-Urbina, J.C.; Pedreño, M.A.; Bru-Martínez, R. 2011. DIGE analysis of proteome changes accompanying large resveratrol production by grapevine (*Vitis vinifera* cv. Gamay) cell cultures in response to methyl- $\beta$ -cyclodextrin and methyl jasmonate elicitors. *J. Proteomics* 74, 1421-1436.
- Martínez-Márquez, A.; Martínez-Esteso, M.J.; Vilella-Antón, M.T.; Sellés-Marchart, S.; Morante-Carriel, J.A.; Hurtado, E.; Palazon, J.; Bru-Martínez, R. 2017. A tau class glutathione-S-transferase is involved in trans-resveratrol transport out of grapevine cells. *Front. Plant Sci.* 8, e1457.
- Martínez-Márquez, A.; Morante-Carriel, J.A.; Palazon, J.; Bru-Martínez, R. 2018. *Rosa hybrida* orcinol O-methyl transferase-mediated production of pterostilbene in metabolically engineered grapevine cell cultures. *N. Biotechnol.* 42, 62-70.
- Martínez-Márquez, A.; Morante-Carriel, J.A.; Ramírez-Estrada, K.; Cusidó, R.M.; Palazon, J.; Bru-Martínez, R. 2016. Production of highly bioactive resveratrol analogues pterostilbene and piceatannol in metabolically engineered grapevine cell cultures. *Plant Biotechnol. J.* 14, 1813-1825.

- Matencio, A.; Dhakar, N.K.; Bessone, F.; Musso, G.; Cavalli, R.; Dianzani, C.; Garcia-Carmona, F.; Lopez-Nicolas, J.M.; Trotta, F. 2020. Study of oxyresveratrol complexes with insoluble cyclodextrin based nanosponges: Developing a novel way to obtain their complexation constants and application in an anticancer study. *Carbohydr. Polym.* 231, 115763.
- Matencio, A.; Garcia-Carmona, F.; Lopez-Nicolas, J.M. 2016. Encapsulation of piceatannol, a naturally occurring hydroxylated analogue of resveratrol, by natural and modified cyclodextrins. *Food Funct.* 7, 2367.
- Matencio, A.; Garcia-Carmona, F.; Lopez-Nicolas, J.M. 2017. The inclusion complex of oxyresveratrol in modified cyclodextrins: A Thermodynamic, structural, physicochemical, fluorescent and computational study. *Food Chem.* 232, 117-184.
- Mathew, S.; Adlercreutz, P. 2013. Regioselective glycosylation of hydroquinone to  $\alpha$ -arbutin by cyclodextrin glucanotransferase from *Thermoanaerobacter* sp. *Biochem. Eng. J.* 79, 187-193.
- Mathew, S.; Hedström, M.; Adlercreutz, P. 2012. Enzymatic synthesis of piceid glycosides by cyclodextrin glucanotransferase. *Process Biochem.* 47, 528-532.
- Medina-Bolivar, F.; Condori, J.; Rimando, A.M.; Hubstenberger, J.; Shelton, K.; O'Keefe, S.F.; Bennett, S.; Dolan, M.C. 2007. Production and secretion of resveratrol in hairy root cultures of peanut. *Phytochemistry* 68, 1992-2003.
- Mendes, C.; Meirelles, G.C.; Barp, C.G.; Assreuy, J.; Silva, M.A.S.; Ponchel, G. 2018. Cyclodextrin based nanosponge of norfloxacin: Intestinal permeation enhancement and improved antibacterial activity? *Carbohydr. Polym.* 195, 586-592.
- Mennini, N.; Cirri, M.; Maestrelli, F.; Mura, P. 2016. Comparison of liposomal and NLC (nanostructured lipid carrier) formulations for improving the transdermal delivery of oxaprozin: Effect of cyclodextrin complexation. *Int. J. Pharm.* 515, 684-691.
- Miksits, M.; Maier-Salamon, A.; Aust, S.; Thalhammer, T.; Reznicek, G.; Kunert, O.; Haslinger, E.; Szekeres, T.; Jaeger, W. 2005. Sulfation of resveratrol in human liver: Evidence of a major role for the sulfotransferases SULT1A1 and SULT1E1. *Xenobiotica* 35, 1101-1119.
- Mitsuda, N.; Iwase, A.; Yamamoto, H.; Yoshida, M.; Seki, M.; Shinozaki, K.; Ohme-Takagi, M. 2007. NAC transcription factors, NST1 and NST3, are key regulators of the formation of secondary walls in woody tissues of *Arabidopsis*. *Plant Cell* 19, 270-280.
- Morales, M.; Bru, R.; García-Carmona, F.; Ros-Barceló, A.; Pedreño, M.A. 1998. Effect of dimethyl- $\beta$ -cyclodextrins on resveratrol metabolism in Gamay grapevine cell cultures before and after inoculation with *Xylophilus ampelinus*. *Plant Cell Tiss. Org. Cult.* 53, 179-187.
- Nabavi, S.; Samec, D.; Tomczyk, M.; Milella, L.; Russo, D.; Habtemariam, S.; Suntar, I.; Rastrelli, L.; Daglia, M.; Xiao, J.; Giampieri, F.; Battino, M.; Sobarzo-Sánchez, E.; Nabavi, S.F.; Yousefi, B.; Jeandet, P.; Xu, S.; Shirooie, S. 2020. Flavonoid biosynthetic pathways in plants: versatile targets for metabolic engineering. *Biotechnol. Adv.* 39, 107461.
- Nivelle, L.; Hubert, J.; Courot, E.; Jeandet, P.; Aziz, A.; Nuzillard, J.M.; Renault, J.H.; Clément, C.; Martiny, L.; Delmas, D.; Tarpin, M. 2017. Anti-cancer activity of resveratrol and derivatives produced by grapevine cell suspensions in a 14 L stirred bioreactor. *Molecules* 22, 474.

- Nonomura, S.; Kanagawa, H.; Makimoto, A. 1963. Chemical constituents of polygonaceous plants. I. Studies on the components of Ko-jo-kon (*Polygonum cuspidatum* Sieb Et Zucc.). *Yakugaku Zasshi* 83, 988-990.
- Nopo-Olazabal, C.; Hubstenberger, J.; Nopo-Olazabal, L.; Medina-Bolivar, F. 2013. Antioxidant activity of selected stilbenoids and their bioproduction in hairy root cultures of Muscadine grape (*Vitis rotundifolia* Michx.). *J. Agric. Food Chem.* 61, 11744-11758.
- Novotny, J.A.; Chen, T.Y.; Terekhov, A.I.; Gebauer, S.K.; Baer, D.J.; Ho, L.; Pasinetti, G.M.; Ferruzzi, M.G. 2017. The effect of obesity and repeated exposure on pharmacokinetic response to grape polyphenols in humans. *Mol. Nutr. Food Res.* 61, 1700043.
- Oliva, E.; Mathiron, D.; Bertaut, E.; Landy, D.; Cailleu, D.; Pilard, S.; Clément, C.; Courot, E.; Bonnet, V.; Djedaini-Pilard, F. 2018. Physico-chemical studies of resveratrol, methyl-jasmonate and cyclodextrins interactions : an approach to resveratrol bioproduction optimization. *RSC Adv.* 8, 1528-1538.
- Osmond, G.W.; Augustine, C.K.; Zipfel, P.A.; Padussis, J.; Tyler, D.S. 2012. Enhancing melanoma treatment with resveratrol. *J. Surg. Res.* 172, 109-115.
- Paczkowska, M.; Mizera, M.; Piotrowska, H.; Szymanowska-Powalowska, D.; Lewandowska, K.; Goscianska, J.; Pietrzak, R.; Bednarski, W.; Majka, Z.; Cielecka-Piontek, J. 2015. Complex of rutin with  $\beta$ -cyclodextrin as potential delivery system. *PLoS ONE* 10, e0120858.
- Palminteri, M.; Dhakar, N.K.; Ferraresi, A.; Caldera, F.; Vidoni, C.; Trotta, F.; Isidoro, C. 2021. Cyclodextrin nanosponge for the GSH-mediated delivery of resveratrol in human cancer cells. *Nanotheranostics* 5, 197-212.
- Pezzuto, J.M. 2011. The phenomenon of resveratrol: redefining the virtues of promiscuity. *Ann. NY Acad. Sci.* 1215, 123-130.
- Pinho, E.; Grootveld, M.; Soares, G.; Henriques, M. 2014. Cyclodextrins as encapsulation agents for plant bioactive compounds. *Carbohydr. Polym.* 101, 121-135.
- Poinssot, B.; Vandelle, E.; Bentéjac, M.; Adrian, M.; Levis, C.; Brygoo, Y.; Garin, J.; Sicilia, F.; Coutos-Thévenot, P.; Pugin, A. 2003. The endopolygalacturonase 1 from *Botrytis cinerea* activates grapevine defense reactions unrelated to its enzymatic activity. *Mol. Plant Microbe Interact.* 16, 553-564.
- Prysyazhna, O.; Wolhuter, K.; Switzer, C.; Santos, C.; Yang, X.; Lynham, S.; Shah, A.M.; Eaton, P.; Burgoyne, J.R. 2019. Blood pressure-lowering by the antioxidant resveratrol is counter-intuitively mediated by oxidation of cGMP-dependent protein kinase. *Circulation* 140, 126-137.
- Pushpalatha, R.; Selvamuthukumar, S.; Kilimozhi, D. 2018. Carbonyl and carboxylate crosslinked cyclodextrin as a nanocarrier for resveratrol: *in silico*, *in vitro* and *in vivo* evaluation. *J. Incl. Phenom. Macrocycl. Chem.* 92, 261-272.
- Pushpalatha, R.; Selvamuthukumar, S.; Kilimozhi, D. 2019. Cyclodextrin nanosponge based hydrogel for the transdermal co-delivery of curcumin and resveratrol: Development, optimization, *in vitro* and *ex vivo* evaluation. *J. Drug Deliv. Sci. Technol.* 52, 55-64.
- Qian, Y.; Lynch, J.H.; Guo, L.; Rhodes, D.; Morgan, J.A.; Dudareva, N. 2019. Completion of the cytosolic post-chorismate phenylalanine biosynthetic pathway in plants. *Nat. Comm.* 10, 15.
- Rafati, N.; Zarrabi, A.; Caldera, F.; Trotta, F.; Ghias, N. 2019. Pyromellitic dianhydride crosslinked cyclodextrin nanosponges for curcumin-controlled release: formulation, physicochemical characterization and cytotoxicity investigations. *J. Microencapsul.* 36, 715-727.

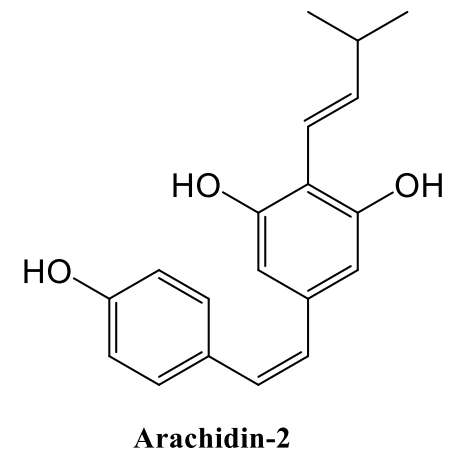
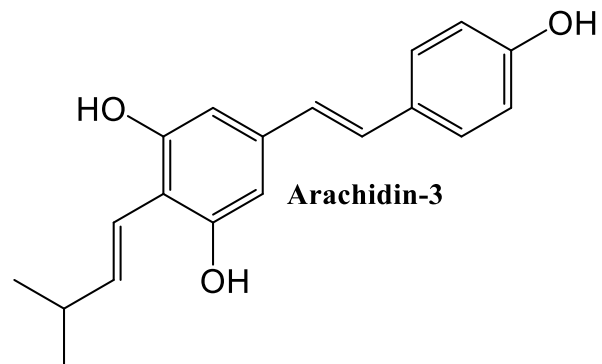
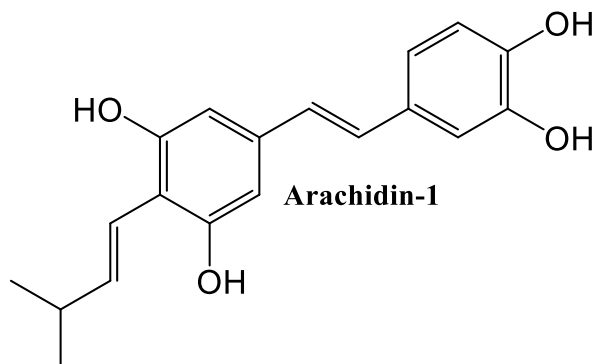
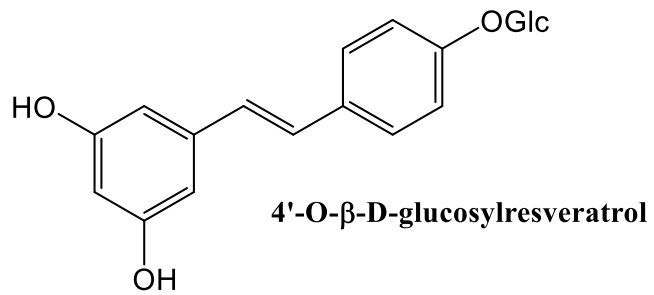
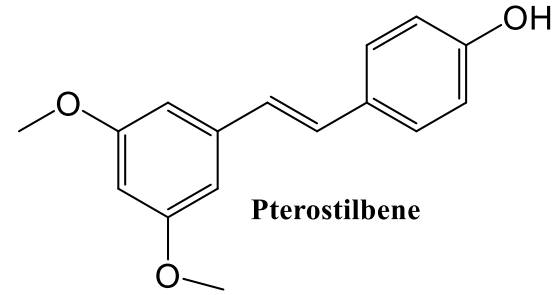
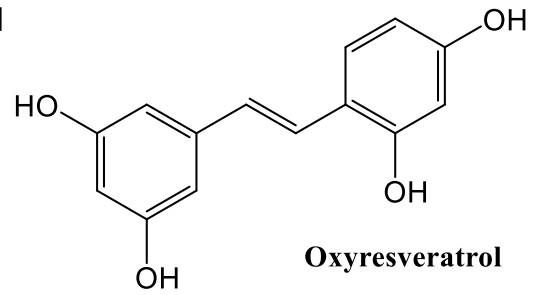
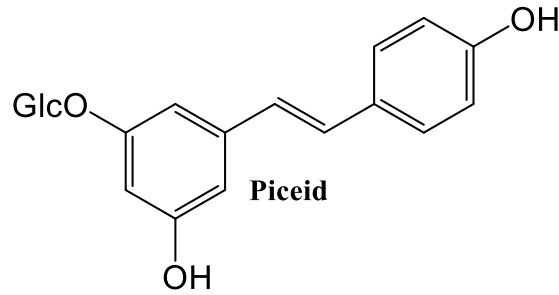
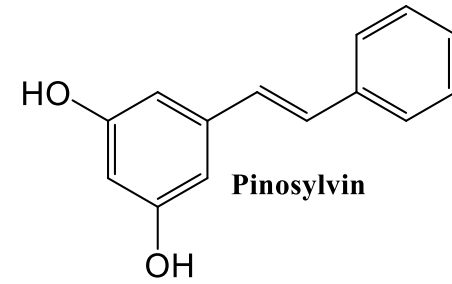
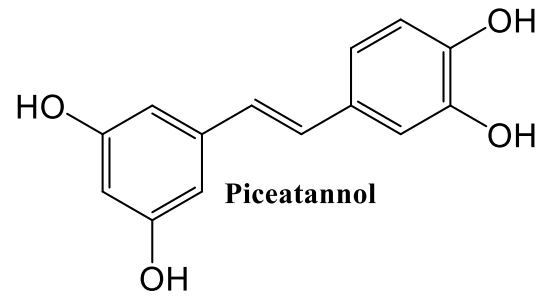
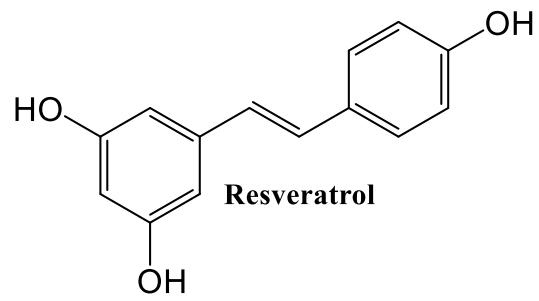
- Rao, M.R.; Chaudhari, J.; Trotta, F.; Caldera, F. 2018. Investigation of cyclodextrin-based nanosponges for solubility and bioavailability enhancement of rilpivirine. *AAPS PharmSciTech.* 19, 1-12.
- Rauf, A.; Imran, M.; Butt, M.S.; Nadeem, M.; Peters, D.G.; Mubarak, M.S. 2018. Resveratrol as an anti-cancer agent: A review. *Crit. Rev. Food Sci. Nutr.* 58, 1428-1447.
- Regev-Shoshani, G.; Shoseyov, O.; Bilkis, I.; Kerem, Z. 2003. Glycosylation of resveratrol protects it from enzymic oxidation. *Biochem. J.* 374, 157-163.
- Renaud, S.; De Lorgeril, M. 1992. Wine, alcohol, platelets, and the French paradox for coronary heart disease. *Lancet* 339, 1523-1526.
- Rivière, C.; Pawlus, A.D.; Mérillon, J.M. 2012. Natural stilbenoids: Distribution in the plant kingdom and chemotaxonomic interest in Vitaceae. *Nat. Prod. Rep.* 29, 1317-1333.
- Ruhlmann, A.; Antovic, D.; Muller, T.; Urlacher, V.B. 2017. Regioselective hydroxylation of stilbenes by engineered cytochrome P450 from *Thermobifida fusca* YX. *Adv. Synth. Catal.* 359, 984-994.
- Sabadini, E.; Cosgrove, T.; do Carmo Edigio, F. 2006. Solubility of cyclomaltooligosaccharides (cyclodextrins) in H<sub>2</sub>O and D<sub>2</sub>O: A comparative study. *Carbohydr. Res.* 341, 270-274.
- Saenger, W.; Jacob, J.; Gessler, K.; Steiner, T.; Hoffmann, D.; Sanbe, H.; Koizumi, K.; Smith, S.M.; Takaha, T. 1998. Structures of the common cyclodextrins and their larger analogues - beyond the doughnut. *Chem. Rev.* 98, 1787-1802.
- Sandilya, A.A.; Natarajan, U.; Priya, M.H. 2020. Molecular view into the cyclodextrin cavity: Structure and hydration. *ACS Omega* 5, 25655-25667.
- Santamaria, A.R.; Antonacci, D.; Caruso, G.; Cavaliere, C.; Gubbiotti, R.; Laganà, A.; Valletta, A.; Pasqua, G. 2010. Stilbene production in cell cultures of *Vitis vinifera* L. cvs Red Globe and Michele Palieri elicited by methyl jasmonate. *Nat. Prod. Res.* 24, 1488-1498.
- Sapino, S.; Carlotti, M.E.; Caron, G.; Ugazio, E.; Cavalli, R. 2009. *In silico* design, photostability and biological properties of the complex resveratrol/hydroxypropyl- $\beta$ -cyclodextrin. *J. Incl. Phenom. Macrocycl. Chem.* 63, 171-180.
- Sharma, R.; Pathak, K. 2011. Polymeric nanosponges as an alternative carrier for improved retention of econazole nitrate onto the skin through topical hydrogel formulation. *Pharm. Dev. Technol.* 16, 367-376.
- Shen, T.; Wang, X.N.; Lou, H.X. 2009. Natural stilbenes: An overview. *Nat. Prod. Rep.* 26, 916-935.
- Shende, P.K.; Trotta, F.; Gaud, R.S.; Deshmukh, K.; Cavalli, R.; Biasizzo, M. 2012. Influence of different techniques on formulation and comparative characterization of inclusion complexes of ASA with  $\beta$ -cyclodextrin and inclusion complexes of ASA with PMDA cross-linked  $\beta$ -cyclodextrin nanosponges. *J. Incl. Phenom. Macrocycl. Chem.* 74, 447-454.
- Shimoda, K.; Kubota, N.; Hamada, H.; Hamada, K. 2015. Synthesis of resveratrol glycosides by plant glucosyltransferase and cyclodextrin glucanotransferase and their neuroprotective activity. *Nat. Prod. Comm.* 10, 995-996.
- Siemann, E.H.; Creasy, L.L. 1992. Concentration of the phytoalexin resveratrol in wine. *Am. J. Enol. Vitic.* 43, 49-52.
- Silva, F.; Figueiras, A.; Gallardo, E.; Nerin, C.; Domingues, F.C. 2014. Strategies to improve the solubility and stability of stilbene antioxidants: A comparative study between cyclodextrins and bile acids. *Food Chem.* 145, 115-125.

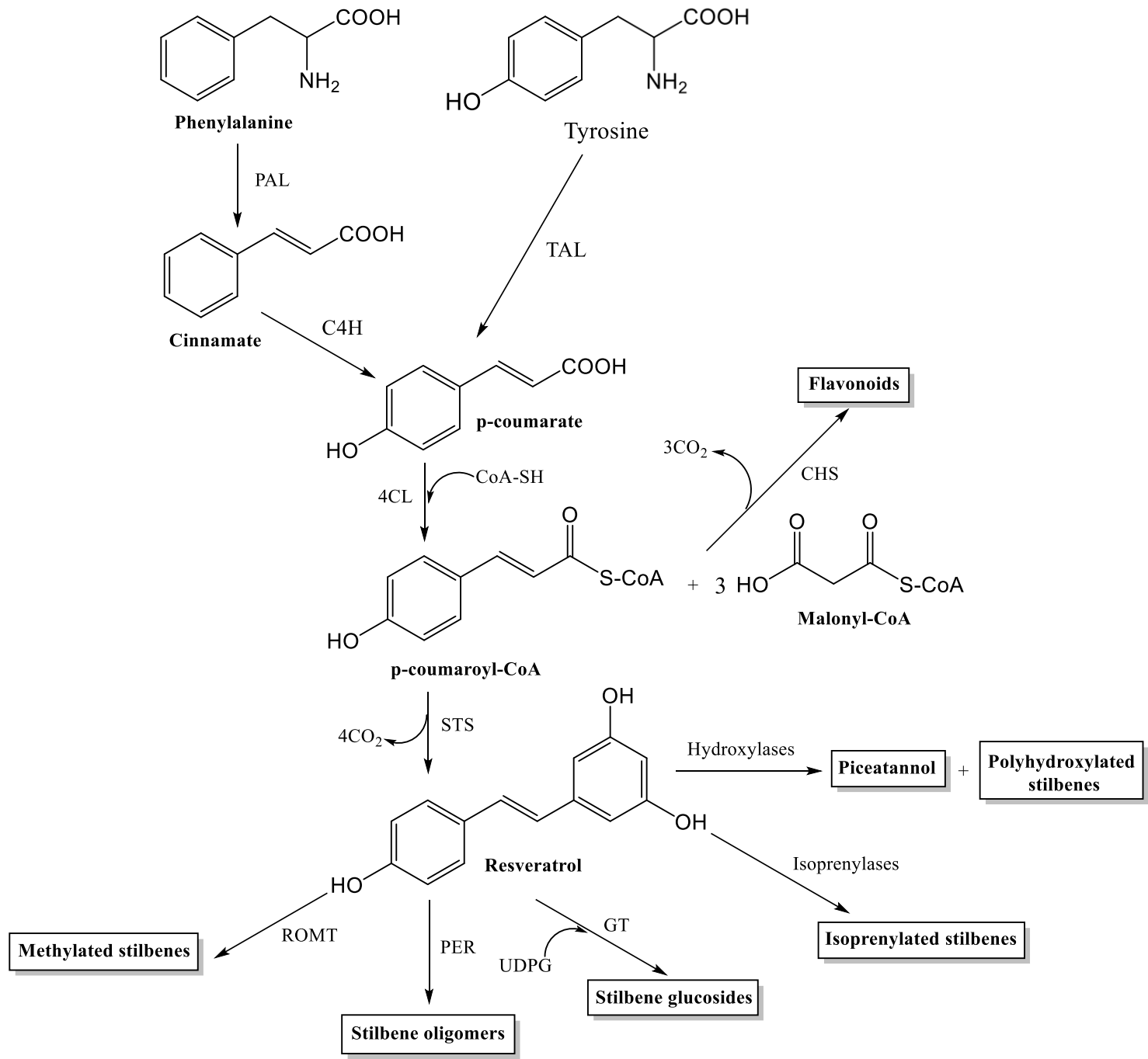
- Silva, A.F.R.; Monteiro, M.; Resende, D.; Braga, S.S.; Coimbra, M.A.; Silva, A.M.S.; Cardoso, S.M. 2021. Inclusion complex of resveratrol with  $\gamma$ -cyclodextrin as a functional ingredient for lemon juices. *Foods* 10, 16.
- Sirerol, J.A.; Feddi, F.; Mena, S.; Rodriguez, M.L.; Sirera, P.; Aupi, M.; Perez, S.; Asensi, M.; Ortega, A.; Estrela, J.M. 2015. Topical treatment with pterostilbene, a natural phytoalexin, effectively protects hairless mice against UVB radiation-induced skin damage and carcinogenesis. *Free Radic. Biol. Med.* 85, 1-11.
- Smoliga, J.M.; Blanchard, O. 2014. Enhancing the delivery of resveratrol in humans: if low bioavailability is the problem, what is the solution? *Molecules* 19, 17154-17172.
- Snyder, S.A.; Goliner, A.; Chiriach, M. 2011. Regioselective reactions for programmable resveratrol oligomer synthesis. *Nature* 474, 461-464.
- Soo, E.; Thakur, S.; Qu, Z.; Jambhrunkar, S.; Parekh, H.S.; Popat, A. 2016. Enhancing delivery and cytotoxicity of resveratrol through a dual nanoencapsulation approach. *J. Colloid Interface Sci.* 462, 368-374.
- Soussi, D.; Danion, J.; Baulier, E.; Favreau, F.; Sauvageon, Y.; Bossard, V.; Matillon, X.; Turpin, F.; Belgsir, E.M.; Thuillier, R.; Hauet, T. 2019. Vectisol formulation enhances solubility of resveratrol and brings its benefits to kidney transplantation in a preclinical porcine model. *Int. J. Mol. Sci.* 20, 2268.
- Springer, M.; Moco, S. 2019. Resveratrol and its human metabolites - Effects on metabolic health and obesity. *Nutrients*, 11, 143.
- Stella, V.J.; Rajewski, R.A. 2020. Sulfobutylether- $\beta$ -cyclodextrin. *Int. J. Pharm.* 583, 119396.
- Stella, V.J.; Rao, V.M.; Zannou, E.A.; Zia, V. 1999. Mechanisms of drug release from cyclodextrin complexes. *Adv. Drug Deliv. Rev.* 36, 3-16.
- Szejtli, J. 1998. Introduction and general overview of cyclodextrin chemistry. *Chem. Rev.* 98, 1743-1754.
- Takaoka, M. 1939. Resveratrol, a new phenolic compound, from *Veratrum grandiflorum*. *J. Chem. Soc. Jpn.* 60, 1090-1100.
- Tan, C.; Wang, J.; Sun, B. 2021. Biopolymer-liposome hybrid systems for controlled delivery of bioactive compounds: Recent advances. *Biotechnol. Adv.* 48, 107727.
- Tassoni, A.; Fornale, S.; Franceschetti, M.; Musiani, F.; Michael, A.J.; Perry, B.; Bagni, N. 2005. Jasmonates and Na-orthovanadate promote resveratrol production in *Vitis vinifera* cv. Barbera cell cultures. *New Phytol.* 166, 895-905.
- Tayo, L. 2017. Stimuli-responsive nanocarriers for intracellular delivery. *Biophys. Rev.* 9, 931-940.
- Tisserant, L.P.; Aziz, A.; Jullian, N.; Jeandet, P.; Clément, C.; Courrot, E.; Boitel-Conti, M. 2016. Enhanced stilbene production and excretion in *Vitis vinifera* cv. Pinot Noir hairy root cultures. *Molecules* 21,1703-1720.
- Torne, S.; Darandale, S.; Vavia, P.; Trotta, F.; Cavalli, R. 2013. Cyclodextrin-based nanosponges: effective nanocarrier for tamoxifen delivery. *Pharm. Dev. Technol.* 18, 619-625.
- Torres, P.; Poveda, A.; Jimenez-Barbero, J.; Parra, J.L.; Comelles, F.; Ballesteros, A.O.; Plou, F.J. 2011. Enzymatic synthesis of  $\alpha$ -glycosides of resveratrol with surfactant activity. *Adv. Synth. Catal.* 353, 1077-1086.
- Trela, B.C.; Waterhouse, A.L. 1994. Resveratrol: Isomeric molar absorptivities and stability. *J. Agric. Food Chem.* 44, 1253-1257.

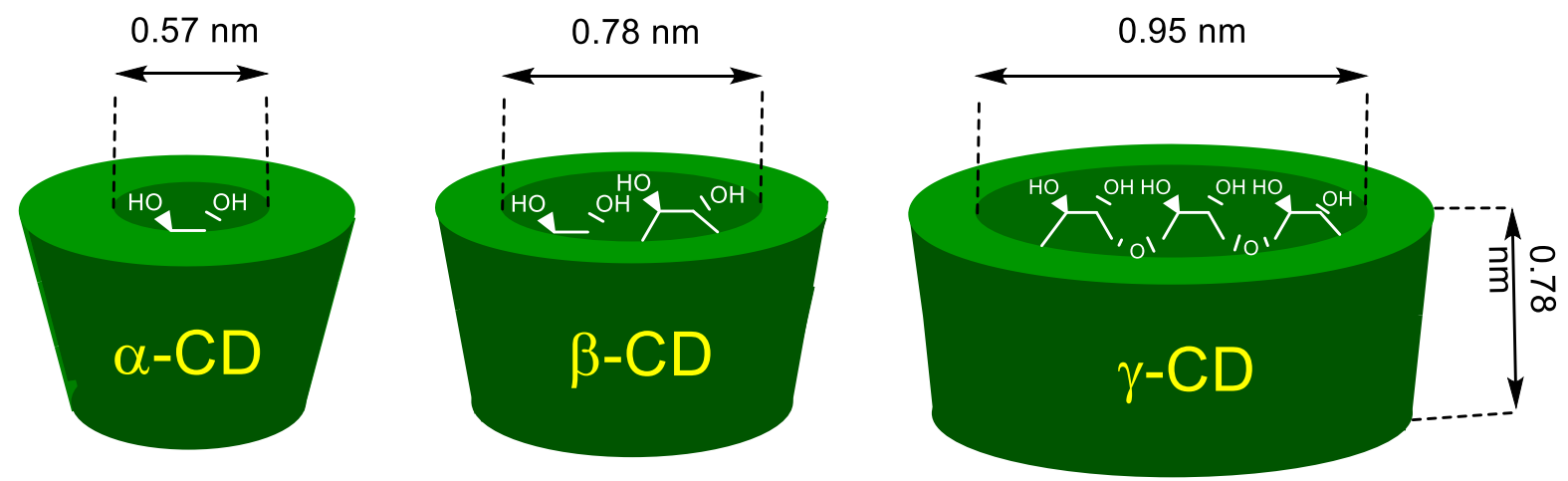
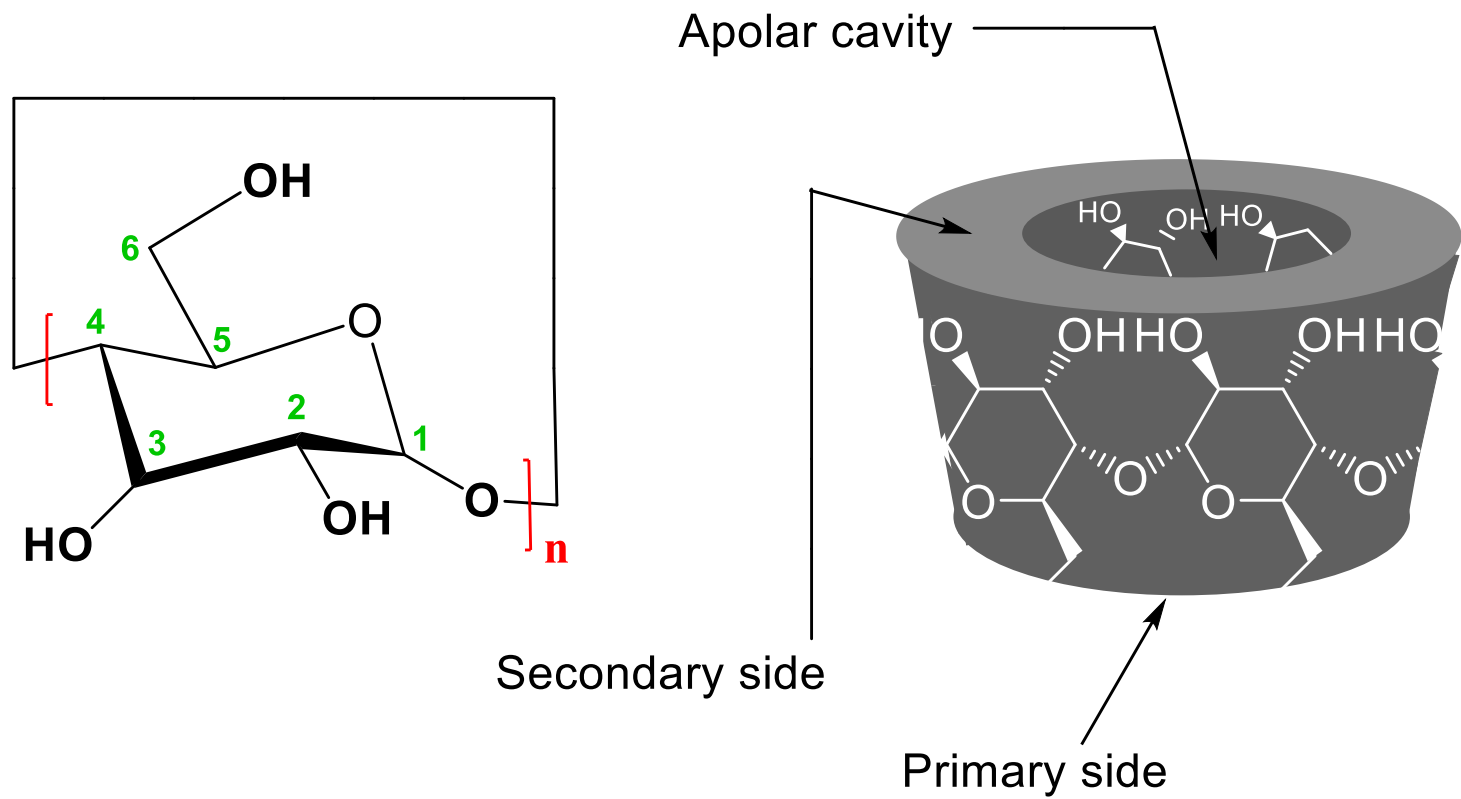
- Trollope, L.; Cruickshank, D.L.; Noonan, T.; Bourne, S.A.; Sorrenti, M.; Catenacci, L.; Caira, M. 2014. Inclusion of *trans*-resveratrol in methylated cyclodextrins: synthesis and solid-state structures. *Beilstein J. Org. Chem.* 10, 3136-3151.
- Trotta, F.; Caldera, F.; Cavalli, R.; Soster, M.; Riedo, C.; Biasizzo, M.; Barretta, G.C.; Balzano, F.; Brunella, V. 2016a. Molecularly imprinted cyclodextrin nanosponges for the controlled delivery of L-DOPA: Perspectives for the treatment of Parkinson's disease. *Expert Opin. Drug Deliv.* 13, 1671-1680.
- Trotta, F.; Caldera, F.; Dianzani, C.; Argenziano, M.; Barrera, G.; Cavalli, R. 2016b. Glutathione bioresponsive cyclodextrin nanosponges. *ChemPlusChem* 81, 439-443.
- Uddin, M.S.; Al Mamun, A.; Rahman, M.M.; Jeandet, P.; Alexiou, A.; Behl, T.; Sarwar, M.S.; Sobarzo-Sanchez, E.; Ashraf, G.M.; Sayed, A.A.; Albadrani, G.M.; Peluso, I.; Abdel-Daim, M.M. 2021. Natural products for neurodegeneration: Regulating neurotrophic signals. *Oxid. Med. Cell. Longev.* 2021, 8820406.
- Uddin, M.S.; Al Mamun, A.; Tanvir Kabir, M.; Ahmad, J.; Jeandet, P.; Sarwar, M.S.; Ashraf, G.M.; Aleya, L. 2020. Neuroprotective role of polyphenols against oxidative stress-mediated neurodegeneration. *Eur. J. Pharmacol.* 886, 173412.
- Vandelle, E.; Poinssot, B.; Wendehenne, D.; Bentéjac, M.; Pugin, A. 2006. Integrated signaling network involving calcium, nitric oxide, and active oxygen species but not mitogen-activated protein kinases in BcPG1-elicited grapevine defenses. *Mol. Plant Microbe Interact.* 19, 429-440.
- Vannozzi, A.; Wong, D.C.J.; Höll, J.; Hmam, I.; Matus, J.T.; Bogs, J.; Ziegler, T.; Dry, I.; Barcaccia, G.; Lucchin, M. 2018. Combinatorial regulation of stilbene synthase genes by WRKY and MYB transcription factors in grapevine (*Vitis vinifera* L.). *Plant Cell Physiol.* 59, 1043-1059.
- Varoni, E.M.; Lo Faro, A.F.; Sharifi-Rad, J.; Iriti, M. 2016. Anticancer molecular mechanisms of resveratrol. *Front. Nutr.* 3, 8.
- Venuti, V.; Cannava, C.; Cristiano, M.C.; Fresta, M.; Majolino, D.; Paolino, D.; Stancanelli, R.; Tommasini, S.; Ventura, C.A. 2014. A characterization study of resveratrol/sulfobutylether- $\beta$ -cyclodextrin inclusion complex and *in vitro* cancer activity. *Colloids Surf. B* 115, 22-28.
- Vera-Urbina, J.C.; Selles-Marchart, S.; Martinez-Esteso, M.J.; Pedreño, M.A.; Bru-Martinez, R. 2013. Production of grapevine cell biomass and resveratrol in custom and commercial bioreactors using cyclodextrins and methyl jasmonate as elicitors, in: Delmas, D. (Ed.), *Resveratrol: source, production, and health benefits*. Nova Science Publishers Inc, New York, pp. 19-39.
- Vestergaard, M.; Ingmer H. 2019. Antibacterial and antifungal properties of resveratrol. *Int. J. Antimicrob. Agents* 53, 716-723.
- Wajs, E.; Nielsen, T.T.; Larsen, K.L.; Frago, A. 2016. Preparation of stimuli-responsive nano-sized capsules based on CD polymers with redox or light switching properties. *Nano Research* 9, 2070-2078.
- Walle, T. 2011. Bioavailability of resveratrol. *Ann. N. Y. Acad. Sci.* 1215, 9-15.
- Walle, T.; Hsieh, F.; DeLegge, M.H.; Oatis, J.E.; Walle, K. 2004. High absorption but very low bioavailability of oral resveratrol in humans. *Drug Metab. Dispos.* 32, 1377-1382.
- Walle, T.; Walle, U.K.; Sedmerer, D.; Klausner, M. 2006. Benzo[A]pyrene-induced oral carcinogenesis and chemoprevention: studies in bioengineered human tissue. *Drug Metab. Dispos.* 34, 346-350.

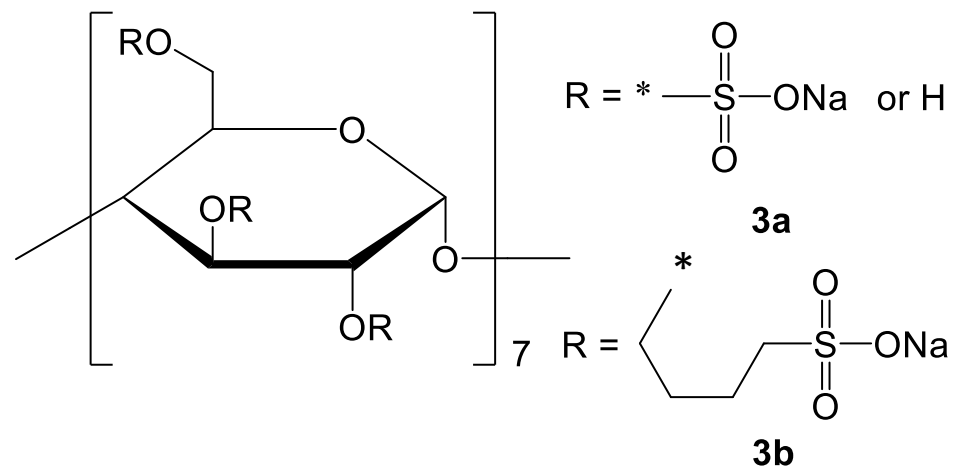
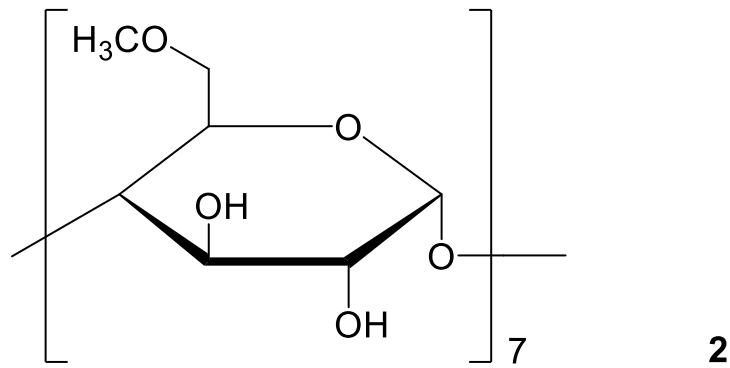
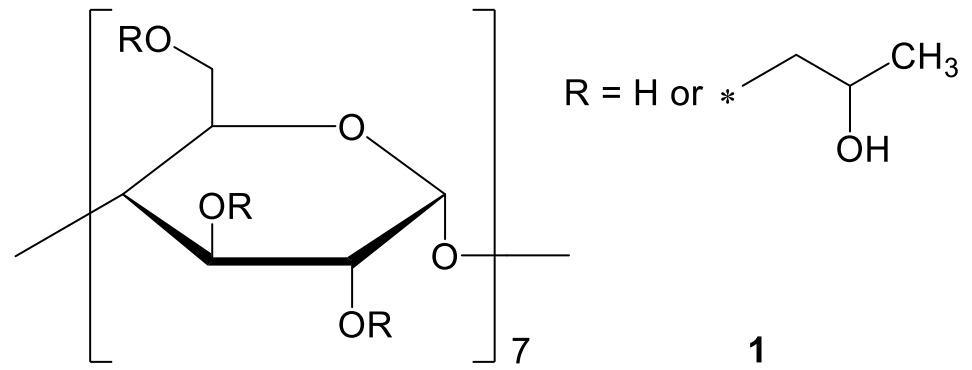


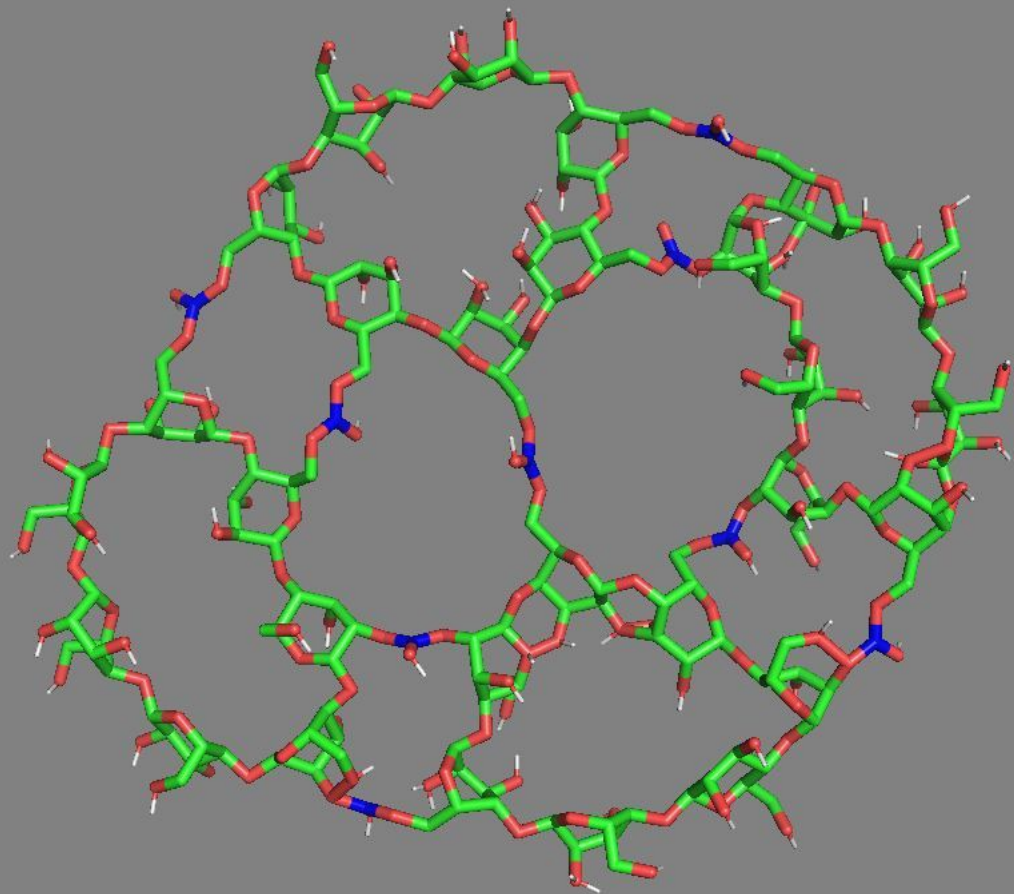
- Wang, X.; Parvathaneni, V.; Shukla, S.K.; Kulkarni, N.; Muth, A.; Kunda, N.K.; Gupta, V. 2020. Inhalable resveratrol-cyclodextrin complex loaded biodegradable nanoparticles for enhanced efficacy against non-small cell lung cancer. *Int. J. Biol. Macromol.* 164, 638-650.
- Wightman, E.L.; Haskell-Ramsay, C.F.; Reay, J.L.; Williamson, G.; Dew, T.; Zhang, W.; Kennedy, D.O. 2015. The effects of chronic trans-resveratrol supplementation on aspects of cognitive function, mood, sleep, health and cerebral blood flow in healthy, young humans. *Br. J. Nutr.* 114, 1427-1437.
- Wong, R.H.X.; Howe, P.R.C.; Buckley, J.D.; Coates, A.M.; Kunz, I.; Berry, N.M. 2011. Acute resveratrol supplementation improves flow-mediated dilatation in overweight/obese individuals with mildly elevated blood pressure. *Nutr. Metab. Cardiovasc. Dis.* 21, 851-856.
- Wong, D.C.J.; Matus, J.T. 2017. Constructing integrated networks for identifying new secondary metabolic pathway regulators in grapevine: recent applications and future opportunities. *Front. Plant Sci.* 8, e505.
- Wong, K.H.; Riaz, M.K.; Xie, Y.; Zhang, X.; Liu Q.; Chen, H.; Bian, Z.; Chen, X.; Lu, A.; Yang, Z. 2019. Review of current strategies for delivering Alzheimer's disease drugs across the blood-brain barrier. *Int. J. Mol. Sci.* 20, 381.
- Wong, K.H.; Xie, Y.; Huang, X.; Kadota, K.; Yao X.S.; Yu, Y.; Chen, X.; Lu, A.; Yang, Z. 2020. Delivering crocetin across the blood-brain barrier by using  $\gamma$ -cyclodextrin to treat Alzheimer's disease. *Sci. Rep.* 10, 3654.
- Wu, B.; Basu, S.; Meng, S.; Wang, X.; Hu, M. 2011. Regioselective sulfation and glucuronidation of phenolics: Insights into the structural basis. *Curr. Drug Metab.* 12, 900-916.
- Wu, M.; Cao, Z.; Zhao, Y.; Zeng, R.; Tu, M.; Zhao, J. 2016. Novel self-assembled pH-responsive biomimetic nanocarriers for drug delivery. *Mater. Sci. Eng. C Mater. Biol. Appl.* 64, 346-353.
- Yang, T.; Fang, L.; Nopo-Olazabal, C.; Condori, J.; Nopo-Olazabal, L.; Balmaceda, C.; Medina-Bolivar, F. 2015. Enhanced production of resveratrol, piceatannol, arachidin-1, and arachidin-3 in hairy root cultures of peanut co-treated with methyl jasmonate and cyclodextrin. *J. Agric. Food Chem.* 63, 3942-3950.
- Yang, T.; Fang, L.; Sanders, S.; Jayanthi, S.; Rajan, G.; Podicheti, R.; Thallapuranam, S.K.; Mockaitis, K.; Medina-Bolivar, F. 2018. Stilbenoid prenyltransferases define key steps in the diversification of peanut phytoalexins. *J. Biol. Chem.* 293, 28-46.
- Yasayan, G.; Sert, B.S.; Tatar, E.; Küçükgüzel, I. 2020. Fabrication and characterization studies of cyclodextrin-based nanosponges for sulfamethoxazole delivery. *J. Incl. Phenom. Macrocycl. Chem.* 97, 175-186.
- Zamboni, A.; Vrhovsek, U.; Kassemeyer, H.H.; Mattivi, F.; Velasco, R. 2006. Elicitor-induced resveratrol production in cell cultures of different grape genotypes (*Vitis* spp.). *Vitis* 45, 63-68.
- Zordosky, B.N.M.; Robertson, I.M.; Dyck, J.R.B. 2015. Preclinical and clinical evidence for the role of resveratrol in the treatment of cardiovascular diseases. *Biochim. Biophys. Acta Mol. Basis Dis.* 1852, 1155-1177.

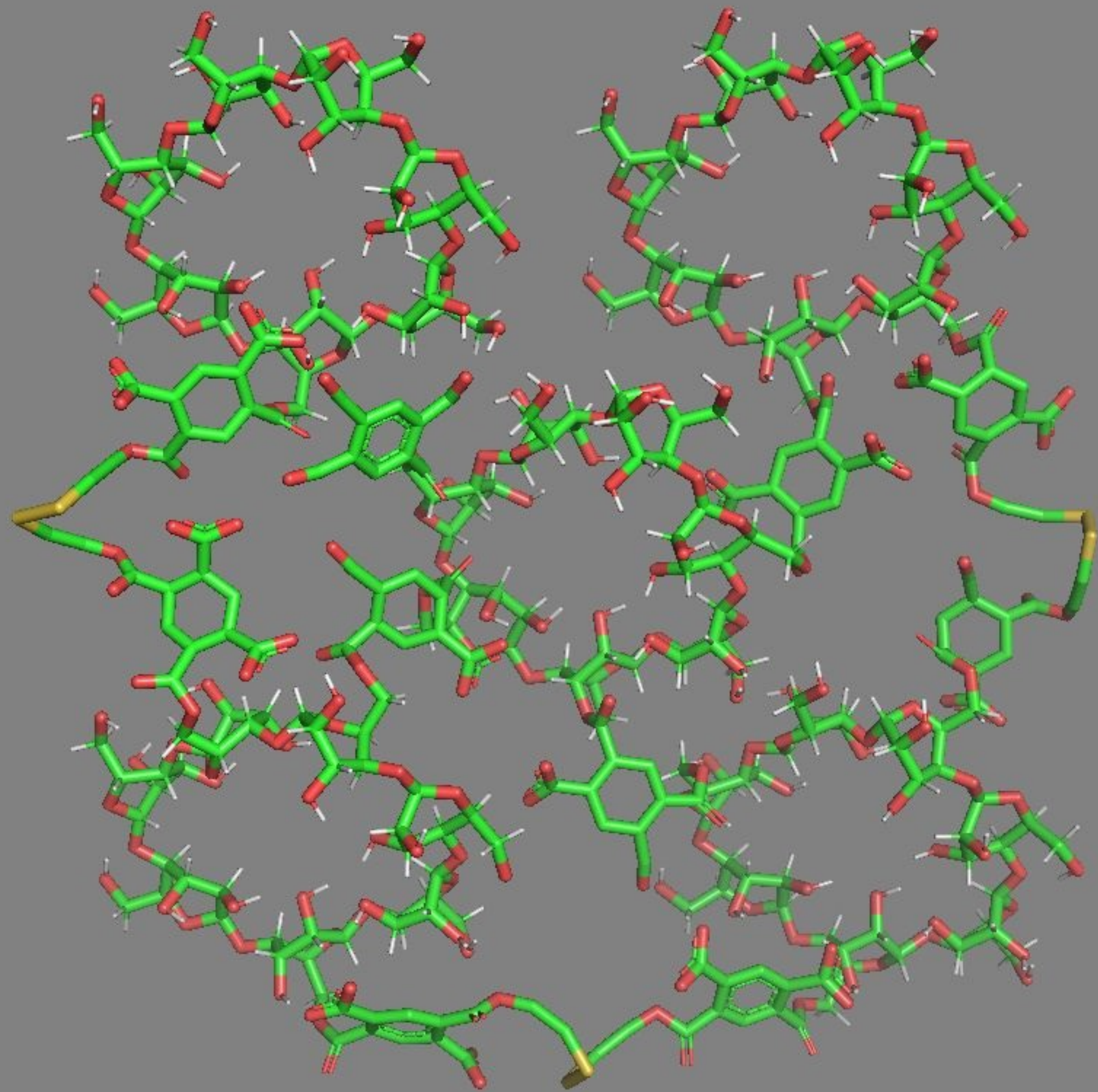


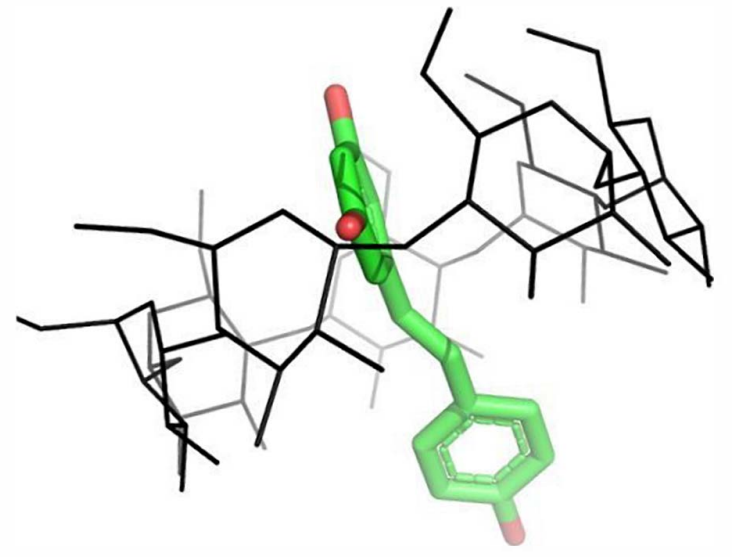
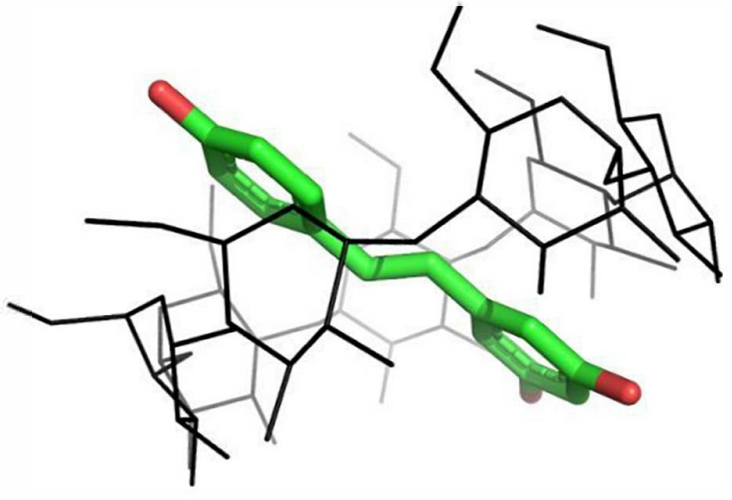
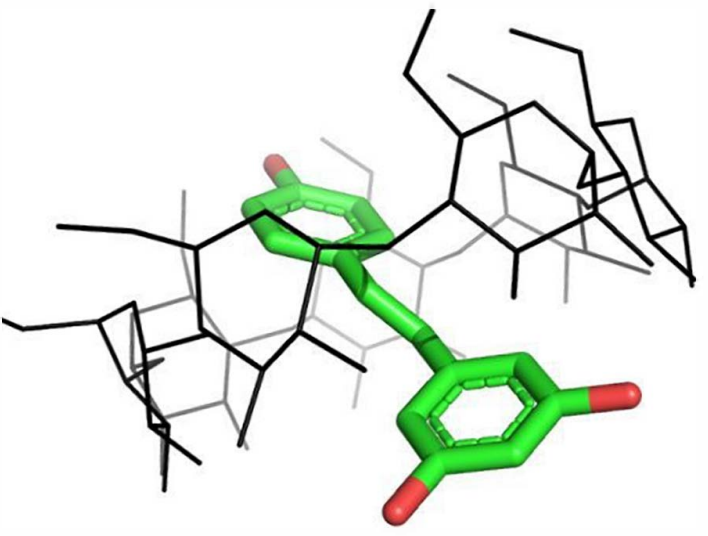
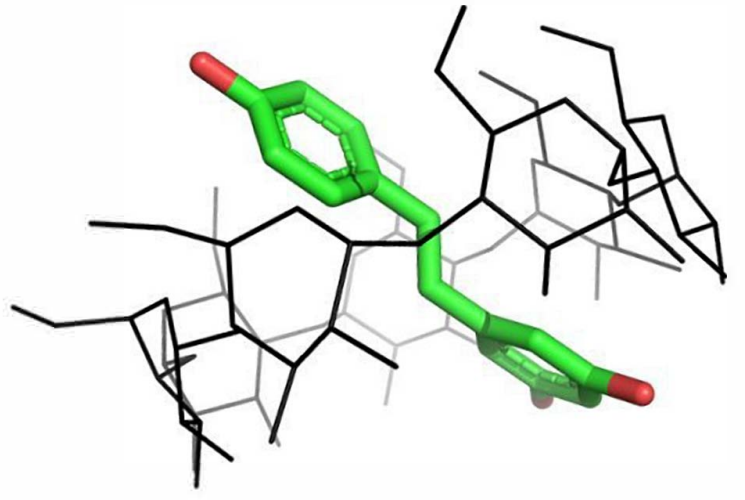
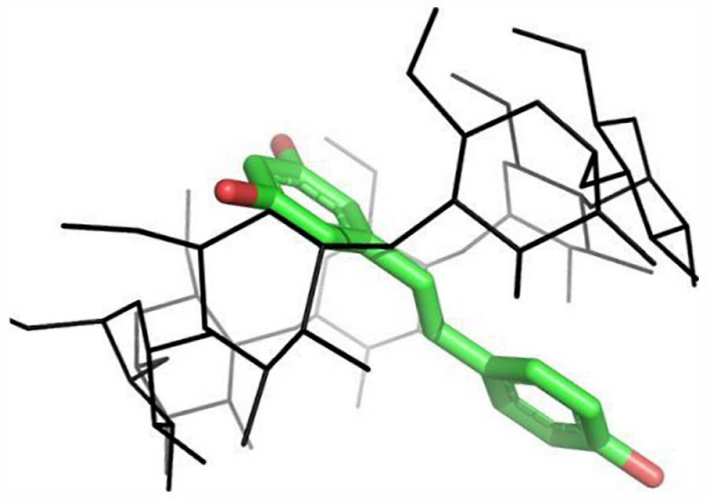
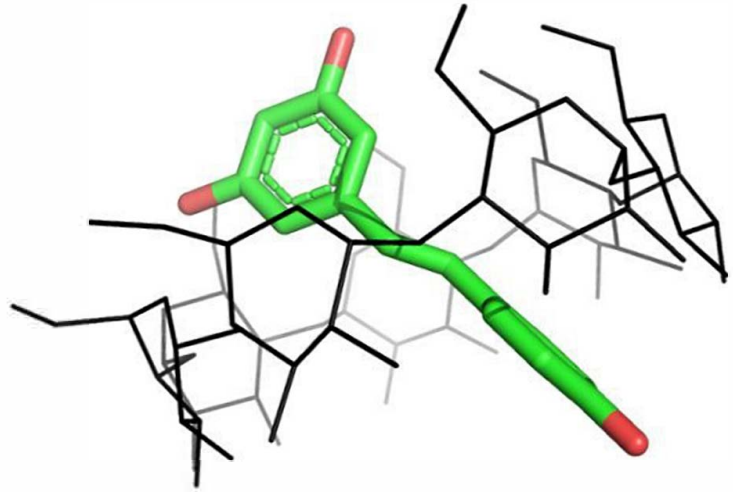






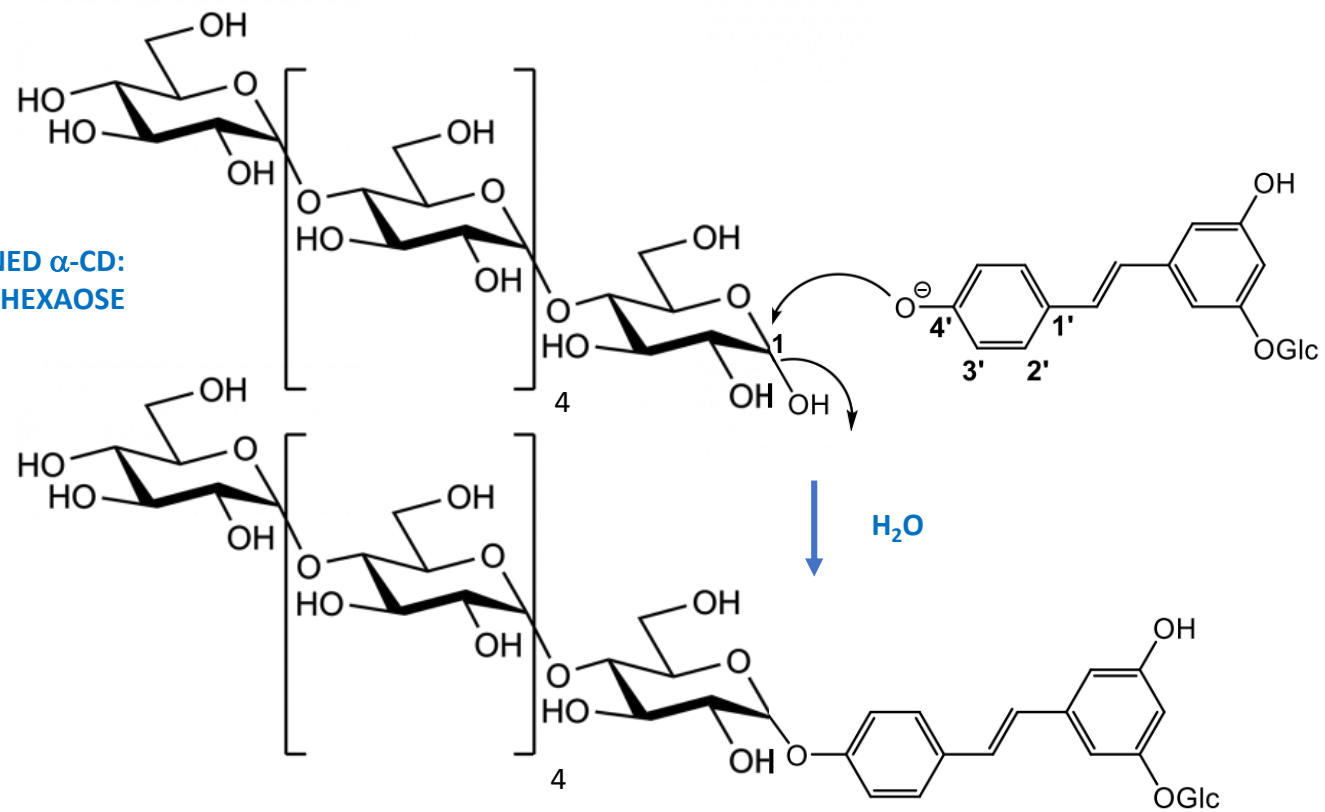




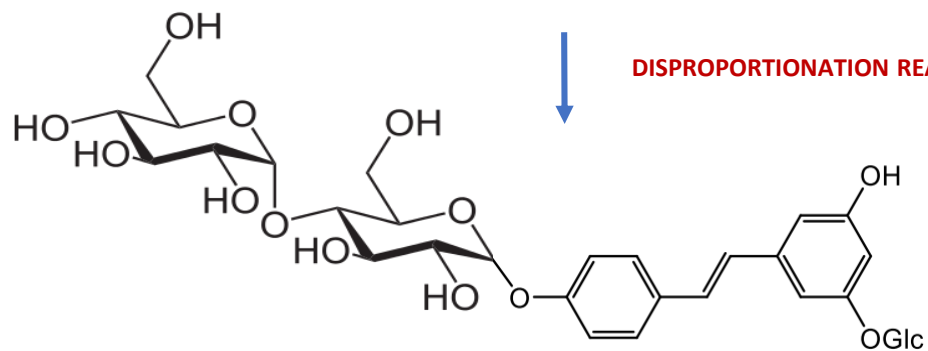




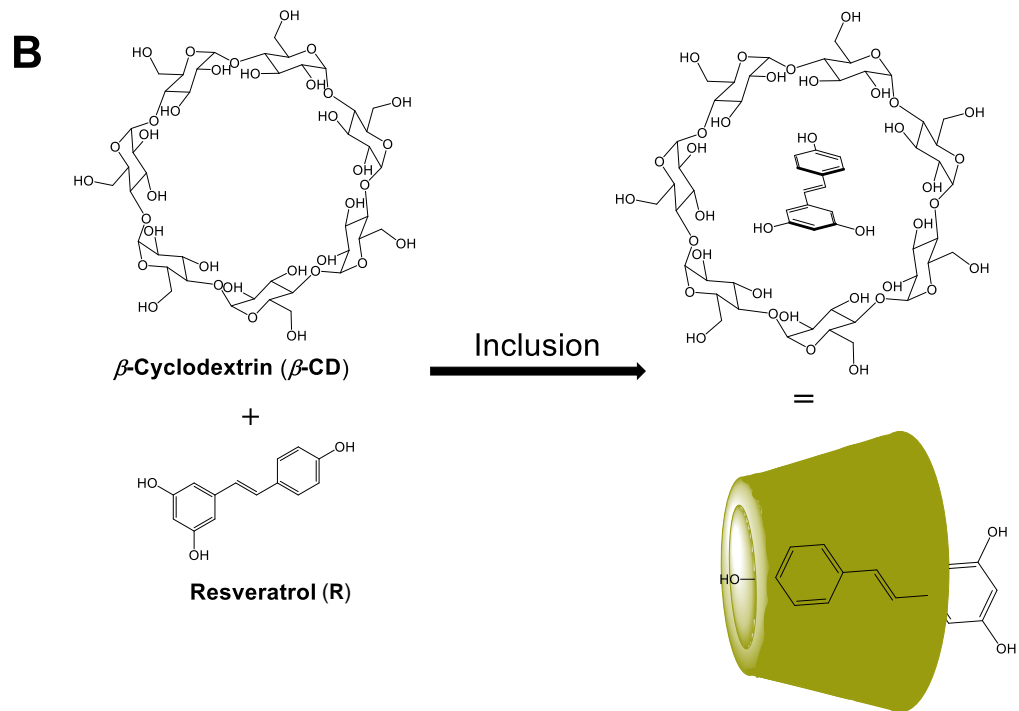
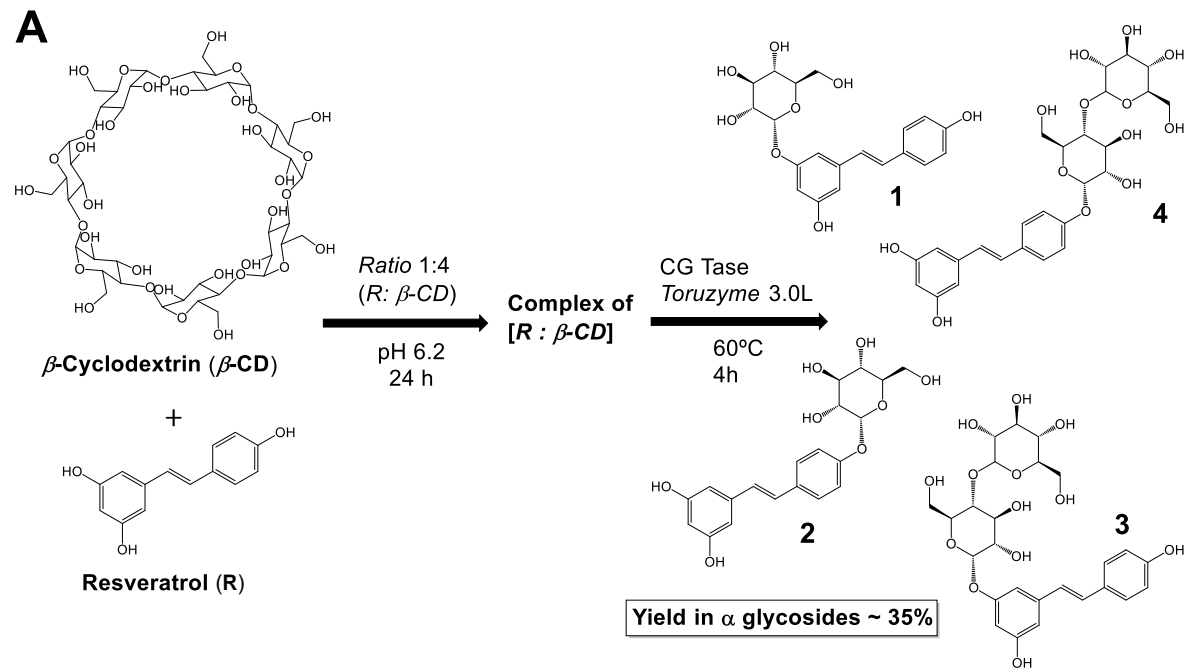
**OPENED  $\alpha$ -CD:  
 $\alpha$ -MALTOHEXAOSE**



**DISPROPORTIONATION REACTIONS**



**PicG3 + various glucosides**



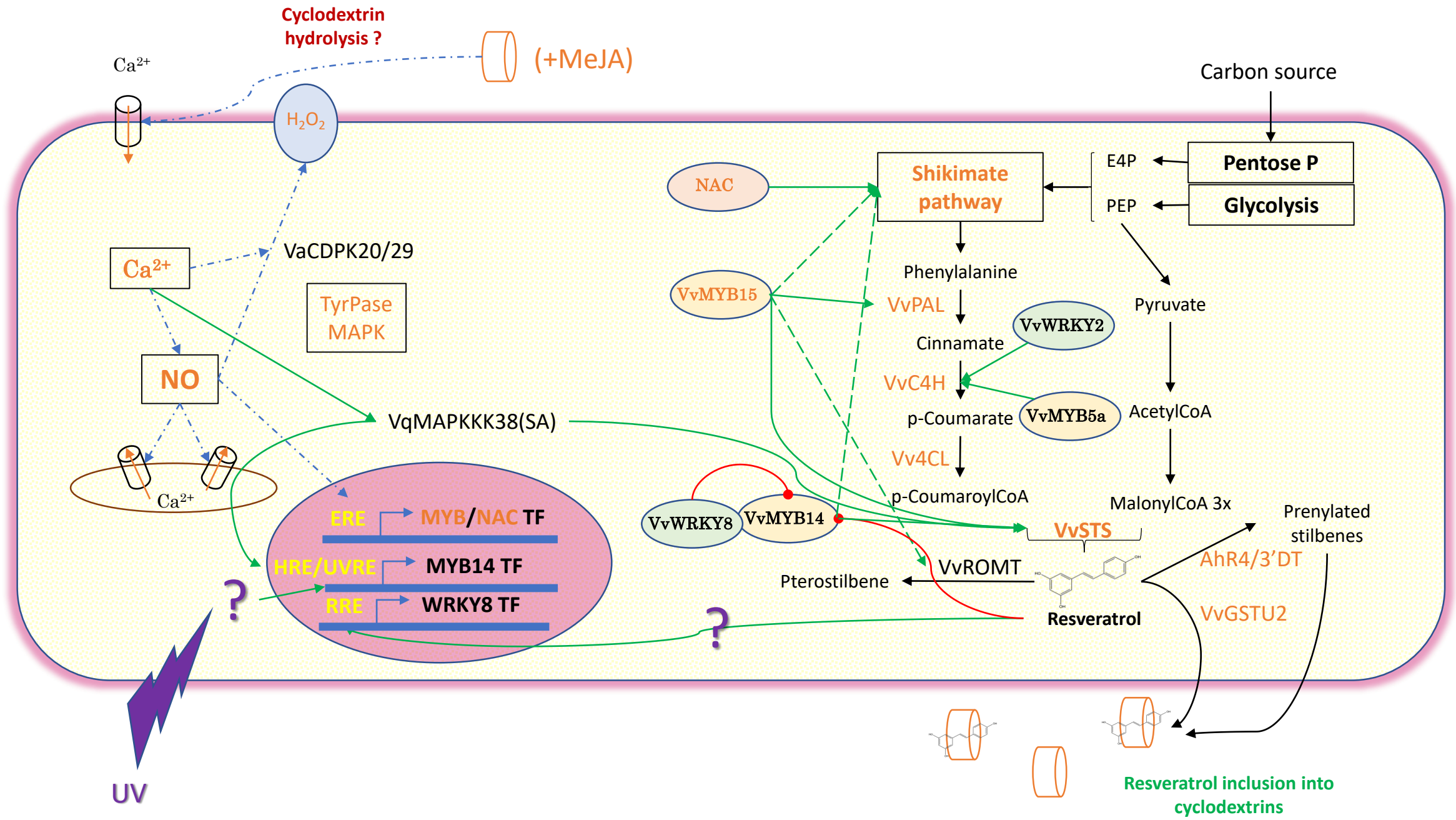


**Table 1: Some parameters of stilbenes/cyclodextrins inclusion complexes**

Abbreviations:  $K_s$ : stability constant; CD, cyclodextrin;  $\beta$ -CD,  $\beta$ -cyclodextrin; G2- $\beta$ -CD, maltosyl- $\beta$ -cyclodextrin; HP- $\beta$ -CD, 2-hydroxypropyl- $\beta$ -cyclodextrin; DM- $\beta$ -CD, dimethylated- $\beta$ -cyclodextrin; RAMEB- $\beta$ -CD, randomized methylated- $\beta$ -CD, Me- $\beta$ -CD, methylated  $\beta$ -cyclodextrin; nr, not reported; PLGA, Poly (lactic-co-glycolic) acid; EE, entrapment efficiency; DL, drug loading; Resv-NS, resveratrol-nanosponge; Oxyresv-NS, oxyresveratrol-nanosponge; w/w, weight/weight ratio; GSH, glutathione

Type of CD	Stilbenes	Stoichiometry	$K_s$ values	Stilbene solubility increase	Stilbene loading	Stilbene release	Refs
$\beta$ -CD	Resveratrol	1:1	2057 M <sup>-1</sup>	2-fold	nr	nr	Bertache et al. (2006)
HP- $\beta$ -CD	Resveratrol	1:1	1588 M <sup>-1</sup>	nr	nr	nr	
DM- $\beta$ -CD	Resveratrol	1:1	2604 M <sup>-1</sup>	8-fold	nr	nr	
$\beta$ -CD	Resveratrol	nr	4317 ± 338 M <sup>-1</sup>	nr	nr	nr	Lucas-Abellan et al. (2007)
G2- $\beta$ -CD	Resveratrol	nr	5130 ± 421 M <sup>-1</sup>	nr	nr	nr	
HP- $\beta$ -CD	Resveratrol	1:1	3.17 × 10 <sup>5</sup> M <sup>-1</sup>	59500-fold	nr	nr	Das et al. (2008)
RAMEB- $\beta$ -CD	Resveratrol	1:1	4.41 × 10 <sup>5</sup> M <sup>-1</sup>		nr	nr	
$\beta$ -CD	Pinosylin	1:1	5181 ± 233 M <sup>-1</sup>	nr	nr	nr	Lopez-Nicolas et al. (2009a)
HP- $\beta$ -CD	Pinosylin	1:1	12112 ± 761 M <sup>-1</sup>	nr	nr	nr	
$\beta$ -CD	Pterostilbene	1:1	8120 ± 440 M <sup>-1</sup>	nr	nr	nr	Lopez-Nicolas et al. (2009b)
HP- $\beta$ -CD	Resveratrol	1:1	24880 ± 1020 M <sup>-1</sup>	nr	nr	nr	
HP- $\beta$ -CD	Pterostilbene	1:1	17520 ± 981 M <sup>-1</sup>	8-fold	nr	nr	
$\beta$ -CD	Resveratrol	1:1	1815 M <sup>-1</sup>	nr	nr	nr	Lu et al. (2009)
HP- $\beta$ -CD	Resveratrol	1:1	6778 M <sup>-1</sup>	nr	nr	nr	
HP- $\beta$ -CD	Resveratrol	1:1	3189 M <sup>-1</sup>	increases with CD concentration	nr	nr	Sapino et al. (2009)
HP- $\beta$ -CD	Resveratrol	nr	nr	nr	nr	nr	Berta et al. (2010)
$\beta$ -CD	Resveratrol	nr	nr	8.55 to 12.57-fold depending on CD concentration	nr	nr	Lu et al. (2012)
HP- $\beta$ -CD	Resveratrol	nr	nr	24.31 to 50.49-fold depending on CD concentration	nr	nr	

HP- $\beta$ -CD	Resveratrol	1:1	$1682 \pm 49 \text{ M}^{-1}$		nr	nr		Silva et al. (2014)
HP- $\beta$ -CD	Pterostilbene	1:1	$11730 \pm 13 \text{ M}^{-1}$	4-6 log fold-increase	nr	nr		
HP- $\beta$ -CD	Pinosylin	1:2	$14 \pm 2.3 \text{ M}^{-1}$		nr	nr		
Sulfobutylether- $\beta$ -CD	Resveratrol	1:1	$10114 \text{ M}^{-1}$	37-fold (from 0.03 mg/mL to 1.1 mg/mL)	nr	nr		Venuti et al. (2014)
RAMEB- $\beta$ -CD	Resveratrol	1:1	$1482.9 \pm 13.7 \text{ M}^{-1}$	400-fold	80%		Increased by 1.5-fold within 60 min	Duarte et al. (2015)
HP- $\beta$ -CD	Piceatannol	1:1	$14048 \pm 702 \text{ M}^{-1}$	nr	nr	nr		Matencio et al. (2016)
HP- $\beta$ -CD HP- $\beta$ -CD	Resveratrol loaded in liposomes	nr		nr	+3.08%		67.7% within 24h	Soo et al. (2016)
	Resveratrol complexed with HP- $\beta$ -CD and inclusion in liposomes	nr	nr	nr	+6.23%		100% within 24h	
	Both complexation of resveratrol in liposomes and in HP- $\beta$ -CD included in liposomes	nr	nr	nr	+11.6%		94.4% within 24h	
$\beta$ -CD Me- $\beta$ -CD HP- $\beta$ -CD	Oxyresveratrol Oxyresveratrol Oxyresveratrol	1:1 1:1 1:1	$590.00 \text{ M}^{-1}$ $606.65 \text{ M}^{-1}$ $435.53 \text{ M}^{-1}$	nr nr nr	nr nr nr	nr nr nr		Matencio et al. (2017)
$\beta$ -CD Me- $\beta$ -CD HP- $\beta$ -CD	Polydatin Polydatin Polydatin	1:1 1:1 1:1	$798 \text{ M}^{-1}$ $1106 \text{ M}^{-1}$ $1308 \text{ M}^{-1}$	6.4-fold increase 7.9-fold increase 9-fold increase	nr nr nr	nr nr nr		Li et al. (2018)
$\beta$ -CD HP- $\beta$ -CD	Oxyresveratrol Oxyresveratrol	1:1 1:1	$1897.54 \pm 81.14 \text{ M}^{-1}$ $35864.72 \pm 3415.89 \text{ M}^{-1}$	30-fold increase (0.47 mg/mL to 14.44 mg/mL) 100-fold increase (0.47 mg/mL to 47.33 mg/mL)	20% increase 20% increase	nr nr		He et al. (2019)
HP- $\beta$ -CD HP- $\beta$ -CD HP- $\beta$ -CD HP- $\beta$ -CD	Resveratrol Oxyresveratrol Piceatannol Pterostilbene	nr	nr	nr	nr	nr		Lim et al. (2020)

Sulfobutylether- $\beta$ -CD + PLGA	Resveratrol	nr	nr	66-fold (from 0.03 mg/mL to 2.0 mg/mL)	EE: 29.1% DL: 0.72%	95.7% resv release within 30 min	Wang et al. (2020)
$\gamma$ -CD	Resveratrol	1:1	nr	9-fold increase in lemon juice	nr	nr	Silva et al. (2021)
<b>NANOSPONGES</b>							
Carbonyl nanosponge	Resveratrol	1:2/1:4	nr	33-fold increase (Resv-NS 1:2) 48-fold increase (Resv-NS 1:4)	30% increase (Resv-NS 1:2) 40% increase (Resv-NS 1:4)	5-fold increase (Resv-NS 1:2) 9-fold increase (Resv-NS 1:4) within 2h	Ansari et al. (2011b)
Carbonyl nanosponge (NS-I) Carboxylate nanosponge (NS-II)	Resveratrol	nr	nr	51 to 161 and 167 $\mu$ g/mL (NS-I 1:2;1:4) 51 to 152 and 156 $\mu$ g/mL (NS-II 1:2;1:4)	91.52% (NS-I) 90.81 (NS-II)	3-fold increases (NS-I and NS-II)	Pushpalatha et al. (2018)
Carbonyl nanosponge in hydrogels	Curcumin and resveratrol	nr	nr	nr	nr	10-fold increase including a lag phase with curcumin and 2.5 fold-increase with no lag phase with resveratrol compared to unloaded compounds	Pushpalatha et al. (2019)
Carbonyl nanosponge	Resveratrol Oxyresveratrol	-	nr	3-fold for resveratrol (40 to 120 $\mu$ g/mL) 2-fold for oxyresveratrol (600 to >1000 $\mu$ g/mL)	9.47 to 14% increase (Resv-NS 1:2 and 1:6 w/w ratio) 11.93 to 16.78% increase (Oxyresv-NS 1:2 and 1:6 w/w ratio)	5-fold increase (47.74% increase for resveratrol within 24h) ca 60% increase for oxyresveratrol within 24h	Dhakar et al. (2019)
Carbonyl nanosponge	Resveratrol Oxyresveratrol	1:4	$K_{app}$ (apparent association constant) values: Oxyresv- $\beta$ -CD 1:4, 3917.89 $\pm$ 392.79 $M^{-1}$ Resv- $\beta$ -CD 1:4, 4466.48 $\pm$ 446.65 $M^{-1}$	nr	39.75% increase (Oxyresv- $\beta$ -CD-NS 1:4)	Diffusion profile of Oxyresv-NS slower than that of free oxyresveratrol within 12h, pH dependent	Mattencio et al. (2020)
$\alpha$ , $\beta$ and $\gamma$ -CD polymers	Resveratrol	nr	nr	nr	4.5% increase for $\alpha$ and $\gamma$ -CD polymers 6.7% increase for $\beta$ -CD polymers	Respectively 11%, 6% and 12% resveratrol release for $\alpha$ , $\beta$ and $\gamma$ -CD polymers within 24h	Haley et al. (2020)

---

GSH-responsive nanosponge	Resveratrol	nr	nr	4-fold increase (46 to 201 µg/mL)	9.95% increase for Resv-β-CD-NS 1:2 (w/w) and 16.12% increase for Resv-β-CD-NS 1:4 (w/w)	2-fold increase with 10 mM GSH 5-fold increase with 20 mM GSH	Palminteri et al. (2021)
---------------------------	-------------	----	----	-----------------------------------	--	--	--------------------------

---

**Table 2: Some pharmacokinetic parameters of stilbenes or stilbene-cyclodextrin complexes**

Abbreviations:  $C_{max}$ ; maximum plasma concentration;  $T_{max}$ , maximal time to reach  $C_{max}$ ; AUC, area under the curve; CMC, carboxymethyl cellulose; CD, cyclodextrin;  $\beta$ -CD,  $\beta$ -cyclodextrin; RAMEB- $\beta$ -CD, randomized methylated-  $\beta$ -CD, Carbonyl-NS, carbonyl-nanosponge; Carboxylate-NS, carboxylate-nanosponge; HP- $\beta$ -CD, 2-hydroxypropyl- $\beta$ -cyclodextrin

Stilbene formulation	Doses (mg/kg)	Mode of administration	$C_{max}$ (ng/mL)	$T_{max}$ (min)	AUC <sub>0-t</sub> (ng x h/mL)	Bioavailability, F (%)	Refs
CMC suspension	Resveratrol (25)	Oral	270 ± 60	5-15	485 ± 114	38.4 ± 9.02	Das et al. (2008)
CMC suspension	Resveratrol (50)	Oral	430 ± 90	60-90	981 ± 49	38.8 ± 1.96	
RAMEB- $\beta$ -CD	Resveratrol (25)	Oral	860 ± 190	5-15	480 ± 24	38.0 ± 1.91	
RAMEB- $\beta$ -CD	Resveratrol (50)	Oral	1750 ± 720	5-15	1009 ± 186	39.9 ± 7.38	
Resveratrol alone	Resveratrol (20)	Oral	496 ± 49	120	2080 ± 56	nr	Pushpalatha et al. (2018)
Carbonyl-NS	Resveratrol (20)	Oral	1107 ± 105	36	4145 ± 155	199.33 (F <sub>relative</sub> )	
Carboxylate-NS	Resveratrol (20)	Oral	1225 ± 111	30	3917 ± 263	188.37 (F <sub>relative</sub> )	
HP- $\beta$ -CD	Resveratrol (10)	Intravenous	15720 ± 3192	2	2836 ± 223	--	Kong et al. (2020)
HP- $\beta$ -CD	Resveratrol (50)	Oral	1997 ± 1167	22	2352 ± 1737	16.68 ± 12.16	
HP- $\beta$ -CD	Resveratrol (20)	Orotracheal	7156 ± 1637	7.8	5280 ± 565	92.95 ± 9.69	
HP- $\beta$ -CD	Resveratrol (2.3)	Inhalation	148 ± 86	142	390 ± 104	76.31 ± 10.74	



**Table 3: Reported bioactivities of stilbenes/cyclodextrins inclusion complexes**

Abbreviations: CD, cyclodextrin; NS, nanosponge;  $\beta$ -CD,  $\beta$ -cyclodextrin; HP- $\beta$ -CD, 2-hydroxypropyl- $\beta$ -cyclodextrin; DMBA, 7,12-dimethylbenz[a]anthracene; DM- $\beta$ -CD, dimethylated- $\beta$ -cyclodextrin; RAMEB- $\beta$ -CD, randomized methylated- $\beta$ -CD, Me- $\beta$ -CD, methylated  $\beta$ -cyclodextrin; nr, not reported; PLGA, poly (lactic-co-glycolic) acid; Resv-NS, resveratrol-nanosponge; Oxyresv-NS, oxyresveratrol-nanosponge; DMSO, dimethylsulfoxide; w/w, weight/weight ratio; GSH-Resv-NS, glutathione responsive nanosponge

Stilbenes	Type of study	Type of CD or NS	Biological input	Refs
Resveratrol	<i>in vitro</i>	$\beta$ -CD HP- $\beta$ -CD	No significant increase in DPPH radical scavenging and antioxidant activities between resveratrol and Resv- $\beta$ -CD or resveratrol and Resv-HP- $\beta$ -CD Better efficiency of Resv-HP- $\beta$ -CD against Resv- $\beta$ -CD regarding antiradical and antioxidant activities	Lu et al. (2009)
Resveratrol	<i>in vitro</i>	HP- $\beta$ -CD	No significant increase in antiradical and lipoperoxidation activities between resveratrol and Resv-HP- $\beta$ -CD Significant increase in resveratrol accumulation in porcine skins with use of Resv-HP- $\beta$ -CD	Sapino et al. (2009)
Resveratrol	<i>in vitro</i> and <i>in vivo</i>	HP- $\beta$ -CD in suspension in a cream (Resv-HP- $\beta$ -CD-cream) or in a mouthwash (Resv-HP- $\beta$ -CD-mouthwash)	Higher cytotoxicity of Resv-CD formulations compared to resveratrol on DMBA-induced oral squamous cell carcinoma (HCPC-I cell line) <i>in vitro</i> (24-72 h) <i>In vivo</i> prevention of exophytic lesions displaying oral squamous cell carcinoma characters. Order efficiency was: Resv-HP- $\beta$ -CD-cream > Resv-HP- $\beta$ -CD-mouthwash > free Resv	Berta et al. (2010)
Resveratrol	<i>in vitro</i>	Carbonyl- $\beta$ -CD-NS	Higher cytotoxicity of Resv-NS compared to resveratrol on DMBA-induced cancer cells of buccal mucosa (HCPC-I cell line) Higher permeation of Resv-NS through pig skin Two-fold higher accumulation of Resv-NS in rabbit mucosa	Ansari et al. (2011b)
Resveratrol	<i>in vitro</i>	$\beta$ -CD HP- $\beta$ -CD	Dramatic morphological alterations of cell membranes of HeLa (human cervical carcinoma) cells with CD formulations of resveratrol but not with free resveratrol Decreased viability of HeLa cells and Hep3B (human hepatocellular liver cancer) cells with CD resveratrol formulations vs low cell viability inhibition with free resveratrol	Lu et al. (2012)
Resveratrol	<i>in vitro</i>	Sulfobutylether- $\beta$ -CD	Weak decrease (-65%) in the cell viability of human breast cancer cells (MCF-7 cell line) with the CD resveratrol inclusion complex when compared to resveratrol alone (-50%) within 72 h	Venuti et al. (2014)
Resveratrol	<i>in vitro</i>	RAMEB- $\beta$ -CD	Strong antioxidant activity of resveratrol and Resv-CD but without any significant differences between free and internalized resveratrol No significant differences reported in the reduction in cell viability of Caco-2 cells (human epithelial colorectal carcinoma) cells between free and CD-included resveratrol	Duarte et al. (2015)
Resveratrol	<i>in vitro</i>	i) Resveratrol loaded in liposomes (RL) ii) Resveratrol complexed with HP- $\beta$ -CD and inclusion in liposomes (RCL) iii) Both internalization of resveratrol in liposomes and in HP- $\beta$ -CD and inclusion in liposomes (RL-CL)	Antiproliferative effect on HT-29-colon cancer cells within 24 h. All inclusion complexes (RL, RCL and RL-CL) displayed higher antiproliferative activities than free resveratrol. The increase in cytotoxicity was in the following order: RL-CL > RCL > RL > R	Soo et al. (2016)

Pterostilbene	<i>in vivo</i>	HP- $\beta$ -CD	Preservation of left ventricular function in infarcted rats following oral administration of the pterostilbene-HP- $\beta$ -CD. No comparison with free pterostilbene was made precluding any conclusion regarding the effect of the inclusion process	Lacerda et al. (2018)
Polydatin (3-O- $\beta$ -D-resveratrol glucoside)	<i>in vitro</i>	$\beta$ -CD Me- $\beta$ -CD HP- $\beta$ -CD	Increased antioxidant activity (as determined by measuring reducing power values) of inclusion complexes with polydatin compared to free polydatin in the following order: HP- $\beta$ -CD>Me- $\beta$ -CD> $\beta$ -CD Increased DPPH radical scavenging activity of inclusion complexes with polydatin compared to free polydatin in the following order: HP- $\beta$ -CD> Me- $\beta$ -CD> $\beta$ -CD	Li et al. (2018)
Resveratrol	<i>in vitro</i>	Carbonyl- $\beta$ -CD nanosponge (Resv-NS-I) Carboxylate- $\beta$ -CD nanosponge (Resv-NS-II)	Decrease of the cell viability (1.7-fold lower IC <sub>50</sub> values) of human breast adenocarcinoma cells (MCF-7 cell line) with the CD resveratrol nanosponges, Resv-NS-I and Resv-NS-II, when compared to resveratrol alone	Pushpalatha et al. (2018)
Resveratrol and oxyresveratrol	<i>in vitro</i>	Carbonyl- $\beta$ -CD nanosponge for resveratrol (Resv-NS) and oxyresveratrol (Oxyresv-NS)	Increased DPPH radical scavenging activity of inclusion nanosponges (Resv-NS and Oxyresv-NS) compared to free stilbenes Decrease of the cell viability of DU-145 prostate cancer cells upon stilbene inclusion with nanosponges compared to free stilbenes	Dhakar et al. (2019)
Resveratrol and curcumin	<i>in vitro</i>	Carbonyl- $\beta$ -CD nanosponge	Dose-dependent decrease in the cell viability of MCF-7 human breast adenocarcinoma cells with Resv-NS and curcumin-NS, respectively	Pushpalatha et al. (2019)
Resveratrol	<i>in vivo</i>	Vectisol® ( $\beta$ -CD)	Beneficial effects upon kidney transplantation in a porcine model: slow-down of the loss of renal functions and beginning of histological lesions, decrease of apoptosis and oxidative stress Improvement of kidney preservation	Soussi et al. (2019)
Resveratrol	<i>in vivo</i>	Polymerized $\alpha$ , $\beta$ and $\gamma$ -CDs	Prolonged antioxidant effect of resveratrol on intracortical microelectrodes used for neurological diseases' treatment	Haley et al. (2020)
Pterostilbene	<i>in vitro</i>	HP- $\beta$ -CD	7.5-fold decrease of the minimum inhibiting concentration and 4 fold-decrease of the minimum bactericidal concentration with pterostilbene CD-inclusion vs free pterostilbene in DMSO against <i>Fusobacterium nucleatum</i> , a periodontitis-associated pathogen	Lim et al. (2020)
Oxyresveratrol	<i>in vitro</i>	Carbonyl-nanosponge	1.5-fold increase, 4 fold-increase and 6 fold-increase in the inhibition of cell viability of, respectively, prostate (PC-3) cancer cell line and colon (HT-29 and HCT-116) cancer cell lines with oxyresveratrol nanosponges vs free oxyresveratrol	Matencio et al. (2020)
Resveratrol	<i>in vitro</i>	Sulfobutylether-CDs + PLGA	15.39-fold decrease in the IC <sub>50</sub> against cell viability of non-small cell lung cancer (NSCLC) A549 cell line and 50 fold-decrease for the H358 cell line vs unloaded resveratrol. 1.7-fold increase in caspase-3 levels in the A549 cancer cell line vs unloaded resveratrol.	Wang et al. (2020)

---

Resveratrol	<i>in vitro</i>	GSH-responsive nanosponge	Preferential entry of GSH-Resv-NS in cancer cells No toxicity of unloaded nanosponges on normal human fibroblasts Decreased viability of OVCAR-3 human ovarian cancer cells and MDA-MB-231 human triple-negative breast cancer cells with GSH-Resv-NS compared to normal human fibroblasts and normal MCF10-A human mammary epithelial cells	Palminteri et al. (2021)
Resveratrol	<i>in vitro</i>	$\gamma$ -CD	Conservation over time of the antiradical ABTS <sup>•+</sup> capacity of lemon juice with $\gamma$ -CD resveratrol complexation compared to juice supplemented with free resveratrol	Silva et al. (2021)

---

**Table 4: Green synthesis of stilbene glucosides using cyclodextrins**

Abbreviations: CD, cyclodextrin;  $\alpha$ -CD,  $\alpha$ -cyclodextrin;  $\beta$ -CD,  $\beta$ -cyclodextrin; CGTase, Cyclodextrin glucosyltransferase; nr, not reported; Pic, piceid; DMSO, dimethylsulfoxide

Reaction conditions	Stilbene acceptor	Glucosides obtained	Biological input and effect on solubility	Refs
Starch $\rightarrow$ CD as glucose donor in DMSO/Na acetate buffer 10:34 (V/V) at pH 5.6 and 60°C with the CGTase from <i>Thermoanaerobacter</i>	Resveratrol (200 mg)	3- <i>O</i> - $\alpha$ -D-glucosyl-resveratrol (28.4 mg); 4'- <i>O</i> - $\alpha$ -D-glucosyl-resveratrol (20.5 mg); 3- <i>O</i> - $\alpha$ -D-maltosyl-resveratrol (12 mg); 4'- <i>O</i> - $\alpha$ -D-maltosyl-resveratrol (10.5 mg); 4'- <i>O</i> - $\alpha$ -D-maltotriosyl-resveratrol (6.1 mg) and 3,4'- <i>O</i> - $\alpha$ -D-diglucosyl-resveratrol (4.1 mg)	Glucoside solubilities: 2 g/L, that is, 5.4-fold increase and 67 fold-increase in solubility compared to piceid (0.37 g/L) and resveratrol (0.03 g/L). Decrease in the antioxidant activity of glucosides compared to resveratrol	Torres et al. (2011)
$\alpha$ -CD as glucose donor in 0.02 M citrate phosphate buffer with 5% methanol (V/V) at pH 6.0 and 40°C with the CGTase from <i>Bacillus macerans</i>	Piceid (2.56 mM)	Numerous glucosylated derivatives of piceid (PicG <sub>2</sub> , PicG <sub>3</sub> , etc...) not quantified (peak areas)	nr	Mathew et al. (2012)
$\alpha$ -CD as glucose donor in 50 mM citrate buffer at pH 5.6 and 37°C with a CGTase of unspecified origin	4'- <i>O</i> - $\beta$ -D-glucosyl resveratrol (50 mg)	4'- <i>O</i> - $\beta$ -D-maltosyl-resveratrol; (30% yield); 4'- <i>O</i> - $\beta$ -D-maltotriosyl-resveratrol; (22% yield); 4'- <i>O</i> - $\beta$ -D-maltotetraosyl-resveratrol (12% yield) and 4'- <i>O</i> - $\beta$ -maltopentaosyl-resveratrol (6% yield)	Increase in the Inhibition of the phosphodiesterase activity (IC <sub>50</sub> = 112 $\mu$ M for 4'- <i>O</i> - $\beta$ -D-maltosyl-resveratrol) compared to resveratrol (187 $\mu$ M). Potent applications in neurology	Shimoda et al. (2015)
Starch $\rightarrow$ CD as glucose donor in water + DMSO 20% (V/V) at 60°C with the CGTase from <i>Thermoanaerobacter</i>	Pterostilbene (5 mg)	4'- <i>O</i> - $\alpha$ -D-glucosyl pterostilbene (0.12 mg) and an uncharacterized pterostilbene diglucoside (0.06 mg)	Increase in pterostilbene aqueous solubility from 0 to 0.1 g/L. 40% decrease in the antioxidant activity of 4'- <i>O</i> - $\alpha$ -D-glucoside of pterostilbene as well as a significantly lower toxicity on HT-29 colon cancer cells compared to the aglycone	Gonzalez-Alfonso et al. (2018)
$\beta$ -CD as glucose donor in 2-[ <i>N</i> -morpholino-]ethanesulfonic acid buffer at pH 6.2 and 80°C with the CGTase from <i>Thermoanaerobacter</i>	Resveratrol (2 g)	Resveratrol (89.22 mg); 3- <i>O</i> - $\alpha$ -D-glucosyl-resveratrol (366.6 mg); 4'- <i>O</i> - $\alpha$ -D-glucosyl-resveratrol (255.5 mg); 3- <i>O</i> - $\alpha$ -D-maltosyl-resveratrol (137.9 mg); 4'- <i>O</i> - $\alpha$ -D-maltosyl-resveratrol (85.16 mg)	Reduced antioxidant activities of the 3 and the 4'- <i>O</i> - $\alpha$ -D-glucosides of resveratrol (respectively 40 and 70% of that of resveratrol)	Marié et al. (2018)
$\beta$ -CD as glucose donor in phosphate buffer at pH 6.2 and 80°C with the CGTase from <i>Thermoanaerobacter</i> . Reaction mixture coupled to a membrane process	Resveratrol	Shift of the glucosylation yield from 35% to 50% compared to the results of Marié et al. (2018)	nr	Ioannou et al. (2021)